Identification of the activities of the antiviral innate immune sensor STING in CD4+ T lymphocytes

Silvia Cerboni

Université Paris Descartes

BioSPC

Unité Immunité et Cancer, INSERM U932, Institut Curie

Identification of the activities of the antiviral innate immune sensor STING in CD4+ T lymphocytes

Par Silvia Cerboni

Thèse de doctorat de Immunologie

Dirigée par Nicolas Manel

Présentée et soutenue publiquement le 21Novembre 2016

Devant un jury composé de :

Oliver Fackler (Rapporteur)

Robert Weil (Rapporteur)

Vassili Soumelis (Examiner)

Damien Arnoult (Examiner)

Nicolas Manel (Directeur de thèse)

Table of Abbreviations

2-BP= 2-bromopalmitate
AGS= Aicardi-Goutières syndrome
AIDS= Acquired immune acquired syndromes
ALR=AIM2-like receptor
AMFR= Autocrine Motility Factor Receptor
AMPK= Protein Kinase AMP-Activated Catalytic Subunit Alpha 1
APC= Antigen-Presenting Cell
ASC= PYD And CARD Domain Containing
ATG9a= autophagy 9
BST2= Bone Marrow Stromal Cell Antigen 2
c-AMP= cyclic adenosine monophosphate
c-diAMP= cyclic dimeric adenosine monophosphate
c-diGMP= cyclic dimeric guanosine monophosphate
c-GMP= cyclic guanosine monophosphate
CARD= caspase recruitment domain
CBD= Cyclic Binding Domain/Central globular domain
CDN= Cyclic dinucleotides
cGAMP= Cyclic GMP-AMP
cGAS= Cyclic GMP-AMP Synthase
CMA= 10-carboxymethyl-9-acridanone
CMV= Cytomegalovirus
CTD= C-Terminal Domain
CTT= C-Terminal Tail
DAI= DNA-dependent Activator of IFN-regulatory factors
DAMP= Damage-Associated Molecular Pattern
DC= Dendritic Cell
DDX58= dead/H box 58
DENV= Dengue virus
DMXAA= 5,6-dimethylxanthenone-4-acetic acid
DNAI= DNA dependent activator of IRF's
DNASE2= deoxyribonuclease II
dsDNA= double strand DNA
dsRNA= double strand RNA
ECMV= Encelophalomyocarditis virus
eIF2= Eukaryotic Translation Factor 2
ER= Endoplasmic Reticulum
ERGIC= ER-Golgi intermediate compartment
HCV= Hepatitis C virus
HIV-1= Human Immunodeficiency Virus 1
HIV-2= Human Immunodeficiency Virus 2
HLAC= Human Lymphoid Aggregate Culture
HPV= Human Papilloma Virus
HSV= Herpes Simplex virus
IFI16= Interferon gamma-Inducible protein 16
IFITM= IFN-induced transmembrane protein
IFN-I = type I IFN
IFN-II= type II IFN

IFN-III= type III IFN
IFN= Interferon
IKK-α= Inhibitor Of Kappa Light Polypeptide Gene Enhancer In B-Cells, Kinase alpha
IKK-β= Inhibitor Of Kappa Light Polypeptide Gene Enhancer In B-Cells, Kinase Beta
IKK-γ= Inhibitor Of Kappa Light Polypeptide Gene Enhancer In B-Cells, Kinase gamma
INSIG1= Insulin Induced Gene 1
IRES= Interferon Stimulated Response Elements
IRF3= Interferon regulatory factor 3
IRFs= Interferon Regulatory Factors
ISG= Interferon Stimulated Gene
ISG15= Interferon induced protein 15
ISGF3= IFN-Stimulated Gene Factor 3
JAK= Janus Kinase
LAT= Linker for activation of T cells
LGP2= Laboratory of Genetics and Physiology 2
LGP2=Laboratory of Genetics and Physiology 2
LRRFIP1= Leucine-Rich Repeat Flightless-Interacting Protein 1
LTNP= Long-Term Non-Progressors
MAM= Mitochondria-Associated Membrane
MAVS= Mitochondrial Adaptor Antiviral Signaling
MDA5= Melanoma Differentiation Associated Gene 5
MDDC= Monocytes-Derived Dendritic Cell
MEF= Mouse Embryonic Fibroblasts
MHC= Major Histocompatibility Complexes
MX1= Dynamin Like GTPase 1
MX2= Dynamin Like GTPase 2
MyD88= Myeloid Differentiation primary response 88
NF-kB= Nuclear Factor kappa-light-chain-enhancer of activated B cells
NFKBI/IκBα= NFKB Inhibitor Alpha
NLRC3= NLR family CARD domain containing 3
NTase= Nucleotidyl Transferase
OAS= 2'-5'Oligoadenylate Synthase
PAMP= Pathogen Associated Molecular Pattern
PAMP= Pattern-Recognition-Pathogen-Associated-Molecules
pDC= plasmacytoid Dendritic Cell
PKR= Protein Kinase R
Poly(I:C)= PolyInosinic-PolyCytidylic acid
PRR= Pattern Recognition Receptors
PYHIN= Pyrin and HIN domain containing protein
RIG-I = Retinoic Acid Inducible Gene-I
RLR= RIG-I-like receptors
RNaseL= Ribonuclease L
RNF26= Ring Finger Protein 6
RNF5= Ring Finger Protein 5
RSAD2= Radical S-adenosyl methionine Domain-containing protein 2
SAMHD1= Sterile alpha motif and histidine-aspartate domain 1 protein
SIV= Simian Immunodeficiency virus

SLE= Systemic Lupus Erythematous
SNP= Single Nucleotide Polymorphism
ssDNA= single strand DNA
ssRNA= single strand RNA
STAT= Signal Transducer and Activator of Transcription
STING= Stimulator of Interferon genes
TBK1= TANK-binding kinase 1
TCR= T Cell Receptor
Tfh= follicular helper T cell
Th= helper T cell
TLR=Toll-like receptor
TM= TransMemebrane
TMEM173= Transmembrane protein 173
TNFa= Tumor necrosis factor a
Treg= regulatory T cell
TREX1= Three prime repair exonuclease 1
TRIF= TIR-domain containing adaptor inducing Interferon b
TRIM25= Tripartite motif containing 25
TRIM32= Tripartite motif containing 32
TRIM56= Tripartite motif containing 56
TRIM5α = TRIpartite Motif-containing protein 5α
TYK= Tyrosine Kinases
ULK1= UNC51-like kinases
VAPS= Vascular And Pulmonary Syndrome
ZDHHC1= Zinc Finger DHHC-Type Containing 1

1 Résumé

Le corps humain est quotidiennement exposé à de nombreux micro-organismes et le système immunitaire est responsable du maintien de son intégrité. Suite à une infection, le système immunitaire inné déclenche une réponse rapide, non spécifique à l'agent pathogène, et amorce le système immunitaire adaptatif qui lui permet de contenir et d'éliminer spécifiquement le pathogène. Tous les virus et de nombreuses bactéries entrent dans le cytosol des cellules hôtes et commencent à se répliquer. Bien que les acides nucléiques possèdent une structure universelle, l'ADN du soi est présent dans les noyaux et les mitochondries. L'accumulation d'ADN dans le cytosol va déclencher une puissante réponse antivirale innée. Celle-ci a lieu après l'activation de la voie de signalisation cGAS-STING qui conduit à la production de d'interféron de type I et de cytokines pro-inflammatoires dues respectivement à l'activation des facteurs de transcription IRF-3 et NF-kB. De récentes découvertes ont montré que le VIH-1 échappe efficacement à l'infection et à la détection par les cellules dendritiques myéloïdes (DCs) dans le cytosol, tandis que l'ADN du VIH-2 est détectée via la voie cGAS-STING dans les DCs, induisant leur maturation. La maturation des DCs par la détection de VIH-2 induit potentiellement des réponses immunes adaptatives et pourrait contribuer au contrôle antiviral des patients infectés par VIH-2. Toutefois, comment la détection immunitaire du VIH-2 par les DCs module la susceptibilité des lymphocytes T CD4 naïfs à l'infection par VIH et leur profil effecteur auxiliaire n'est toujours pas connus.

Pour répondre à ces questions, nous avons développé un modèle in-vitro de lymphocytes T CD4+ naïfs co-cultivés avec des cellules dendritiques préalablement exposées à VIH-1 ou VIH-2, ou d'autres stimuli de contrôle. Nous avons montré que la détection de VIH-2 par les cellules dendritiques conduisait à l'acquisition partielle d'une résistance à l'infection dans les lymphocytes CD4+ naïfs. Cette résistance est liée à l'induction de gènes stimulés par l'interféron. Nous avons montré que le profil T_{VIH-2} est caractérisé par la production d'IFNγ rappelant le profil des lymphocytes T auxiliaires de type 1 (Th1). Nous avons généré les profils d'expression géniques correspondant par micropuces. Nous avons réalisé une analyse exploratoire sur les différences d'expression des gènes à partir des micropuces et nous avons produit une liste de gènes candidats comme facteurs de résistance dans les lymphocytes T CD4+.

Bien que le rôle de STING dans l'immunité innée et les voies de signalisation ait été largement décrit, son implication dans l'immunité adaptative reste inconnue. Dans de précédentes études, une nouvelle mutation de gain de fonction a été identifiée dans le gène codant pour STING dans une famille caucasienne non-consanguine. Le mutant constitutivement actif STING-V155M, est localisé de façon permanente dans l'appareil de Golgi et active la voie STING-TBK1-IRF3. Les patients porteurs de cette mutation présentent une signature IFN de type 1 dans leur sérum. L'analyse des paramètres cliniques de ces patients montre une diminution de leurs lymphocytes T mémoires et une augmentation de leur fraction des lymphocytes T naïfs par rapport aux sujets contrôles. Pour évaluer l'activité de STING dans les lymphocytes, nous avons développé un modèle *in vitro* de lymphocytes T CD4+ transduits avec STING WT ou d'autres mutants de STING. Nous avons démontré que STING induit une

activité antiproliférative des lymphocytes T CD4+. Cette activité est indépendante du recrutement de TBK1, IRF3 et de l'action de l'IFN de type I, mais il active les DCs. En outre, cet effet antiprolifératif des cellules par STING est dépendant de sa localisation au Golgi et induit des erreurs lors de la mitose. En conclusion, nos découvertes révèlent l'activité intrinsèque antiproliférative d'un senseur innée dans des cellules appartenant au système immunitaire adaptatif.

Nos découvertes contribuent à étendre le paradigme de l'immunité innée par l'examen de l'impact de signaux innés dans les cellules de l'immunité adaptative. Nous avons trouvé que les lymphocytes T CD4+ ne sont pas seulement façonnés par des signaux extrinsèques induits par des cellules spécialisées de l'immunité innée, mais ils sont aussi influencés par des activités intrinsèques de détecteurs innés. Un concept émergeant de notre travail est que les détecteurs innés pourraient adopter des activités distinctes dans les cellules de l'immunité adaptative. En conséquence, il sera important de comprendre comment les cellules de l'immunité adaptative intègrent ces signaux extrinsèques et intrinsèques pour produire une immunité protective.

2 Introduction

2.1 The Immune System

The human immune system is constantly exposed to microorganisms such as viruses, bacteria and fungi. However, this exposure only occasionally leads to an infectious disease in healthy individuals. This is due to several lines of defense that protect our body from infectious agents. For an infection to occur, pathogens have to enter the body and pass physical barriers like the skin and chemical protection such as acidic body fluids. Should this early defense fail, pathogens are met by the immune system, a complex network of tissues, cells and molecules which has evolved multiple mechanisms to combat pathogens. In vertebrates, the immune system is composed of innate immune and adaptive immunity. While the innate immune system is responsible for pathogen detection and a quick, rather unspecific response, the adaptive immune acts relatively late but in a highly pathogen-specific manner. Innate and adaptive immune defense complement each other for the eradication of the infection in the host as the adaptive immune system is activated by innate immune system [1].

2.2 Pathogen sensing by the innate immune system

The innate immune system is a network of cells formed during early development, which protects the newborn from potentially lethal infections. Its components are generated from hematopoietic precursors in the bone marrow and develop into several distinct cell lineages: Granulocytes (composed of neutrophils, eosinophils and basophils), Macrophages and Dendritic Cells (DCs). While Granulocytes are the major cell population in the blood, macrophages are mostly restricted to mucosal defense in the tissues while DCs are patrolling both blood and tissues. As their name suggests, granulocytes contain many granules with potent cytotoxic molecules that can be released to kill a pathogen once it is recognized. Macrophages are specialized in phagocytosis, a term that describes the uptake of a pathogen into the cell followed by intracellular lysis of the pathogen. Macrophages are equally potent in restoring tissue homeostasis after an infection has been successfully resolved. Dendritic cells are the key player linking the early innate to the adaptive immune response. They are so called antigen-presenting cells (APC), specialized in digesting pathogens into small pieces (antigens) which are then presented on major histocompatibility complexes (MHC) to cells of the adaptive immune system.

The ability to mount an adequate immune response to clear an infection is based on the recognition of the pathogen. The innate immune system is responsible for this recognition. Innate immunity relies on a limited array of germ-line encoded innate immune "sensors", termed pattern recognition receptors (PRRs). PRRs recognize conserved structures of different pathogens, known as pathogen-associated-molecules (PAMPs) and can be found on the surface and the cytosol of all innate immune cells. Recognition of PAMPs in turn triggers a wide range of downstream effects in the cell

that may lead to the induction of an immune response [2, 3] such as degranulation in granulocytes or phagocytosis in macrophages. In DCs pathogen recognition leads to maturation and expression of the co-stimulatory molecules CD80/86, which is required for the activation of naïve T lymphocytes. Like PAMPs, damage-associated-molecular-patterns (DAMPs) also trigger innate immune responses through PRR-mediated recognition. DAMPs are molecule that belong to the host organism but are only released upon cell stress or damage [4]. The recognition of PAMPs and DAMPs by PRRs will be discussed in detail below.

2.3 **Innate sensing shapes adaptive immunity**

The adaptive immune system consists of mainly two cell types: B cells that are generated in the bone marrow and T cells that mature in the thymus. In contrast to the germ line-encoded PRRs of the innate immune system, adaptive immune cells have evolved a process of somatic gene rearrangement to generate an enormous repertoire of receptors, each specific for a single antigen. Since each cell undergoes a separate gene rearrangement event, practically every T or B cell has a unique receptor expressed on its surface. Since the repertoire of lymphocyte receptors is generated randomly, they are not necessarily specific for pathogen-derived antigens. In fact, T and B cells can bind self-antigens. To avoid autoimmunity, these self-reactive cells are controlled and negatively selected in the bone marrow (B cells) or in the thymus (T cells). Mature T cells, that express a rearranged T cell receptor (TCR), can express either the CD8 or CD4 glycoprotein on their surface. CD8+ T cells are termed cytotoxic T cells, are activated via interactions with antigen presented on MHC class I and are highly potent cytotoxic cells. CD4+ T cells are activated by antigens presented on MHC class II and are termed helper T cells (Th) as they boost the immune response by producing a wide range of cytokines and by promoting B cell activation, antibody production and class switch.

After exiting the thymus, naïve T cells migrate from the bloodstream to lymph nodes where they might encounter a cognate antigen presented by an APC. As mentioned above, the activation of the adaptive immune system depends on innate immune cells. In general, activation of an adaptive immune response requires 3 signals: (1) TCR engagement by complexes of cognate antigen bound to MHC molecules, (2) co-stimulatory signals through interaction of T cell CD28 and APC-expressed CD86, and (3) the secretion of soluble mediators from DCs. Extrinsic signals, such as cytokines and chemokines, are responsible for the attraction of other immune cells and are indispensable for differentiation of naïve CD4+ T cells into effector and memory T cells. T cell differentiation into a functionally distinct lineage depends on the cytokine milieu at the time of activation [5]. While the cytokine IL-4 is associated with T cell differentiation into the helper 2 lineage (Th2) that is effective against parasites, IL-12 and interferon α,β and γ (IFN α,β and γ) are associated with Th1 cells which take action against intracellular pathogens [6]. In the presence of TGFβ, T cells can also differentiate into Th17 cells, fighting off extracellular bacteria and fungi or regulatory T cells (Treg) that are crucial to immune homeostasis and prevent autoimmunity. Here, we were particularly interested in Th1 cells as they are involved in the elimination of intracellular pathogens. During differentiation, the expression of the Th1-specific transcription factor t-bet enhances the production of IFNγ and other Th1 key cytokines. These cytokines then participate in a positive feedback loop further

promoting T cell activation as well as providing pro-survival signals to other cells of the immune system such as macrophages, CD8+ T cells and natural Treg.

Finally, a specific subset of activated T helper cells, so-called follicular helper cells (Tfh), are crucial for an effective immune response as they bridge CD4+ T cell immunity and B cell activation. Through another MHC-dependent and antigen-specific activation between cognate B- and Tfh cells, B cells become licensed to produce large amounts of soluble B cell receptor, also termed antibodies. Antibodies are highly specific, mark intruding pathogens and help cells of the innate immune system to perform more efficient degranulation and phagocytosis. They are among the most potent effectors of the immune system [7] (Fig.1).

After activation, CD4+ T cells migrate to peripheral tissues and inflamed sites to facilitate destruction of infected targets. The majority of effector cells die after antigen clearance, but a small population develops into long-lived memory T cells [8]. Given the variety of adaptive immune responses, what dictates the global nature of the final immune response? Evidence is emerging that the quality of innate pathogen sensing determines the outcome of adaptive immunity. In the following section we focus on how different pathogens can be sensed by different PRRs creating a broad spectrum of innate immune activation.

2.4 Sensing by the innate immune system through PRRs

PRRs are a heterogeneous group of receptors involved in the recognition of different PAMPs/DAMPs [2, 3]. They can be subdivided into different categories based on their localization within the cell. PRRs are either found on the cell surface, in endosomal compartments or in the cytosol. Another system of classification is based on their ligand specificity, which can range from bacterial peptidoglycans and lipopolysaccharides to viral RNAs and DNAs. Most PRRs share the same mechanism of signal transduction. After binding to a PAMP/DAMP, a PRR interacts with a downstream adaptor protein resulting in the activation of terminal effector proteins like caspases and transcription factors. Pro-inflammatory cytokines, chemokines and IFNs are secreted and ultimately they trigger a second wave of autocrine and paracrine signaling resulting in the induction of an immune response. The details of these pathways are described below.

2.4.1 TLRs: extrinsic innate sensors

Among the several types of PRRs the best studied belong to the Toll-like-receptors (TLR) family. All the 10 TLRs expressed in humans, are type I transmembrane proteins and they are mainly expressed in DCs, monocytes and macrophages. They are either found in the plasma membrane, such as TLR1, 2, 4, 5, 6 and 10, or in the endosomal compartments such as TLR3, 7/8 and 9 [9-11]. TLRs present on the cell surface recognize extracellular lipids and bacterial or viral proteins while the endosomal TLRs detect nucleic acids. TLR3 was found to be involved in the sensing of long dsRNAs by stimulating cells with the synthetic analog poly(I:C) [12]. While TLR7/8 detects single-stranded RNA and TLR9 detects hypomethylated CpG-rich DNA from pathogens. Additionally, TLR7 and TLR8 were shown to play roles in the

sensing of ssRNA in a species-specific manner [9, 13]. The function of TLR7 has been studied in the context of human immunodeficiency virus 1 (HIV-1) infection. Plasmacytoid dendritic cells (pDCs) constitutively express TLR7 but not MDDC [14]. It has been reported that when pDCs detect HIV-1 derived RNA, large amounts of type I IFN (IFN-I) are secreted. This innate response requires TLR7 sensing of viral nucleic acids in endosomes [15, 16].

TLR signaling occurs through the intracellular adaptor proteins, Myeloid Differentiation primary response 88 (MyD88) and TIR-domain containing adaptor inducing Interferon b (TRIF). Activation of TLRs induces activation of Nuclear Factor kappa-light-chain-enhancer of activated B cells (NF-kB) and transcription of proinflammatory cytokines such as TNFa or IL-6. Sensing of viral ssRNA by TLR7 and DNA by TLR9 leads to MyD88-dependent and IRF7-mediated IFNβ production. Alternatively, this pathway can lead to NF-kB and IRF4 and IRF5 activation and subsequent production of type I and II interferon (IFN-I, IFN-II) and pro-inflammatory cytokines [9-11] [15, 16].

2.4.2 Cytosolic Innate Immune sensing

The basic structure of nucleic acids is universally shared between unicellular and multicellular organisms. The immunostimulatory effect of nucleic acids on cells has been known for more than 50 years. Indeed, self-DNA is well compartmentalized in the nucleus and in mitochondria. However, detection of DNA in the cytosol triggers strong immune responses. The accumulation of foreign nucleic acids occurs when viruses and also many bacteria enter into the cytosol of a host to start their replication. Viral RNA and DNA are recognized as PAMP in most viral infections. The detection of cytosolic nucleic acids is an important mechanism by which pathogens are sensed and protective immune responses are generated. In general, activation of nucleic acid sensors leads to indirect antiviral activity *e.g.* through the production of IFN-I which has pleiotropic antiviral effects (discussed in detail below). At the same time IFN-I further augments the expression of nucleic acid sensors in a positive feedback loop.

However, maintaining host recognition of foreign nucleic acids is a big challenge considering that pathogens have evolved mechanisms to evade the innate immune sensing. In the past few years a significant body of work has identified cytosolic nucleic acid sensors that trigger innate immune responses. Thus, much progress has been made in the identification of cytosolic RNA and DNA innate sensors.

2.4.2.1 Cytosolic RNA sensors

Given that TLRs recognize only extracellular or endosomal RNAs/DNAs due to their localization, and the observation that IFN-I can be detected in cell lines lacking TLR3/7/8, more studies explored the existence of TLR-independent RNA sensing pathways [17]. Indeed, the RIG-I-like receptors (RLR) family was found to comprise 3 members of cytosolic RNA sensors. Retinoic Acid Inducible-I (RIG-I) is activated by 5' tri- or di- phosphorylated RNA (dsRNA ≥ 19 bp), Melanoma Differentiation Associated Gene 5 (MDA5) detects long RNA with strong secondary structures (dsRNA ≥ 300 bp) while Laboratory of Genetics and Physiology 2 (LGP2) also

recognizes RNA but its mechanism is not yet fully resolved. It has been proposed that LGP2 acts as a modulator by inhibiting RIG-I and facilitating MDA5 signaling [18]. Both RIG-I and MDA5 signal through Mitochondrial Adaptor Antiviral Signaling (MAVS) by the interaction of their CARDs domains. In turn the engagement of MAVS provides a platform for downstream activation of TANK-binding kinase 1 (TBK1) and NF-kB [19]. Thus, an amplification of RLR signaling and a rapid induction of cytokine expression occurs [10, 11] [13] [18] [20, 21] [22].

However a second class of RNA sensors has been identified due to their direct antiviral activity. The 2'-5'Oligoadenylate Synthase (OAS) family is involved in the recognition of cytosolic dsRNA and counts four members (OAS1, OAS2, OAS3 and OASL) in humans. They belong to the superfamily of Nucleotidyl Transferases (NTases) [23]. Upon RNA sensing, OASs synthesize 2'-5' oligoadenylates that activate Ribonuclease L (RNaseL). RNaseL in turn cleaves viral ssRNA, thus interfering with viral replication while at the same time producing ligands for RIG-I. This mechanism synergizes OAS antiviral activity with IFN-I production by RLR signaling [24, 25] [26-29]. Another member of this second class of RNA sensors is Protein Kinase R (PKR), a serine/threonine kinase, which binds cytosolic dsRNA. Its activation leads to eIF2 phosphorylation and subsequent suppression of mRNA translation which prevents viral replication [30].

2.4.2.2 Cytosolic DNA sensors

A decade ago, only TLR9 was known to sense foreign DNA in the endosomes, but the list of cytosolic DNA sensors has grown rapidly. This includes DNA-dependent Activator of IFN-regulatory factors (DAI), RIG-I via RNA polymerase III, Leucine-Rich Repeat Flightless-Interacting Protein 1 (LRRFIP1), DEAD/H box peptides: DHX9, DHX36 and DDX41, Cyclic GMP-AMP Synthase (cGAS) and Interferon gamma-Inducible protein 16 (IFI16) [31] [32] [33] [34] [35, 36].

However, many of the studies on the reported sensors did not provide a detailed molecular mechanism that explains the translation of the DNA sensing to IFN-I response. Which pathways are essential in inducing IFN expression in response to DNA needs to be clarified in the field. One report has provided genetic evidence that 13 members of the Aim2-like receptors (ALRs) are not essential for IFN-I responses to cytosolic dsDNA [37].

To date, cGAS is the only cytosolic DNA sensor that has been supported with a detailed biochemical mechanism and crystallography data. For example, IFI16, a member of ALR family, was reported to act as a DNA sensor and to be critical for IFN-I response. It is supposed to sense viral DNA upstream of Stimulator of Interferon Genes (STING), an important signaling adaptor protein for DNA sensors (discussed in detail below), [38]. However, a CRISPR/Cas9 approach showed that human fibroblasts deficient for IFI16 still mount normal IFN responses [37]. Nonetheless, IFI16 has been reported to trigger pyroptosis, an inflammatory cell-death, upon DNA sensing of an abortive HIV-1 infection in non-permissive bystander CD4+ T cells [39, 40].

It has been suggested that cytosolic DNA receptors could engage two different

inflammatory signaling pathways. Briefly, the first pathway results in the production of IFN-I and pro-inflammatory cytokines through the transcription activity of Interferon regulatory factor 3 (IRF-3) and NF-kB that is coordinated by the ER-associated protein STING. The second pathway is activated by members of NOD-like receptor (NLR) and ARL family and it is characterized by the assembly of an 'inflammasome complex' that leads to caspase-1-dependent activation and secretion of inflammatory cytokines such as IL-1β and IL-18 [31, 32] [41, 42]. In the following, we will focus on the first pathway.

2.5 STING is the universal innate adaptor of cytosolic nucleic acid sensing

2.5.1 STING structure and conservation over species

Human *TMEM173* gene encodes for STING (also called MITA, IRIS or NET23), a protein consisting of 379 amino acids which is characterized by three functional domains: a cytoplasmic C-terminal tail (CTT, amino acids 342-379) important to transduce downstream signals, a central globular domain (CBD, amino acids 155-341) which contains dimerization and ligand binding sites, and four N-terminal transmembrane motifs (amino acids 1-154) that localize STING in the endoplasmic reticulum (ER) at steady state [43] (Fig.2).

Crystallography analysis of the C-terminal domain (CTD) reveals that STING exists as a V-shaped dimer even in absence of its ligand [44]. The dimer interface generates a hydrophobic trough where the bacterial second messenger c-di-GMP or mammalian-derived 2'-3'-cGAMP bind [44]. The mechanism of STING activation upon ligand binding is still under study; possibly binding of its ligand induces conformational changes that lead to the recruitment/release/activation of downstream signaling molecules and which allow for its translocation to the Golgi/ERGIC compartments, a hallmark of activation [45].

Evolutionary analysis revealed several functional homologs of STING, from protozoan to vertebrate species. The N-terminal domain is generally conserved in vertebrates, with exception of birds. It also exists in protozoan and metazoan species with four TM domains while fewer than four TM domains are found in STING homologs among arthropods and birds. All STING homologs contain the conserved cyclic-binding-domain (CBD) and a dimerization domain (DD) suggesting that the STING function to bind cyclic dinucleotides (CDNs) is evolutionary conserved and that the production of IFN was acquired later in vertebrate innate immunity. Indeed, the CTT of STING is only conserved in vertebrates [46].

2.5.2 STING is the sensor of cyclic dinucleotides

STING was originally described as a novel transmembrane protein interacting with MHC class II, however further studies are needed to clarify the importance of this discovery [47]. At the same time, three other groups independently described STING as the key innate sensor of CDNs [43, 48, 49]. Further studies demonstrated that

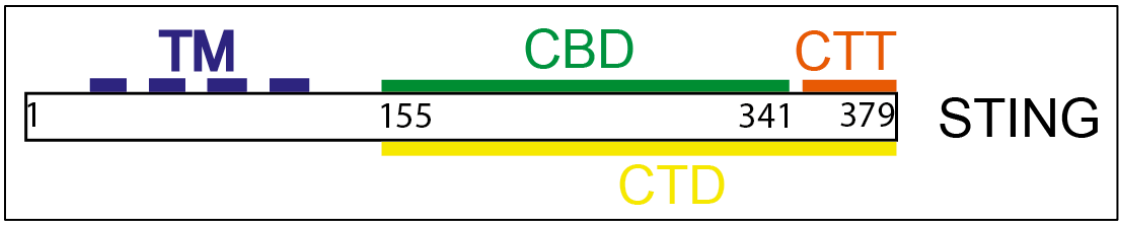

Fig.2. Human STING protein structure.

STING is a protein of 379 amino acids characterized by three functional domains: a cytoplasmic C-terminal tail (CTT, amino acids 342-379) important to transduce downstream signals, a central globular domain (CBD, amino acids 155-341) which contains dimerization and ligand binding sites, and four N-terminal transmembrane motifs (amino acids 1-154) that localize STING in the ER at steady state. C-terminal domain (CTD) comprises the CBD and CTT (155-379).

STING has a fundamental role in IFN-I production both in knockdown and overexpressing experiments in different cells [43, 50]. Cyclic di nucleotides *e.g.* c-AMP, c-GMP, c-di-AMP and c-diGMP, have been well studied and characterized as second messengers in prokaryotes. They regulate a multitude of physiological processes including biofilm formation, virulence and motility [51-53]. Only recently, CDNs have been recognized as potent second messengers of innate immune responses in mammalian cells [54]. Here, STING has been found to be the direct sensor CDNs and acts as an adaptor for downstream signaling that leads to IFN-I production.

Indeed, in eukaryotic cells, STING can bind directly to CDNs, such as c-di-GMP and c-di-AMP, which can be secreted by intracellular bacteria like *Listeria monocytogenes* [55-58]. However, also eukaryotic cells, transfected with DNA, can synthesize the cyclic dinucleotide cGAMP [59]. This production is mediated by cGAS, which senses cytosolic DNA and catalyses the synthesis of cGAMP from AMP and GMP. While bacterial c-diAMP or c-diGMP are constituted by two nucleotides bound via a canonical 3'-5' phosphodiester linkage, cGAMP was later shown to have a canonical 3'-5' linkage and a non canonical 2'-5' phosphodiester bond (c[G(2',5')pA(3',5')p]) [60-63]. Eukaryotic cGAMP binds to STING with 300 fold higher affinity than the other CDNs [63], which might explain its potent properties in triggering STING-dependent downstream signaling [60, 61]. Thus, the innate immune system has evolved a mechanism to respond to pathogens upon sensing the second messengers, either produced by bacteria themselves or by an enzymatically active DNA sensor. However, structural studies did not clarify completely how signal transduction is facilitated downstream of STING.

Nonetheless, given the central role of STING in innate DNA sensing, efforts have been made to identify synthetic ligands that can be used to trigger STING-dependent antiviral and antibacterial immune responses. Structural and functional analyses of STING show its versatility in the recognition of natural and synthetic ligands such as CMA (10-carboxymethyl-9-acridanone) and DMXAA (5,6-dimethylxanthenone-4-acetic acid). However, it has been shown that these compounds bind STING and induce STING-dependent IFN-I production only in mice and they are not effective in activating human STING, probably due to differences in the amino acid sequence of the CBD of STING [64-66].

2.5.3 STING localization and signaling

At steady-state STING localizes to the ER. However it is not clear yet if the inactive form is present as a monomer or a dimer, due to conflicting results [44, 48, 56-58]. Upon CDN binding, STING traffics from the ER to the Golgi and ERGIC, a tubulovesicular membrane cluster named the ER-Golgi intermediate compartment. Tanaka *et al.* established a model in which STING forms an activation platform of higher order oligomers. It recruits TBK1 at the CTT and upon TBK1 phosphorylation, through a not yet described mechanism, TBK1 phosphorylates STING at the Ser366. Phosphorylation of STING at this residue is necessary for STING-dependent IRF3 phosphorylation by TBK1. Mutations in Ser366 or Leu374 abolished the interaction between STING and TBK1, suggesting their importance in TBK1 dependent IRF3 activation. Upon IRF3 phosphorylation, IRF3 dimerizes and translocates to the nucleus to induce transcription of IFN-I genes [50, 67]. In a second line of signaling, STING also activates the NF-kB pathway leading to pro-inflammatory cytokine

production [68] (Fig.3). However further investigation is required to clarify all the players involved in the latter signaling pathway. Lastly, STING-dependent activation of TBK1 can also induce activation of STAT6 in a JAK-independent manner followed by the expression of Signal Transducer and Activator of Transcription 6 (STAT6)-dependent chemokines such as CCL2, CCL20, and CCL26. These chemokines contribute to the recruitment of immune cells to combat viral infection [69].

2.5.4 STING post-translational modifications and negative regulation

Given the central role of STING in antiviral innate immunity, many studies have focused on deciphering the molecular mechanisms that regulate STING function. Here we focus on several post-translational modifications that contribute to STING function and its negative regulation.

Two different studies have shown that the ubiquitin ligases TRIM32 and TRIM56 can mediate K63-linked ubiquitination at lysine 150 of STING, facilitating STING interaction with TBK1 and optimal signaling after DNA sensing [70, 71]. However, conflicting results were obtained by using a more stringent two-step immunoprecipitation assay. In this study the authors showed that neither TRIM32 nor TRIM56 were directly capable of ubiquitinating STING. Nonetheless, TRIM32-mediated ubiquitination of STING was partially reduced when Lys150 was modified in the STING sequence [72]. Overall these data suggest that the two enzymes might contribute to STING signaling, but in an indirect fashion, modifying yet unknown partners of STING.

Interestingly, it seems that Lys150 is a critical target site for post-translational regulation of STING. Indeed, it has been shown that the ubiquitin ligase Ring Finger Protein 5 (RNF5) mediates proteasome-dependent STING degradation through K48-linked ubiquitination upon viral infection [73]. Conversely, the E3 ligase Ring Finger Protein 26 (RNF26) attenuates the RNF5-mediated negative regulation through K11-linked polyubiquitination of STING without preventing K63-linked ubiquitination [74]. At the same time, RNF26 has been shown to negatively regulate IFN-I production by promoting IRF3 degradation through autophagy, in the later phase of viral infection [74]. This offers an example of a dual regulation of STING signaling by the same regulator, RNF26, highlighting the complexity of different mechanisms that take place at different times during infection to stabilize and tightly control STING activation and its downstream effects.

STING has also been implicated in antibacterial innate immune responses. The AMFR-INSIG1 complex was identified to be responsible for K27-linked polyubiquitination of STING in antimicrobial signaling. The proposed model interestingly depicts INSIG1 to specifically bind to STING and thus to promote AMFR-STING interaction. It is demonstrated that AMFR, responsible for K27-linked polyubitination of STING, is required to recruit TBK1 onto STING, indicating that TBK1 can selectively bind to K27-linked polyubiquitin chains but not to K63-linked ubiquitination [75]. This regulation of the STING-TBK1 axis by the AMFR-INSIG1 complex leads to speculate about the link between innate immunity and metabolism due to previous studies showing that the AMFR-INSIG1 complex is also responsible

for K48-linked polyubiquitination of HMG-CoA reductase [76], an enzyme involved in cholesterol metabolism. Further studies are needed to elucidate whether STING is involved in metabolism changes after DNA sensing.

A recent report suggested that STING activity is regulated by the serine protease iRhom2. The authors proposed that iRhom2 facilitates STING trafficking, from ER to perinuclear microsomes, through recruitment of the TRAP complex member β (TRAPβ) and by stabilizing STING through the recruitment of the de-ubiquitination enzyme EIF3S5 that removes STING K48-linked polyubiquitin chains [77].

Not only phosphorylation and ubiquitation have been implicated in STING regulation. Recently, palmitoylation of STING at the Golgi has been described to be required for its activation and to induce optimal downstream immune responses. Briefly, it has been demonstrated that mutation of the Cys88/89 residue as well as treatment with palmitoylation inhibitor 2-bromopalmitate (2-BP) abolished STING-dependent IFN-I production. Moreover, different STING genetic variants, which will be discussed below, were tested using both approaches and in all cases the STING-dependent response was inhibited. This discovery opened the possibility to treat cytosolic DNA-dependent autoinflammatory syndromes by interfering with STING palmitoylation [78].

The importance of palmitoylation of STING for its activity is further supported by another work showing that the ER-associated modulator ZDHHC1, which belongs to the DHHC palmitoyl transferase family, facilitates STING higher-order oligomerization followed by TBK1 and IRF3 recruitment. Further studies are required to elucidate whether STING-dependent signaling requires the enzymatic activity of ZDHHC1 [79, 80].

Additional proteins have been identified to interact with STING and to negatively modulate its function. For example, NLRC3, a member of the NLR family intracellular sensors that regulates inflammasome functions, has been reported to associate directly with STING and to compete with TBK1 for STING interaction. NLR family CARD domain containing 3 (NLRC3) reportedly blocks the translocation of STING from the ER to the Golgi and NLRC3 deficiency enhances immune responses. Similarly, $Nlrc3^{-/-}$ mice are more resistant to HSV-1 challenge [81]. These results suggest that members of different innate sensing pathways cooperate in the host to regulate inflammatory responses against intracellular microbial infections.

Another way of regulating STING activity is to regulate its degradation. Recently, autophagy has been reported as a possible mechanism for the negative regulation of STING. Indeed, STING co-localizes with LC3 and Atg9a after DNA stimulation [82]. Moreover, it has been reported that the autophagy related serine/threonine kinase ULK1 phosphorylates STING, resulting in IRF3 inhibition. Phosphorylation of STING occurs at Ser366, the same residue that is phosphorylated by TBK1 and required for IFN-I production [83, 84]. Reportedly, ULK1 function is negatively regulated by Protein Kinase AMP-Activated Catalytic Subunit Alpha 1 (AMPK), a cellular energy sensor, which is released from ULK1 after cGAMP sensing or under starvation-induced cellular stress [84]. Therefore, after dsDNA sensing by cGAS, STING is activated but at the same time, the increasing concentration of CDNs in the

cell trigger a negative feedback mechanism that limit STING activity through ULK-mediated autophagy (Fig.4).
Finally, two other mechanisms have been described to regulate signaling upstream of STING by targeting cGAMP production. It has been reported that Beclin-1, an autophagy related protein, directly interacts with cGAS to inhibit IFN-I production upon HSV-1 infection [85]. Akt is also found to phosphorylate and inhibit cGAS activity, decreasing cGAMP production and subsequent IFN-I production leading to increased HSV-1 infection [86].

2.5.5 Evasion of STING signaling by pathogens

Since STING is involved in antiviral and antimicrobial innate immune responses as well as in diseases caused by protozoan parasites [87]. STING activation and STING-dependent IFN-I production is essential for efficient protection against infection after HSV-1 [43] or *Listeria monocytogenes* [88-90]. These pathogens evolved to have several escape mechanism to circumvent STING-induced immune responses. Moreover, and even though IFN-I exerts a potent antiviral function, some pathogens have successfully developed mechanism to evade the STING-dependent pathway. For example, the NS2B3 protease complex of Dengue virus (DENV) counteracts IFN-I production by directly cleaving STING in human MDDCs, a mechanism that is ineffective in mice due to the inability of the viral protein to cleave murine STING [91, 92].

Furthermore, HCV protein NS4B is reported to interfere with STING pathway in two different studies. One study reports the co-localization of NS4B and STING in the ER that attenuates the STING-TBK1 interaction, while the second study found NS4B and STING co-localization in the mitochondria-associated membranes (MAMs), interrupting the interaction between STING and MAVS [93, 94]. The second study connects STING to RNA virus sensing [43, 48-50], but further studies could not validate the role of STING in IFN-I production upon RNA sensing [69, 88]. Also coronaviruses were found to inhibit STING-mediated activation of IRF3 through the papain-like protease NSP3, resulting in a reduction of IFN-I [95].

Insights about evasion mechanisms of DNA viruses have been reported for HSV-1. It has been shown that STING is activated and required for HSV-1 viral control. However, the same group reported that HSV-1 requires STING in a cell type and context dependent manner for its infection. ICP0 or ICP4 deleted HSV-1 mutants require STING for replication, since viral reproduction was attenuated in STING knockdown cells. However, neither WT nor ICP0 HSV-1 viruses induced STING degradation in human embryonic lung [96].

Another mechanism of evasion is reported for the early HPV E2 protein. The protein interferes with STING transcription followed by a subsequent down regulation of downstream Interferon-Stimulated-Genes (ISGs) [97].

Moreover, the oncogenes E7 from HPV, and E1A from adenoviruses, are described as potent inhibitors of STING-dependent signaling. Indeed, the reported oncogenes bind to the C-terminal domain of STING with the conserved LXCXE motif, pointing towards the key involvement of this domain for downstream signaling [98].

Importantly, the relevance of the cGAS-STING axis has also been described for HIV [99, 100]. HIV sensing and mechanism of evasion of innate immune responses will be discussed in a separate chapter.

2.5.6 Genetic STING variants

Given the central role of STING in innate immune responses upon infection and its involvement in IFN-I induction, genetic studies have focused in the identification of SNPs in the STING sequence in the human population. Modifications in the amino acids sequence of STING might influence its ability to activate innate immune response leading to aberrant IFN-I and inflammatory cytokines production. It is critical to understand how STING mutations change the susceptibility of individuals to infections in IFN-I dependent diseases. 12 different haplotypes are described for STING with an incidence of 57.9% for WT, 20.4% for HAQ, 13.7% for R232H, 5.2% for AQ and 1.5% for R293Q and other mutants (R71H, G230A, HQ) (Fig.5). All of these haplotypes have been studied for their ability to bind CDNs and to induce type I IFN production [101, 102]. It appears that STING variants R232H or R293Q are poorly or not responsive to bacterial CDNs but efficiently respond to cGAMP, respectively. While HAQ and AQ haplotypes are activated by all CDNs, they showed a reduced ability to stimulate downstream signaling pathways in 293FT cells [102], for a reason that has yet to be clarified. In mice, the variant T596A has been identified, which is defective in IFN-I induction after stimulation with CDNs [88].

However, some SNPs correspond to gain-of-function mutations, in which case detrimental effects might be observed. Indeed, gain-of-function polymorphisms of STING are shown to trigger constitutive IFN-I production and cause autoimmune and inflammatory syndromes. 5 sporadic cases of activating STING mutations have been reported with patients suffering from vascular and pulmonary syndrome (VAPS) [103]. The newly identified STING variants (N154S, V155M and V147L) potently stimulate the type I IFN promoter in *in vitro* expression assays in 293 cells, demonstrating for the first time that STING variants may induce inflammatory diseases [103]. A follow-up study has provided further information regarding the mechanism of activation and localization of the STING-V155M variant. It is proposed that the substitution of the residue V to M at position 155, which falls within the dimerization domain, might stabilize the position M271 in the same monomer, which creates stronger interaction with W161 of the other monomer. The formation of stronger inter-monomers sulfur-aromatic interaction is predicted to induce the "closed conformation" typically induced by CDNs binding at the dimer interface. Moreover, the V155M variant has been found in the Golgi and ERGIC in patients' fibroblasts in absence of CDN ligands, supporting the constitutive-active nature of this mutant [104]. Indeed, patients carrying the V155M variant, show elevated levels of IFN-I in the serum and PBMCs display an ISG-signature. This hyperproduction of IFN-I might be the main cause for the chronic inflammation, variable autoimmunity and pulmonary syndrome [104].

2.6 **STING-dependent IFN-I production**

2.6.1 IFNs and ISGs

IFN is a soluble factor secreted by cells upon detection of PAMPs or DAMPs by transmembrane and cytosolic receptors. It has been described for the first time in 1957 as a factor able to interfere with viral infection [105, 106].

The IFN family is composed of several proteins divided into 3 main groups: IFN-I, II and III. While IFN-II is a sole cytokine, IFN-I and III encode for many cytokines. All IFNs signal through the JAK-STAT signaling pathway, after binding to the IFN receptor, which is composed of 2 different subunits, depending on the type of IFN that is considered [107] (Fig.6). While IFN-II is produced by immune cells such as T lymphocytes and NK cells [108] and is important in anti-bacterial immunity [109], IFN-I can be produced by almost all cell types depending on the type of stimulus. However, some cells of the immune system, such as plasmacytoid DCs, are specialized in the IFN-I secretion which function is to prevent the spread of infectious agents, in particular viral pathogens. IFN-I is also proposed to modulate innate immune responses by counteracting pro-inflammatory pathways and cytokine production. It can also modulate the adaptive immune response by promoting T and B cells pathogen-specific immune responses. Depending on the context, IFN-I production can lead to beneficial outcomes, as discussed below, or have detrimental effects in the host, as will be discussed in a separate chapter.

After binding of IFN-I to its receptor (IFNAR), the activation of JAK1-TYK2 leads to STAT1 and STAT2 heterodimerization and translocation into the nucleus, where they assemble with IRF9 to form the Interferon StimuIated Gene Factor 3 (ISGF3) complex. ISGF3 in turn binds to its specific consensus sequences in the DNA, known as Interferon Stimulated response elements (ISREs) thereby activating the transcription of hundreds of ISGs [110-113].

The ISGs are a heterogeneous group of genes with multiple functions. ISGs have anti-tumor, anti-angiogenic, immunomodulatory, apoptotic, cell cycle inhibitory and anti-viral among the most studied functions.

Within the wide group of ISGs, IRFs represent a group of transcription factors that are expressed at baseline and are induced by IFN-I in a STAT-dependent mechanism. In addition, IRFs reinforce the IFN response due to overlap of the consensus motifs of IRF elements with ISREs. Thus IRFs, including IRF1, IRF7, IRF8 and IRF9 can bind and activate many of the same ISGF3 target genes and their contribution is likely to regulate transcription of a second group of ISGs, which requires *de novo* protein synthesis [114].

Due to the IFN antiviral effect, ISGs have been recently extensively studied for the identification of viral restriction factors as it will be discussed in the following chapter.

Restriction factors and antiviral antagonists

Restriction factors are germ-line encoded factors that mediate innate immune responses, in a cell-intrinsic manner. Their function is to detect and respond to viral infection without previous exposure to the pathogen. Thus, their main biological function is to block viral replication. Most of the known restriction factors have a viral antagonist, a viral protein that has evolved to evade the restriction factor dependent innate response. Therefore, restriction factors show evolutionary 'signatures' of genetic conflict, defined as positive selection towards the mutations that confer a fitness advantage for the host under pathogen pressure. While the restriction factor exerts selective pressure on viral replication, the virulent pathogen exerts fitness cost on the host. Thus, while mutations that allow the restriction factor to block the virus are preferentially inherited, the virus in turn evolves specifically to escape the new restriction factor. Finally both, host and virus have evolved. Indeed, almost all restriction factors contain genetic signature of this "arms race" [115, 116].

A common feature of restriction factors and their viral antagonists is their direct interaction, which determines their co-evolution. The identification of domains of interaction is clearly important for understanding viruses' evolution in humans and it might also contribute to the design of drugs to target and block viral infection. However, due to the higher viral mutation rate, the virus eventually evolves resistance mechanisms. Due to the tight relation between the restriction factor and the viral antagonists, specific viral inhibition without impacting host functions is difficult to achieve.

Among the different mechanisms adopted by viruses to escape host restrictions, the degradation of SAMHD1 by Vpx is particularly interesting. The HIV-2 accessory protein Vpx, which is absent in HIV-1, targets the host restriction factor SAMHD1 to degradation by the proteasome. Vpx directly binds SAMHD1 and the Cul4-DDB1-DCAF1 E3 ligase complex, which ubiquitinates SAMHD1 for proteasomal degradation [117, 118]. Many viral antagonists share the same mechanism of targeting restrictions factors for proteasomal degradation[119, 120]. Others antagonists work by mimicking the restriction factor substrates [121], by protein sequestration and by subcellular re-localization [122, 123].

Restriction factors can be induced by IFN-I, are directly induced by the virus or are constitutively expressed such as APOBEC3 [124, 125]. The latter example suggests an IFN-I independent, more ancient role for some restriction factors in protecting the host genome from viral invasion.

However, many, but not all, restriction factors are ISGs and several overexpression- or silencing-based *in vitro* screens of ISGs- have been performed to understand their antiviral functions. Only few genes have been fully characterized *in vivo* and overall ISGs seem to target conserved phases of the viral replication cycle in the host [18, 126]. However, ISGs probably exert a more specific rather than broad antiviral activity as demonstrated upon challenge with several human and animal viruses [112]. However, combined deletion of pairs of ISGs has demonstrated considerable redundancy in the ISGs effector mechanisms [112, 127]. These restriction factors, IFN-I induced, act at different levels such as viral fusion, remodeling of the

cytoskeleton, post-transcriptional regulation as well as post-translational modifications. Dynamin Like GTPase 1 (MX1) was one of the first ISGs to be identified for its strong antiviral activity during viral entry [128, 129]. MX1 is found to be a potent cell-restriction factor against a broad range of pathogenic viruses, while its homologue MX2 has been recently identified as a potent HIV restriction factor [130-132]. The mechanism of antiviral activity of both MX1 and MX2 is similar. They act at the level of nuclear entry and prevent the viral cDNA to reach the host DNA and thus prevent its integration, a fundamental step of the HIV replication cycle [128, 129, 133]. The antiviral mechanism of MX2 is proposed to be CypA-dependent. Indeed silencing of CypA or binding of CypA to the viral capsid prevent MX2 antiviral restriction [134].

In the context of HIV infection, other ISGs have been described to block HIV-1 viral fusion such as IFITM2 and IFITM3 [135-137]. While IRF1, IRF7, UNC84B, RIG-I [112], tetherin [138], TIM-1 [139], APOBEC3G [140], TRIM5a [141, 142] and ISG15 [143] interfere with HIV replication and budding (Fig.7). However, some ISGs (ADAR, FAM46C, LY6E, MCOLN2) have been demonstrated to enhance viral replication, proving the duplicity of IFN functions as further discussed in the manuscript.

2.6.2 Type-I-Interferonopathies

The detrimental effect of IFN-I in the mammalian system is not a recent concept and has been reported as early as 1980 [144]. However, it was only recently, in 2011, that Mendelian disorders such as the Aicardi-Goutières syndrome (AGS), spondyloenchondrodysplasia, and cases of systemic lupus erythematosus (SLE) with complement deficiency, were grouped as interferonopathies for which IFN-I up-regulation is their common pathological feature [145].

The classification of interferonopathies coincides with the great progress in the understanding of the crosstalk between nucleic acid sensing, innate immune responses and IFN signaling pathways.

Type I interferonopathies are characterized by overactive innate signaling with devastating inflammatory consequences on the adaptive system that eventually lead to the development of autoimmunity [145]. Aberrant IFN-I production and development of type I interferonopathies are proposed to depend on genetic mutations which leads to several mechanisms such as: (1) accumulation of nucleic acids in the cytosol due to deficient clearance (*e.g.* TREX1) or oversupply of nucleotides (*e.g.* SAMHD1), (2) constitutive, ligand-independent activation of nucleic acid sensors or adaptors (*e.g.* STING, DDX58), (3) enhanced response to ligand (*e.g.* IFIH1), (4) modification of nucleic acid content (*e.g.* RNASEH2, ADAR1), (5) defective negative regulation (*e.g.* ISG15) or other components of the type I IFN signaling pathways [146].

All the patients carrying a loss of function mutation in one of the above reported genes, showed an increased in IFN-I signature in peripheral blood [146].

However, as there is clinical overlap between the different disorders, such as for SAVI and AGS, different interferonopathies might manifest distinctly. For example,

SAVI patients do not show a neurological disorder but they have been reported with pulmonary disorders, while AGS patients show strong neurological disorders [147]. The phenotypic differences observed among individuals might be explained by the diverse functional activities of the above reported molecules, their tissue specific expression levels and patterns of gene regulation.

2.7 **Biology of HIV-1 and HIV-2**

2.7.1 General HIV-1 and HIV-2 innate immune extrinsic regulation of adaptive immunity

The human immunodeficiency virus (HIV) is a diploid ssRNA retrovirus with a strong tropism for CD4+ T cells. After HIV entry into target cells, the viral ssRNA is reverse transcribed into ssDNA by the HIV-encoded reverse transcriptase [148]. This process occurs in the capsid core, where viral integrase then binds specifically the full-length HIV-1 DNA ends to form a pre-integration complex that ensures viral DNA integration into the host genome [149]. However, only few copies of viral DNA integrate, and the majority of viral DNA remains in the cytosol available for innate sensing unless clearance by host enzymes occurs [150]. This makes HIV an attractive model system to study the importance of cytosolic DNA sensors for viral infections.

In nature, two types of HIV have been described: HIV-1 [151, 152] and HIV-2 [153, 154]. HIV-1 is closely related to the simian immunodeficiency virus (SIV) from chimpanzees. It has spread worldwide and 98% of untreated HIV-1-infected people progress to develop the Acquired Immunodeficiency Syndrome (AIDS).

HIV-1 has been isolated for the first time in 1983 [152, 155], while the related HIV-2 virus was identified in 1986. It has been described as the causative agent of AIDS in 1981 and it is responsible for the pandemic observed since the 1980s. HIV-2 is closely related to SIV from sooty mangabeys. It is mainly restricted to West Africa and much less pathogenic than HIV-1 [156, 157]. Even though the two HIVs share many biological features, such as the ability to infect CD4+ T cells and a high propensity of genetic variability, most of HIV-2 infected people become long-term-non-progressors (LTNP) and less than 25% of untreated HIV-2 infected people progress to a disease which is clinically indistinguishable from the AIDS caused by HIV-1 [158] [159].

Understanding why HIV-2 infection is less pathogenic and better controlled by the immune system can provide insights into HIV-1 related diseases [156]. Several studies have investigated the HIV-2 specific immune response, suggesting that HIV-2 viral control is associated with high numbers of polyfunctional HIV-Gag-specific CD8+ T cells. Similarly, the frequency of HIV specific CD4+ T cells is increased in HIV-2 patients compared to HIV-1 infected subjects at the same stage of disease. Moreover, increased T cell responses correlate with lower viral replication and good prognosis [160-164]. Finally, HIV-1 individuals dually infected with HIV-2 seem to progress slower to AIDS as compared to individuals infected only by HIV-1, suggesting a level of cross-protection that may be immune in nature [165] (Fig.8). Overall, these observations suggest that the human immune system is capable of

mounting a more effective immune response against HIV-2 than HIV-1. However, how the immune system contributes to the control of HIV-2 infection is not well understood yet.

First, I will present the genome organization and replication cycle of HIV-1 and HIV-2, followed by a description of the physiopathology of HIV-1 and HIV-2 in humans, emphasising the similarities and differences between the two viruses.

2.7.2 HIV-1 vs HIV-2 structure

HIV-1 and HIV-2 are lentiviruses that belong to the Orthoretrovirinae family, a subfamily of the Retroviridae. Lentiviruses are characterized by high spontaneous mutations rates and slow disease progression in the infected host. Their transmission is only possible through the exchange of body fluids and, most importantly, they cannot be eradicated from infected cells. Lentiviruses, unlike other retroviruses, are characterized by their ability to infect non-dividing cells, particularly of the mononuclear phagocyte lineage [166]. Due to their rather flexible genome and their potential of infecting many forms of non dividing cells, lentiviruses have become one of the most widely used vectors for gene transfer.

HIV is an obligate intracellular parasite, which requires reverse transcription of the viral genome for its replication. Thus, it exists either as a viral particle (virion), budding from the plasma membrane of an infected cell, or as a provirus, where its viral DNA has integrated into the host genome.

At the structural level, HIV virions have a spherical morphology with a diameter of around 100 nm. They are composed of a nucleoprotein core surrounded by a host cell derived envelope which carries surface and transmembrane glycoproteins (gp120 and gp41 Env, respectively for HIV-1) [167]. The viral core contains an electron dense p24 Gag capsid protein and encloses two copies of single-stranded genomic viral RNA. Its genome is stabilised by RNA-binding proteins and multiple complementary nucleic acid regions. The viral enzymes (RT, RNase, H and integrase, IN), tRNA and some accessory proteins are also contained in the core of the viral particle [166]. Moreover, virions may contain other molecules (e.g. signaling molecules, etc...) from the host cell [168].

While HIV-1 and HIV-2 are similar in structure some minor differences remain. While gp160 is the precursor for the derived glycoproteins gp120 and gp41 of HIV-1, the HIV-2 glycoproteins gp125 and gp36 originate from the smaller precursors gp140. These differences are due to differences in gene size [169] and HIV-2 glycoproteins have a lower affinity for the CD4 receptor [170]. Also, the capsid protein of HIV-2 is slightly larger than p24 of HIV-1 and is thus named p26.

2.7.3 The viral genome of HIV-1 and HIV-2

The viral genome of HIV-1 is composed of diploid RNA with positive polarity and measures 9,2 kb in length. In comparison, the size of the HIV-2 genome is 9,671kb, 0,4kb more than HIV-1. This difference can be explained in parts by differences in

length of the LTR (long terminal repeat) sequences, flanking each end of the viral genome. They are *cis*-active elements and are required during replication. It has been shown that the viral DNA of HIV-1 is preferably integrated in the coding and transcriptionally active regions of the genome [171-173].
Like all known retroviruses, the HIV genome encodes for three major structural genes: *gag, env*, and *pol*. In the case of HIV-1, the structural components are derived from the *gag* gene, which encodes a Pr55gag precursor polyprotein. It is cleaved by the HIV-1 protease (encoded by the *pol* gene) into its mature products: matrix (MA or p17), capsid (CA or p24), nucleocapsid (NC, p7), p6 and two spacer proteins (p1 and p2) [174]. The viral enzymes derive from the cleavage of the polyprotein Pr160Gag/Pol generated by ribosomal frame-shifting. Also the envelope proteins are derived from a polyprotein precursor (gp160 Env). However, unlike Gag and Pol, Env is processed by a cellular protease during trafficking to the cell surface, a process that generates surface gp120 and transmembrane gp41 Env proteins [174].

In addition to enzymes and structural proteins, HIV-1 also encodes for a number of regulatory and accessory proteins. Tat is a critical transcriptional activator that binds to a secondary RNA structure, named TAR (Trans-Activation Regulatory element) located at 5'-end of all viral transcripts. It is a crucial driver of viral gene expression [175]. The second regulatory protein, Rev plays a major role in the transport of viral RNAs from the nucleus to the cytoplasm [176]. Vpu, Vif, Vpr and Nef have been termed "accessory" proteins to reflect the fact that they are dispensable for virus replication *in vitro*. The HIV-1 accessory proteins have been studied for their mechanisms to counteract immune detection by the host. Indeed, Nef induces decreased expression of the CD4 receptor, MHC-I and MHC-II, as well as the TCR [177-181]. Vif inhibits the antiviral activity of APOBEC3G [181] and Vpu antagonises the function of Tetherin, also termed BST2. Tetherin induces the retention of virions to the cell membrane [138] while Vpu is involved in the degradation of the CD4 receptor [182]. Vpr plays a role in viral replication by interfering with the G2 phase of the cell cycle. It has been observed that expression of Vpr might favor macrophage infection [183-187].

The overall organization of the genome of HIV-2 is similar to that of HIV-1. Both viruses are 60% homologous with respect to genes such as Gag and Pol and 30 to 40% with respect to other genes and LTRs. The majority of HIV-2 proteins are functionally similar to those of HIV-1. As for HIV-1, Tat is required for expression of the HIV-2 genome transcription [188]. The HIV-2 precursors Gag and Pol seem to require the same process of cleavage observed for HIV-1 and generate similar functional proteins, such as RT and EN (Fig.9).

However, the most important difference between the two strains is the accessory protein Vpx. While HIV-1 encodes for Vpr, which is absent in HIV-2, Vpx is encoded only in HIV-2 but not in HIV-1. Interestingly, Vpx seems to have a different role than Vpr. Recently, Vpx has been extensively studied due to its essential role in HIV replication in dendritic cells, as will be discussed in section 2.7.6.

2.7.4 HIV replication cycle

The HIV replication cycle can be divided into an early and a late phase. The early phase includes the events that occur between virus attachment to the host cell surface and the integration of the viral DNA into the host genome. These early events include virus binding to cell surface receptors, cell entry, reverse transcription of the viral RNA to DNA, uncoating of the viral capsid, nuclear import of viral DNA and DNA integration. The late phase includes the events that regulate viral gene expression to the release and maturation of new virions. It encompasses the transcription of viral genes, export of the viral RNAs from the nucleus to the cytoplasm, translation of viral RNAs to produce the Gag polyprotein precursor (Pr55Gag), the GagPol polyprotein precursor, the viral envelope glycoproteins (Env glycoproteins), and the regulatory and accessory viral proteins, trafficking of the Gag and GagPol precursors and of the Env glycoproteins to the plasma membrane, assembly of the Gag and GagPol polyproteins at the plasma membrane, encapsidation of the viral RNA genome by the assembling Gag hexagonal lattice structures, incorporation of the viral Env glycoproteins, budding off of the new virions from the infected cell and particle maturation.

The first step in the infection of a cell by HIV-1 is the interaction of gp120 with a receptor expressed on the surface of a target cell. Based on their affinity to cell receptors and their function, these glycoproteins provide the tropism of the virus to certain cells, Gp120 has a high affinity for the cellular receptor CD4 and the co-receptors CCR5 or CXCR4. The glycoprotein gp41 then facilitates the fusion of viral and cell membranes by mechanically bringing the two membranes together. After the fusion event, the viral capsid is released into the cell cytoplasm while the viral envelope remains at the level of the cell membrane [167, 189-191]. Viral nucleoprotein complexes form and the reverse transcription complex begins the synthesis of viral DNA using the available cytosolic nucleotides as building blocks. At the end of this process, a viral double-stranded DNA molecule is synthesized, associated with cellular proteins and viral proteins such as MA, RT, IN, NC and Vpr [192-194], together termed the pre-integration complex (PIC).

Once the PIC is generated, it enters the nucleus through the nuclear pore complex without disrupting the nuclear envelope, thus allowing HIV and related retroviruses to replicate in non-dividing cells [195]. However, the exact mechanism is still unknown. Once the complex reaches the nucleus, the viral integrase allows the insertion of viral DNA into the cellular genome [196]. After integration, the formed provirus can be transcriptionally inactive (latency) or enter a phase of active transcription of the viral genome, the beginning of the late phase of viral replication. While the 5'-LTR acts as a viral promoter, the 3'-LTR contains the polyadenylation and termination site required for generation of a functional mRNA. Transcription of the viral genome requires the recruitment of cellular components, such as RNA polymerase II, allowing for the initiation of transcription. The viral protein Tat enhances the efficiency of transcription initiation and elongation. The newly synthesized viral transcripts are spliced using the host cell machinery and transported into the cytosol, where Tat, Nef and Rev proteins are synthesized on ribosomes. The Rev protein is imported back into the nucleus and binds to unspliced RNA, genomic RNA encoding Gag and Pol. Here, Rev enables the transport of viral RNA into the cytoplasm. These transcripts for

structural and enzymatic proteins are translated into proteins at the ER, and are directed to the plasma membrane via the cellular secretion route. Budding of the virions occurs at the plasma membrane in lipid rafts, cholesterol rich regions. Here, viral envelope and Gag proteins interact with each other to initiate the assembly of the virus particle. Once the virions are released, the viral protease cleaves the Gag and Gag-Pol precursors, allowing for virion maturation and thus their infectivity [197].

The viral life cycle is similar for HIV-1 and HIV-2, however HIV-1 infected patients have a higher viral load than HIV-2 infected patients [198-202]. As an explanation, it was proposed that the replication of HIV-2 was slower than that of HIV-1 [200].

Another difference between HIV-1 and HIV-2 is in the use of their co-receptors. Numerous studies have demonstrated that HIV-2 can use alternative co-receptors other than CCR5 or CXCR4 and that some isolates did not require interaction with the CD4 receptor [203]. Thus in the context of DCs, it has been shown that CCR1 is used as an alternative co-receptor for HIV-2 [204, 205]. In other cell types, HIV-2 uses other co-receptors such as CCR2b, CCR3, CCR8, CXCR2, CX3CR1, GPR1, GPR15, and STRL33 [203-211]. It has been proposed that the lower number of glycosylation sites on the V3 loop region of the gp140 of HIV-2, compare to gp160 of HIV-1, allows for a more accessible configuration and for interaction with a wider range of co-receptors [212].

2.7.5 The physiopathology of HIV-1 vs HIV-2

HIV-1, in the absence of treatment, leads to the onset of AIDS in 98% of human cases. Chronic infection with HIV leads to progressive depletion of CD4+ T lymphocytes, disrupting the immune system and leaving the body vulnerable to other infections such as *mycobacteria*, *cryptococcus*, yeast or oncogenic viruses. HIV-1 infection is characterized by three phases defined by the viral load and the number of CD4+ T cells circulating in the blood: 1) the primary infection or acute phase occurs in the first weeks after HIV infection, followed by 2) the asymptomatic phase or clinical latency period that can last several years and 3) the symptomatic phase corresponding to AIDS [213], as it will be discussed in more details in the next sessions.

2.7.5.1 Primary infection or acute phase

Following infection, there is a period of a few days, known as the “eclipse phase”, before viral RNA becomes detectable in the plasma. The initial burst of virus replication during primary HIV-1 infection (PHI), regardless of the route of virus transmission, likely occurs in the gut-associated lymphoid tissue (GALT) [214], where activated $CD4^+CCR5^+$ T cells are present in high numbers [215-217]. During HIV-1 replication in the GALT and, later, in other lymphoid tissues, the plasma viremia (defined as number of HIV RNA copies/ml) increases exponentially and reaches a peak of up to $>10^6$ copies/ml, 14-28 days after initial infection in humans or experimental SIV infection of macaques [218, 219]. At the peak of viremia, $CD4^+$ T cell numbers are already decreased, but return to near normal levels in peripheral

blood later during infection (although not in the GALT) [214, 220, 221]. In the following, the virus spreads widely in the body and forms a latent viral reservoir in lymphoid organs such as thymus, spleen, lymph nodes and gut. During this phase, a HIV-1 specific immune response develops and ensures seroconversion (production of anti-HIV-1 specific antibodies) and virus-specific T cell proliferation. This immune response reduces viral replication and partially restores CD4 + T cells numbers [222, 223].

2.7.5.2 The asymptomatic phase or clinically latent phase

During the acute phase, the activation of both the innate and the adaptive responses causes a significant decrease of virus levels over a 12-20 week period before viremia reaches a more stable level, known as the viral set point [224-227]. The asymptomatic phase can last several years and varies depending on the patient. During this period, the immune response is biased towards Th2 rather than Th1, a shift that has been suggested to play a central role in the progression of HIV infection towards AIDS [228]. However conflicting evidence has accumulated and it remains to be determined whether this provocative hypothesis holds true. With time, the number of CD4+ T lymphocytes in the blood slightly and gradually decreases, due to multifactorial reasons. On the one hand, the elimination of infected cells and on the other hand the large amount of interferon chronically secreted by the immune system both play a role with in the loss of CD4+ T lymphocytes [227, 229-231]. It will be discussed in the following chapter 2.8.

2.7.5.3 The symptomatic phase or AIDS

The final stage of HIV infection is restricted to individuals with peripheral CD4+ T cell counts <200 cells/µl and/or those with an AIDS-defining clinical illness, such as opportunistic infections or tumors. As a consequence of the complete destruction of the lymphoid tissue architecture, which is typically replaced by fibrotic tissue, most of the detected virus is cell-associated [232]. This advanced stage of HIV disease is characterized by profound immune suppression and a loss of anti-HIV-specific cytotoxic T lymphocytes (CTLs) and neutralizing antibodies (Nabs) [233-235].

However, there are exceptions to this typical pathology such as in the Exposed-Uninfected Seronegative individuals (ESN), individuals who are either naturally resistant to HIV, and those who, when infected, spontaneously control either their disease progression and loss of CD4+ T cell counts or their viremia levels. We generally refer to the former group as LTNP, whereas the latter are commonly referred to as Elite or HIV Controllers (ELC/HIC). The ESN phenotype is partially explained by the presence of a 32 base pair deletion mutation of CCR5 in homozygosity (CCR5-Δ32), the viral entry co-receptor indispensable for virus infection [236, 237]. The mutation renders the molecule misfolded and it is absent from the cell surface. However, a substantial fraction of ESN that do not carry this mutation have been described some of which had developed resistance to infection [238], e.g. by producing mucosal IgA against gp41 Env or “natural” anti-CCR5 Ab [239, 240].

An estimated <2% of all infected individuals are LNTP and maintain CD4+ T cells counts >500 cells/µl for at least 7 years post-infection in the absence of anti-retrovial therapy (cART) [241]. In addition to the association with CCR5-Δ32 heterozygosity, other genetic mutations, including CCR2-64I (in linkage disequilibrium with a mutation in the CCR5 promoter region) and several single nucleotide polymorphisms (SNPs) in the MHC Class I, II and III locus have been suggested to contribute to non-progression [242]. Another 1-2% of all infected individuals are ELC/HIC and spontaneously maintain their viremia levels <50 or <2,000 copies of RNA/ml of plasma for at least 12 months [243]. In both populations, the viral reservoir (defined as copies of HIV DNA/10^6 PBMC or equivalent tissue-associated HIV DNA load) is significantly smaller compared to the majority of HIV patients [244-246].

2.7.6 cGAS-STING axis in HIV infection in DCs

Insights into possible between HIV-1 and HIV-2 immune differences originated from the study of DCs. Previous studies have demonstrated that monocyte-derived DCs (MDDCs) are highly refractory to HIV-1 infection [99, 247]. This is due to the presence of the restriction factor SAMHD1 [117, 118, 248], a gene associated with the AGS [249, 250]. SAMHD1 is the only known eukaryotic deoxynucleoside triphosphate triphosphohydrolase (dNTPase). The enzyme is allosterically activated by GTP and selectively cleaves the dATP, dCTP, dTTP and dGTP but not ribonucleotide triphosphates, resulting in the degradation of the cytosolic pool of dNTPs which leads to the restriction of HIV-1 replication at the reverse transcription step [251]. The lack of dNTPs and efficient reverse transcription of HIV-1 prevents the synthesis of viral dsDNA and thus detection of the virus by DCs [247]. In the absence of HIV-1 sensing, MDDCs do not up-regulate co-stimulatory molecules and do not secrete IFN-I [99, 247].

However, the innate response in MDDCs also induced the production IFN-I and ISGs. The mechanism requires the expression of neo-synthesized Gag protein of HIV-1 and interaction with Cyclophilin A (CypA). CypA is a peptididyl prolylisomerase that binds to the viral capsid and is incorporated into viral particles. It is shown that CypA can promote HIV-1 infectivity and replication, although further studies are required to underlying the mechanism [252, 253]. In comparison, HIV-2 is able to productively infect MDDCs, thanks to the presence of the accessory protein Vpx, which inhibits SAMHD1 and which is absent in HIV-1 [254]. In fact, when Vpx protein is added to HIV-1, the virus can infect MDDCs much more efficiently which leads to induction of DC activation and the production of IFN-I [247, 255] (Fig.10). HIV-2 infection of MDDCs similarly activates the DCs and leads to production of IFN-I. This innate recognition of HIV-2 by MDDCs induces better activation of CD4+ and CD8+ T cells, as a result of increased antigen presentation and expression of co-stimulatory molecules in DCs. Simultaneously DCs also induce a partially protective antiviral response in bystander CD4+ T cells, at least through the production of IFN-I [247].

The mechanism of HIV sensing in DCs relies on the detection of viral cDNA in the cytosol. HIV-1 and HIV-2 capsids play an important role in detection of the newly synthesized viral DNA by innate sensors before integration. HIV has evolved mechanisms to escape innate sensing by interacting with host proteins such as CypA

or CPSF6. CypA and CPSF6 prevent premature reverse transcription of HIV-1 in macrophages and thus enable the virus to escape from innate sensing [256, 257]. Viral DNA is detected by the cytosolic DNA sensor cyclic GMP/AMP synthase (cGAS) [59, 99]. cGAS, after binding to the viral DNA, produces cGAMP which interacts with STING leading to the activation of MDDCs and production of IFN-I [59, 99], as discussed earlier.

Of note, the ability of HIV-2 to infect MDDCs was recently challenged by the demonstration that wild-type HIV-2 but not HIV-1 is inhibited at the level of viral fusion [258]. Nonetheless, unpublished results from our lab (Aymeric Silvin et al., manuscript in revision) clearly confirm that primary dendritic cells isolated from blood are highly susceptible to HIV-2 infection, and not HIV-1, due to SAMHD1. Our preliminary evidence indicates that the recently reported block of HIV-2 entry in MDDCs is a side effect of in vitro culture conditions. Thus, the increased ability of HIV-2 over HIV-1 to efficiently infect DCs stands as a valid observation with primary cells and fully wild-type virus, and one of the most striking difference between HIV-1 and HIV-2.

2.7.7 Role of CD4+T lymphocytes during HIV infection

Almost three decades of studies have focused on understanding of how HIV interferes and destroys CD4+ T cells and the unique feature of HIV compared to other human pathogens. Adaptive immune responses elicited by CD4+ T cells are a mechanism evolved by vertebrates to eliminate pathogens in a pathogen-specific manner and to generate an immunological memory. There is ample evidence that CD4+ T cells play a crucial role in the defense against HIV. While maintenance of a CD4+ T cell pool is a critical factor for the slow progression of HIV infection [259]. People infected HIV-1 or -2 who maintain a high CD4+ T cell response against HIV progress more slowly towards acquired immune acquired syndromes (AIDS) [162, 260]. Depletion of CD4+ T cells in macaques infected with SIV amplified the progression to disease, suggesting an active role of CD4+ T cells during infection [261]. During the acute phase the number of memory CD4+ T cells is strongly decreased in the lymphoid system, particularly in the intestine [221, 262]. The loss of CD4+ T cells correlates with the expression of PD-1, a receptor triggering apoptotic cell death [263-265]. The expression of PD-1 correlates with the expression of the transcription factor BLIMP and a lower production of IL-2 [266, 267].

CD4+ T cells might also play a more active role in the defense against HIV. Early studies have demonstrated that CD4+ T cells of HIV-infected patients are unable to proliferate in response to antigens [268]. However, HIV-specific CD4+ T cells are present throughout the infection, though in small numbers [269]. Challenging T cells with a broad spectrum of HIV-derived epitopes showed that HIV-specific CD4+ T cells are directed against the majority of viral proteins with a preponderance of CD4+ T cells specific for Gag and Nef [270]. Further, it has been demonstrated that antiretroviral treatments, given very early during infection, allow for the development of a HIV-1-specific CD4+ T cells response [222]. Further, CD4+ T cells are required for the HIV-specific CD8+ T cell response [259], which dominates the T cell response in patients infected with HIV. The importance of CD4+ T cells in the

defense against HIV is possibly due to their role as cytokine producers and the subsequent activation of other arms of the immune system. IL- 21 is produced by CD4+ T cells and this cytokine which may induce cell proliferation and maturation of CD8+ T cells and B cells [271]. Polyfunctional CD4+ T cells, cells that have acquired the ability to produce many, functionally distinct cytokines, in the mucosal membranes correlated with a slower progression of AIDS [272]. Other studies suggest the presence of CD4+ T cells expressing the cytotoxic molecules perforin and granzyme A as a factor to predict disease outcome [273]. In rhesus monkeys, predominantly Th17 T cells are infected with SIV, which might explain the observed decrease of this cell type in peripheral blood [274]. Th17 cells are actively involved in inflammation and might contribute to viral clearance. Finally, little is known about the role of Tregs in HIV-induced immunopathology although the crucial role of Tregs in the homeostasis of immune response has been long known.

2.7.8 STING-independent IFI16 sensing of abortive HIV replication in CD4+T cells

In the last decade, HIV research has also benefitted from recent progress in the field of innate sensors, which has opened up opportunities to elucidate molecular aspects of the HIV pathogenesis. For a long time, it had been proposed that the loss of CD4+ T cells in HIV infection was due to viral cytopathic effects in activated CD4+ T cells. Using immortalized or activated CD4+ T cells from peripheral blood of HIV patients, apoptosis was found to be the mechanism for CD4+ T cells loss *in vitro* [275]. It was shown that the cell death by apoptosis is mediated by caspase-3 activation [39, 276-280] although the mechanism of viral sensing is not yet known. Interestingly, *in vivo* studies suggest that the percentage of activated CD4+ T cells are too small to justify the massive loss of CD4+ T cells that leads to disease progression [281-283]. It was reported that lymphoid tissue resident, bystander CD4+ T cells are the main population that undergo cell death [281, 284, 285]. Only in the last five years the use of *ex vivo* HLCA system [286] has improved our understanding of the mechanism of CD4+ T cell death during HIV infection. HIV mainly replicates in secondary lymphoid tissues [287] where only 5% of CD4+ T cells are permissive to HIV infection. The remaining 95% are not permissive to infection, probably due to their resting state [288]. Recently an alternative mechanism to apoptosis mediated loss of CD4+ T cells has been proposed. A possible, abortive HIV infection and replication in “bystander” CD4+ T cells could produce viral DNA long enough (500 bps) to be sensed by IFI16 [40], a cytosolic DNA sensor described above. IFI16 in turn activates caspase-1 and a NLR3-independent ASC-dependent inflammasome pathway leading to massive cell death, known as pyroptosis [39] (Fig.11). Cell death, along with the release of pro-inflammatory cytokines such as IL-1b establishes a vicious and detrimental cycle of death [288]. Together, these findings put a different light on the proposed cytotoxic effect of HIV infection in CD4+ T cells. Rather, this is a unique example of a powerful innate immune defense mechanism that might be conserved during evolution to prevent HIV spread through a "form of cellular suicide".

A more recent study tried to shed light on the susceptibility of different CD4+ T cell subsets to HIV infection using *in vitro* models. It has been shown that blood CD4+ T

cells are in a more profound bystander state than their counterparts in lymphoid organs. Neither pyroptosis nor apoptosis could be detected when these cells are infected with HIV-1 [289]. As outlined above the restriction factor responsible for the block of HIV infection is SAMHD1 [290]. Lower expression levels of innate sensors, such as IFI16, STING, cGAS and also components of the inflammasome in peripheral blood compared to lymphoid tissue CD4+ T cells, might explain the differences in restriction of HIV-infection. Cell-free infection of peripheral CD4+ T lymphocytes might not be sufficient to produce enough viral DNA to trigger innate sensors and thus pyroptosis. Another mechanism such as exosome-mediated cGAMP release directly into the cytosol from infected surrounding cells [168, 291] could contribute to activate other innate sensors, such as STING, in CD4+ T cells. Further studies are needed to elucidate HIV sensing in different CD4+ T cell subsets.

2.7.9 Negative regulation of STING-dependent innate response against HIV-1

On the contrary to other viruses, it appears that HIV has evolved less efficiently escape mechanisms to avoid the host innate immune response but it has successfully evolved to exploit them to complete its life cycle [292, 293]. In fact, it has been demonstrated that HIV-1 exploits TREX1 exonuclease activity to escape the innate immune response mediated by the cGAS-STING axis. TREX1 is the most abundant DNase in mammals (also known as DNase III) and is ubiquitously expressed at high levels in immune cells [294]. It has been proposed that TREX1 may be part of the endoplasmic-reticulum-associated SET complex which binds to the HIV-pre-integration complex to prevent viral DNA auto-integration, where TREX1 degrades bulk viral DNA. Experiments performed in Trex-/- MEFs showed that HIV-1 DNA is sensed and triggers type I IFN production even in absence of TREX1 [150]. Therefore, HIV-1 exploits TREX1 function in immune cells to exert a negative regulation on the intrinsic innate response. While formentioned finding in MEFs has been validated in human peripheral blood CD4+ T cells and monocytes-derived macrophages (MDMs) [150], proving its physiological relevance during HIV infection, and the role of TREX1 in human CD4+ T cells and DCs has not been demonstrated to-date. However, as described above, DCs are resistant to HIV-1 infection due to SAMHD1-mediated depletion of the dNTP pool in the cytosol. Indeed, the absence of Vpx in HIV-1 could be evolutionarily interpreted as 1) the inability of HIV-1 to inhibit SAMHD1-mediated restriction or 2) the acquired ability of HIV-1 to avoid the antiviral response in SAMHD1 expressing cells. In any case, resting CD4+ T cells cannot be infected by HIV-1 due to their SAMHD1 activity, however it is not known why TREX1 does not prevent IFI16-mediated pyroptosis in non-permissive lymphoid CD4+ T cells.

Another example of the ability of HIV-1 to take advantage of host restriction is NLRX1, which promotes HIV-1 infection in different cells, including macrophages and DCs. NLRX1 is a mitochondrial NOD-like receptor known to attenuate IFN signaling interfering with the RIG-I/MAVS and TRAF/IKK axis [295, 296], other than inducing ROS [297, 298] and autophagy [299]. NLRX1 was first identified as a host factor required for the early steps of HIV-1 infection in a siRNA-based screen [292], but its function in HIV-1 infection was not further studied. Recently a study

focused on understanding the kinetics of HIV dissemination and infection, using a rhesus monkey SIV mucosal infection model. The study reported that increased expression of NLRX1 correlates with decreased transcription of ISGs, in tissues positive for viral RNA [300]. Moreover, key antiviral ISGs were detected only at day 10 after inoculation [300]. A second study elucidated the mechanism by which NLRX1 suppresses IFN-I production after HIV infection. Here, the authors propose that NLRX1 directly interacts with STING in the MAMs, which then blocks STING-TBK1 association. Thus, NLRX1 is found to be a negative regulator of STING-dependent antiviral signaling [301]. These findings partially address the question whether HIV-1 evolutionarily adapted to exploit host factors for its survival and contribute to clarify the complex puzzle of HIV-1 infection and pathogenesis in human immune cells.

2.8 Dual Impact of IFN-I on CD4+ T cells priming during HIV infection

2.8.1 Impact of IFN-I on CD4+ T cell polarization

IFN-I is an important signal during T lymphocyte activation, since it contributes to CD4+ T cell differentiation into Th1 effector cells [6, 302]. Results from mouse models suggest that IFN-I is required for a fully functional T cell immune response against viruses that include CD4+ T, CD8+ T, B and NK cells [303]. In particular, the role of IFN-I in the generation of memory CD8+ T responses is well established in the ECMV model [304]. However, while triggering an antiviral state, large amount of IFN-I limit the amount of viral antigen, which in turn compromises its capacity to induce an adequate adaptive immune response. In fact, it has been shown that excessive and prolonged exposure to IFN-I can inhibit T cell functions [305, 306]. For instance, IFN-I can induce an anti-proliferative state and pro-apoptotic programs in T cells. Also, the expression of death receptors and their respective ligands, such as TRAIL, FAS and DR5, is positively regulated by IFN, and can lead to apoptosis of CD4+T, CD8+T and B cells [229, 307, 308].

It is believed that the timing of IFN-I stimulation for CD4+ T cells is critical to determine whether CD4+ T cell survive and proliferate or become exhausted and die by apoptosis. It has been proposed that concomitant IFN-I and TCR signaling induces STAT-4 dependent pro-survival, proliferative and effector cell differentiation, [309, 310]. On the other hand, if IFN-I signaling precedes TCR engagement, STAT-1-dependent anti-proliferative and pro-apoptotic programs are induced [311-313].

However, the impact of IFN-I on the quality of the resulting CD4+ T cell response is less clear. It was described that IFN-I modulated the quality and the shape of naïve CD4+ T cell polarization into Th0, Th1, Th2 or Th17 cells in vitro without abrogating their expected T-helper differentiation [314].

2.8.2 Impact of IFN-I on susceptibility to HIV- infection in CD4+ T cells

IFN-I production can exert its antiviral activity in an autocrine and paracrine manner. In vitro experiments have shown that IFN-I can influence the infection efficiency of primary CD4+ T cells by HIV-1 and HIV-2 [131, 247, 314]. IFN-I induces hundreds of ISGs that encode for proteins, including restriction factors, which have been mostly studied for their impact on viral replication [112], as outlined above. Many of the known HIV restriction factors, for instance, are in fact also ISGs: MXB/MX2 [131, 132], SAMHD1 [117, 118] and tetherin [315, 316]. However, which ISGs are responsible for inhibition of HIV infection in primary CD4+ T cells is still incompletely understood with MX2 not being sufficient to explain the overall inhibition. In addition to IFN-I, the susceptibility to infection is also dependent on the CD4+ T cell being a memory or effector cell [317, 318], or the in vitro polarization assay used to generate helper T cells in vitro [314]. In fact, it appears that cytokine-dependent T cell polarization and the IFN-I response are intertwined: there is a subset-specific (context-dependent) effect of IFN-I on its ability to impact HIV-1 and HIV-2 infection [314]. In this work, IFN-I induced less efficient resistance of CD4+ T cells to HIV-1 and HIV-2 in a Th17 context [314]. Interestingly, Th17 cells are preferentially depleted in the gut during HIV-1 infection, consistent with the lack of an effective IFN-I [216].

2.8.3 IFN contribution to HIV immunopathogenesis

In HIV infection, evaluating the positive or negative contribution of IFN-I remains a major question. It is likely that a dual scenario is triggered by IFN-I after HIV-1 infection. While IFN-I production during the active phase, early after HIV-1 infection, might induce partial protection due to a direct antiviral effect and ISGs induction, the persistence of the virus might lead to chronic IFN-I production that is thought to contribute to (or at least correlates with) the chronic overall immune activation state in HIV patients [319, 320]. Indeed, HIV-1 induced immunophatogenesis is characterized by high levels of IFN-I that are presumably mainly produced by pDCs [321]. Indeed, while HIV-1 poorly infects DCs [247] (as described previously), pDCs can sense cell-free virus or HIV-1 infected CD4+ T cells [322]. However, unlike myeloid DCs, sensing of HIV-1 by pDCs leads to the production of copious amounts of IFN-I and inflammatory cytokines. Interestingly, HIV-1 sensing does not trigger pDC maturation and consequently they cannot induce adaptive immune responses [323]. At the stage of chronic infection, HIV-specific CD4+ T lymphocytes display an impaired ability to produce cytokines such as IL-2 and IFNγ, and unregulated exhaustion markers such as PD-1 and have decreased proliferative capacity [324-327].

Recently, the role of IFN-I was experimentally addressed in rhesus macaques during SIV infection [328]. This study reports that on one hand IFNAR blockade reduces antiviral gene expression, increases viral reservoir size and accelerates CD4+ T cell depletion and progression to disease. On the other hand, the sustained administration of IFN-I triggers desensitization to IFN-I with reduced antiviral gene expression and an accelerated loss of CD4+ T cells. Thus, IFN-I can have opposite effects. It is likely

that the timing, duration and the source of type I IFN during SIV, HIV-1 and HIV-2 infection has a major effect on the disease outcome.

3 Rationale

Overall, the lab focuses on understanding the implication of the cGAS-STING innate immune signaling pathway in physiological processes or upon infection, in particular related to pathological condition as for HIV-1 and HIV-2 in DCs. A major question that arose from the initial work of the lab was that it is needed to better understand the subsequent CD4+ T cell responses in HIV-1 vs HIV-2 infection. To do so, efforts have been engaged to study both the *in vitro* priming of CD4+ T cells in HIV-1 vs HIV-2 conditions as well as to characterize the qualities of CD4+ T cells found in HIV-1 vs HIV-2 patients. The ultimate goal is to infer causal relationships between infection and sensing of the virus in DCs and the resulting properties of CD4+ T cells.

The main objective of this thesis is to determine the impact of the activities of the innate sensor STING in CD4+ T lymphocytes, in normal and pathological conditions. More specifically we asked two questions: 1) Can innate immune sensing through STING in DCs can function as an extrinsic mechanism to confer resistance to CD4 T cells? 2) What intrinsic role does STING have in CD4+ T cells and how does it relate to viral infection?

In order to determine the extrinsic role of STING in HIV resistance of CD4+ T cells, we setup a DC:T cell co-culture system to generate CD4+ T cells primed by HIV-2-infected DCs (T_{HIV-2}), HIV-1-infected DCs (T_{HIV-1}), or DCs activated by a series of synthetic reference stimuli. First, we characterized the cells in terms of their susceptibility to infection and T helper polarization. Next, to determine the underlying molecular mechanisms we generated unbiased transcriptional profiles of the cells and a gathered a list of candidate resistance factors in CD4+ T cells. The results will be presented in a first chapter entitled “Regulation of adaptive immunity by HIV sensing in dendritic cells.”

To address the cell-intrinsic role of STING in CD4+ T cells we studied CD4+ T cells harboring a STING gain-of-function mutation that has been identified in a non-consanguineous Caucasian family in a recent report. Patients carrying the mutation showed elevated levels of type I IFN signature in the serum and revealed a reduced fraction of memory T cells compared to age-matched controls. We developed an *in vitro* model using CD4+ T cells transduced with STING WT or other STING mutants to determine the molecular biology behind STING activity in CD4+ T cells. To assess its function on T cell biology, we evaluated the effect of different STING mutants on T cell proliferation. Finally, to investigate the physiological role of STING in CD4+ T cells, we used CD4+ T cells from STING-KO mice and compared to their proliferative capacity to WT CD4+ T cells in response to TCR activation. The results are presented here as manuscript entitled “Intrinsic anti-proliferative activity of the innate sensor STING in T lymphocytes.”

4 Results

4.1 Regulation of adaptive immunity by HIV sensing in dendritic cells

Silvia Cerboni[1], Santy Marques-Ladeira[1], Mathieu Maurin[1], Aurianne Lescure[2], Elaine Del Nery[2] and Nicolas Manel[1]

[1]Immunity and Cancer Department, Institut Curie, PSL Research University, INSERM U932, 75005 Paris, France.
[2]BioPhenics, Institut Curie, 75005 Paris, France.

4.1.1 HIV-2, but not HIV-1, induces activation and type I IFN production in MDDC

Since it is known that HIV-2 generally is better controlled by the immune system than HIV-1, we asked whether innate sensing by DCs contributes to achieve better virus control [160, 162-164]. Thus, we exposed MDDCs to HIV-1, HIV-2 or MVA or different ligands of nucleic acid sensors (poly(IC), poly(dG:dC), R848 as positive controls and measured the expression of the activation marker CD86 and production of pro-inflammatory cytokines. Confirming previous results [99, 247], we show that MDDCs become infected by HIV-2, but not HIV-1, using GFP-expressing lentiviruses (Fig.1A, C) 48hrs after infection. Accordingly, MDDCs upregulated CD86 in response to all control stimuli and HIV-2 but not to HIV-1 infection (Fig.1A, 1B). Next, we determined whether CD86 expression correlates with induction of type I IFN by measuring it in culture supernatants 24 and 48hrs after stimulation using a luciferase reporter cell line. We show that high amounts of type I IFN are produced by MDDCs after stimulation with poly(IC), poly(dG:dC) and MVA but not R848 (Fig.1D, 1E) already after 24hrs. Interestingly, MDDCs also produce type I IFN when infected with HIV-2 at 48 hours post infection but not upon HIV-1 infection.

To further delineate MDDC activation in our experimental model, we measured cytokine production by CBA at 48hrs. (1F-M). We confirm that MDDCs release high amount of the type I IFN-inducible cytokine IP-10 (Fig.1F), when stimulated with poly(IC), poly(dG:dC), MVA and HIV-2 while only moderate levels were detected in response to HIV-1 or R848 stimulation. However, R848 induced significant IL-6 (Fig.1G), IL-12p70 (Fig.1H) and TNF production (Fig.1I) while HIV-1 did not. MDDCs did not produce IL-10 and IL-1β in response to any of the used stimuli (Fig.1J, 1K). In conclusion, while HIV-1 had no measurable effect on activation and cytokine production by MDDCs, HIV-2 infection activated MDDCs similar to poly(IC), poly(dG:dC), MVA, but distinct from R848. Importantly HIV-2 infection also led to type I IFN production, although at later time points than control stimuli.

FIGURE 1

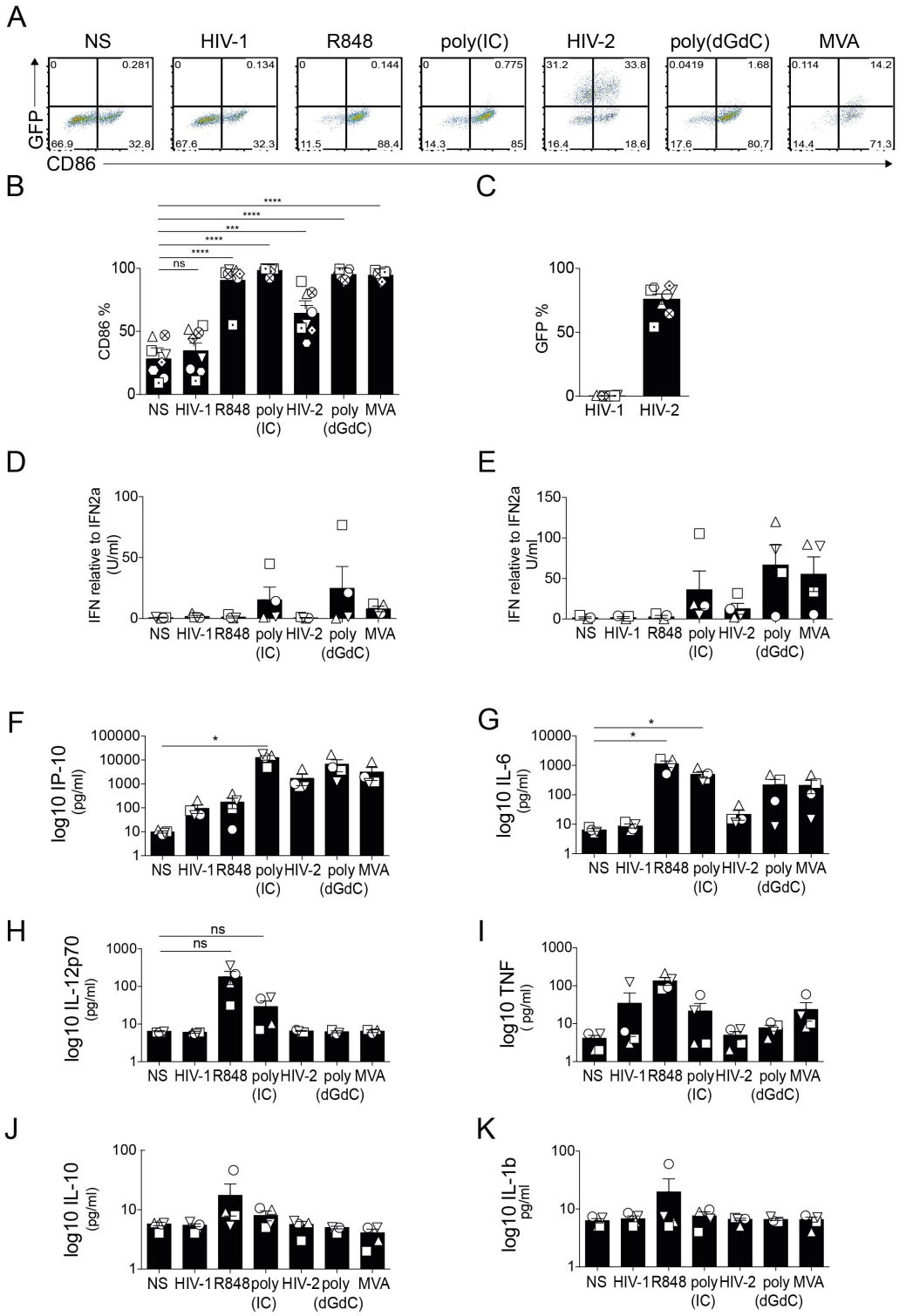
A
NS
HIV-1
R848
poly(IC)
HIV-2
poly(dGdC)
MVA
GFP
CD86
0
0.281
66.9
32.8
0
0.134
67.6
32.3
0
0.144
11.5
88.4
0
0.775
14.3
85
31.2
33.8
16.4
18.6
0.0419
1.68
17.6
80.7
0.114
14.2
14.4
71.3
B
CD86 %
ns
****
***
NS
HIV-1
R848
poly (IC)
HIV-2
poly (dGdC)
MVA
C
GFP %
HIV-1
HIV-2
D
IFN relative to IFN2a (U/ml)
E
IFN relative to IFN2a U/ml
F
log10 IP-10 (pg/ml)
G
log10 IL-6 (pg/ml)
H
log10 IL-12p70 (pg/ml)
I
log10 TNF (pg/ml)
J
log10 IL-10 (pg/ml)
K
log10 IL-1b pg/ml

Fig. 1: MDDCs profile after infection or stimulation.

(A) CD86 and infection (GFP) profile in MDDCs 48 hrs after infection with HIVGFPenv-nef-(G) or HIV2ROD9ΔenvΔnefGFP+(G) or stimulation with control stimuli (representative sample).
(B) CD86 expression as in (A) (n=8 and mean ± sem, one way ANOVA test, Dunnett's correction, ns= not significant and ***/****p< 0,0001).
(C) Infection profile (%GFP) of HIVGFPenv-nef-(G) or HIV2ROD9ΔenvΔnefGFP+(G) in MDDCs after 48 hrs (n=8 and mean ± sem).
(D) Type I IFN activity in supernatant of MDDCs 24 hrs or (E) 48 hrs after infection or stimulation as in (A) (n=4 and mean ± sem).
(F-M) Cytokines concentration in the supernatant of MDDCs 48 hrs after infection or stimulation (n=4 and mean ± sem, Mann Withney test ns= not significant, *p< 0,05).

4.1.2 HIV-2-infected MDDC protect CD4+ T cells from subsequent HIV infection

In order to test whether the differential effects on DC activation by HIV-1 or HIV-2 have an impact on subsequent HIV infection of CD4 T cells, we set-up a novel *in vitro* co-culture system. Briefly, MDDCs activated with HIV-1, HIV-2 or control stimuli were co-cultured with naïve, allogeneic CD4+ T cells. After 8 days, T cells were challenged with different HIV variants and protection from infection was measured as the decrease in virus-infected, GFP expressing cells compared to control conditions 48hrs post challenge. Strikingly, we found that T cell susceptibility to HIV infection strongly depended on which stimulus had been used for MDDC activation. In particular, we show that, while CD4+ T cells that had been exposed to poly(IC), poly(dG:dC), MVA or HIV-2 stimulated MDDCs had become less susceptible to HIV infection, MDDCs infected with HIV-1 or R848 had no protective effect on CD4+ T cells which remained highly susceptible to HIV challenge (Fig.2A-C). To determine whether the type I IFN produced by MDDCs after HIV-2 sensing had an effect on CD4+ T cells, we measured MX1 and OAS1, two IFN-induced genes, in CD4+ T cells by qPCR in a representative donor (Fig.2D, 2E). We demonstrate that the two ISGs are induced in naïve $CD4^+$ T cells by co-culture with allogeneic MDDCs stimulated with HIV-2 or poly(IC), poly(dG:dC), MVA, but not with HIV-1 or R848. We confirmed these results on the protein level in CD4+ T cells using intracellular staining (Fig.2F). Highlighting the link between MX1 upregulation and protection from infection we found a negative correlation between the susceptibility to infection and the MX1 expression in CD4+ T cells in our experimental model (Fig.2G). Finally, using a cocktail of neutralizing antibodies for type I IFN we could decrease MX1 expression to basal levels in CD4+ T cells in all the conditions (Fig.2H), suggesting that type I IFN produced by MDDCs in response to HIV-2 or poly(IC), poly(dG:dC), MVA sensing plays a major role in shaping $CD4^+$ T cell susceptibility to HIV infection.

FIGURE 2

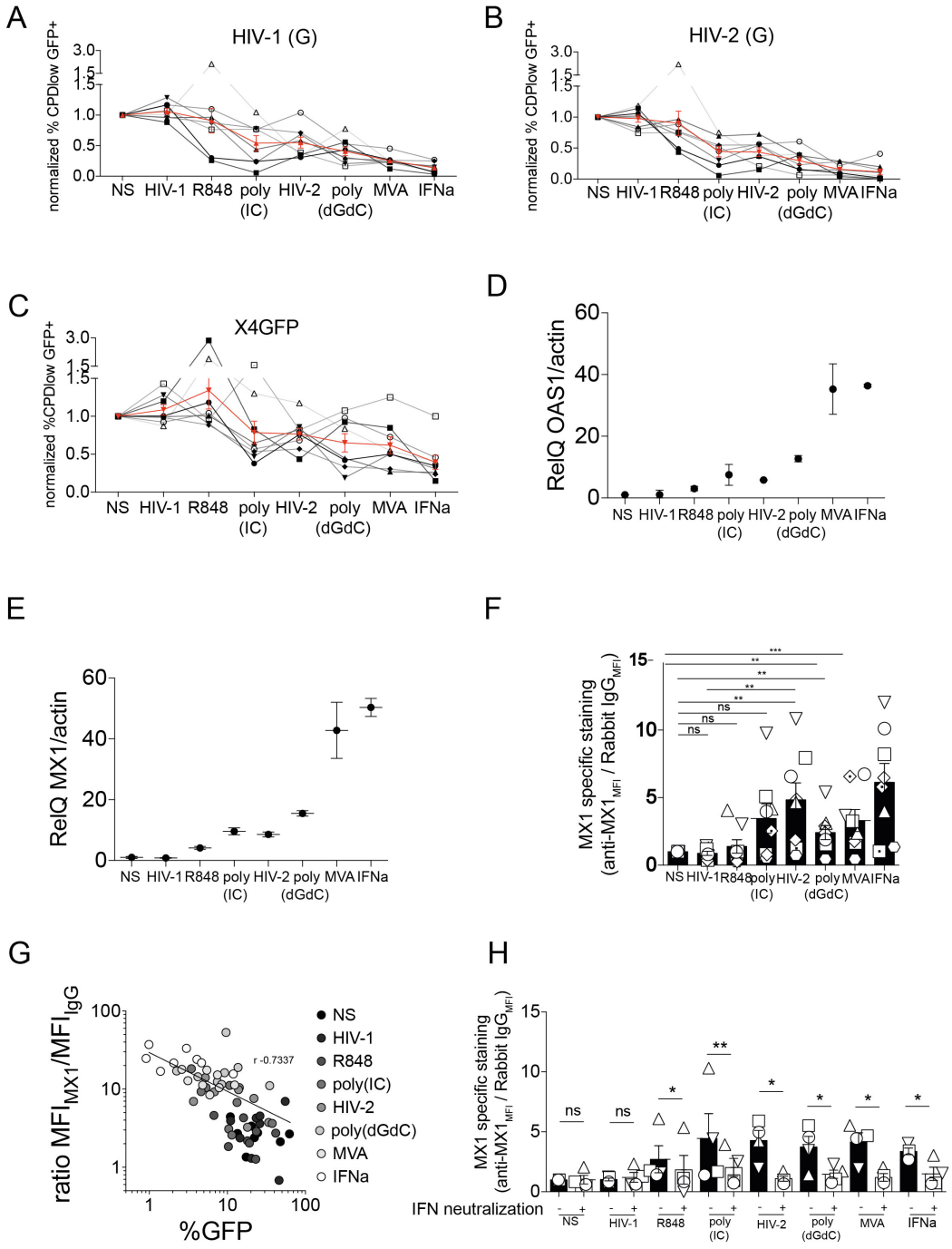
A
HIV-1 (G)
normalized % CPDlow GFP+
NS HIV-1 R848 poly (IC) HIV-2 poly (dGdC) MVA IFNa
B
HIV-2 (G)
normalized % CDPlow GFP+
C
X4GFP
normalized %CPDlow GFP+
D
RelQ OAS1/actin
E
RelQ MX1/actin
F
MX1 specific staining
(anti-MX1MFI / Rabbit IgGMFI)
G
ratio MFIMX1/MFIIgG
%GFP
r -0.7337
NS
HIV-1
R848
poly(IC)
HIV-2
poly(dGdC)
MVA
IFNa
H
MX1 specific staining
(anti-MX1MFI / Rabbit IgGMFI)
IFN neutralization

Fig.2 MDDCs-mediated CD4+ T cells susceptibility to HIV challenge

(A-C) Normalized infection (GFP+) in alive CD4+ T cells 48 hrs after challenge with indicated viruses (n=8 and mean ± sem).
(D) Quantitative measurement of OAS1 and (E) MX1 gene expression related to actinβ in CD4+ T cells 8 days after co-culture with MDDCs in different conditions as reported (one representative donor).
(F) Intracellular MX1 expression as in (D) (n=8 and mean ± sem, Withney test, ns= not significant, *p< 0,05 and **p< 0,01).
(G) Correlation between normalized intracellular MX1 expression and infection (%GFP) in CD4+ T cells, 8 days after co-culture and 48 hours after challenge respectively, in different conditions as reported (n=8 and mean ± sem, Spearman rank test, ****p< 0,0001 and r = 0,7337).
(H) Intracellular MX1 expression in CD4+ T cells 8 days after co-culture with MDDCs in presence of type I IFN neutralization in different conditions as reported (n=8 and mean ± sem, two-tailed t test, ns= not significant, *p< 0,05 and **p< 0,01).

4.1.3 Helper function profile of CD4+ T cells

To examine whether the susceptibility of CD4+ T cells to HIV-infection correlated with a bias in effector T cell differentiation, we sought to measure the T helper profile resulting from the MDDC:CD4+ T cell co-cultures. We re-stimulated T cells with Ionomycin/PMA and performed intracellular cytokine staining (IS) for IL-21 and IFNγ. CD4+ T cells had increased IFNγ production after co-culture with MDDC from all stimulation conditions (Fig.3A) while IL-21 was only produced by T cells that had been activated by R848 stimulated DCs (Fig. 3B). Similar results were found analysing culture supernatants using CBA and on the RNA level using data from microarrays from co-cultured naïve CD4+ T cells (Fig.3C, D). In all experiments, no significant changes in other T helper cell associated cytokines were observed (e.g. IL-4, IL-10, IL-13, IL-17, Fig. 3C). Interestingly, the expression of IFNγ positively correlated with MX1 levels, suggesting that the observed Th1 profile is a direct consequence of the type I IFN production by MDDCs (Fig.3E).
Overall, our data demonstrate that resting naïve CD4+ T cells can acquire a resistance to HIV infection as a result of their priming by DCs stimulated with specific innate signals. This resistance correlates with the expression of standard interferon-stimulated genes, MX1 and IFNγ expression. We thus term this profile $T_{antiviral}$, as a reference to the described Th helper subsets [7].

FIGURE 3

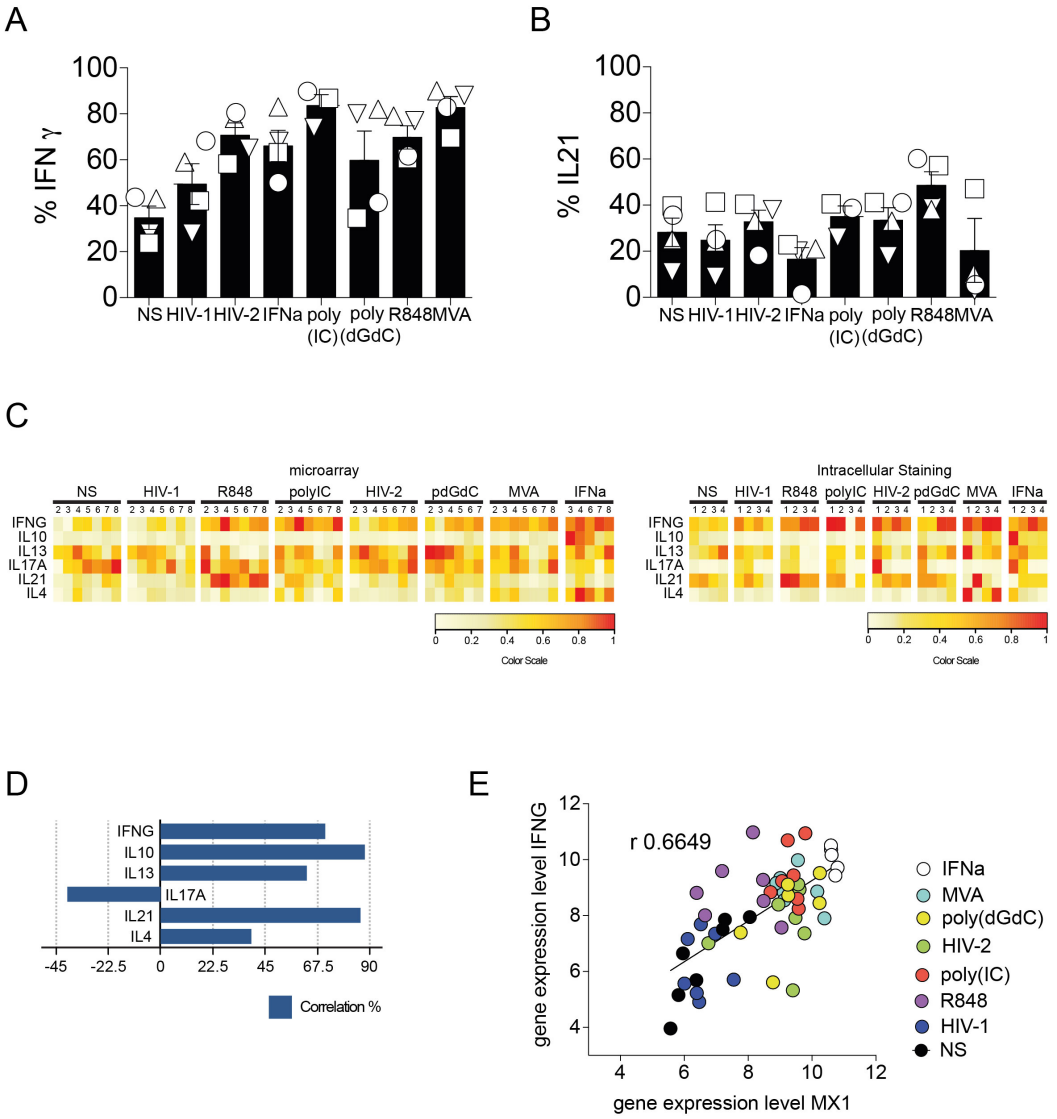
A
% IFN γ
100
80
60
40
20
0
NS HIV-1 HIV-2 IFNa poly (IC) poly (dGdC) R848 MVA
B
% IL21
100
80
60
40
20
0
NS HIV-1 HIV-2 IFNa poly (IC) poly (dGdC) R848 MVA
C
microarray
NS HIV-1 R848 polyIC HIV-2 pdGdC MVA IFNa
IFNG
IL10
IL13
IL17A
IL21
IL4
0 0.2 0.4 0.6 0.8 1
Color Scale
Intracellular Staining
NS HIV-1 R848 polyIC HIV-2 pdGdC MVA IFNa
IFNG
IL10
IL13
IL17A
IL21
IL4
0 0.2 0.4 0.6 0.8 1
Color Scale
D
IFNG
IL10
IL13
IL17A
IL21
IL4
-45 -22.5 0 22.5 45 67.5 90
Correlation %
E
r 0.6649
gene expression level IFNG
12
10
8
6
4
4 6 8 10 12
gene expression level MX1
IFNa
MVA
poly(dGdC)
HIV-2
poly(IC)
R848
HIV-1
NS

Fig.3 Helper function profile of CD4+ T cells

(A) Intracellular IFNγ expression in CD4+ T cells 8 days after co-culture with MDDCs in different conditions (n=4 and mean ± sem).
(B) Intracellular IL21 expression as in (A).
(C) Heat-maps (colour scale) based on the distribution of the different values of the selected cytokines in microarray and intracellular staining (different donors in microarray and IS).
(D) Correlation analysis with Pearson distance represented by % as in (C).
(E) Correlation between MX1 and IFNγ expression value in microarray in CD4+ T cells, 8 days after co-culture in different conditions as reported (n=8 and mean ± sem, Spearman rank test, ****p< 0,0001 and r = 0,6649).

4.1.4 Infection resistance of CD4+ T cells is associated with the induction of type I IFN regulated genes

Next, we sought to generate the unbiased transcriptional profile of the CD4+ T cells obtained by our priming system, in order to discover possible candidates genes participating in the MDDC-mediated protection from HIV infection. We generated Affymetrix data on RNA of sorted T cells 8 days after co-culture from 8 donors (D1-D8). Using Volcano-plots we evaluated the distribution of differentially expressed (DE) genes for each condition over NS (Fig.S1). While no genes were found to be differentially regulated between T_{HIV-1} and the NS condition (Fig.S1) we obtained 943 genes differentially expressed in one or more conditions compared to the NS group (Fig.S2A,B). We used these 943 DE genes for unsupervised clustering into modules using the WGCNA algorithm finding 6 modules. Module 1 contained genes that were differentially regulated in all stimuli associated with HIV infection resistance including HIV-2. Genes of module 2 and 5 showed a similar pattern of regulation but were found to be unchanged in the HIV-2 condition. Module 3 and 4 were specific to regulation in response to R848 or IFNα, respectively. Finally, genes in module 0 are the left over genes (Fig.S3). Given our interest in the genes involved in HIV-2 mediated resistance to HIV infection, we decided to focus our further analysis on module 1 (Fig.3A). Using a functional analysis, we found module 1 genes mainly to be associated with the immune response, the response to virus, antiviral defence and cytokine activity (Fig.3B). Interestingly, we identified MX1 as part of module 1 and as MX1; many other genes have also previously been shown to be regulated by type I IFN.

To confirm that module 1 was indeed representing a type I IFN signature we analysed the transcriptional regulation of module 1 genes. Using the web-tool oPOSSUM 3.0 and Pscan we calculated the over-representation of conserved transcription factor binding sites. We found that Module 1 genes were enriched for binding sites of the transcription factors belonging to the IRF and STAT families, two families that have been best described to regulate a type I IFN signature (Fig. 3C, 3D).

FIGURE 4

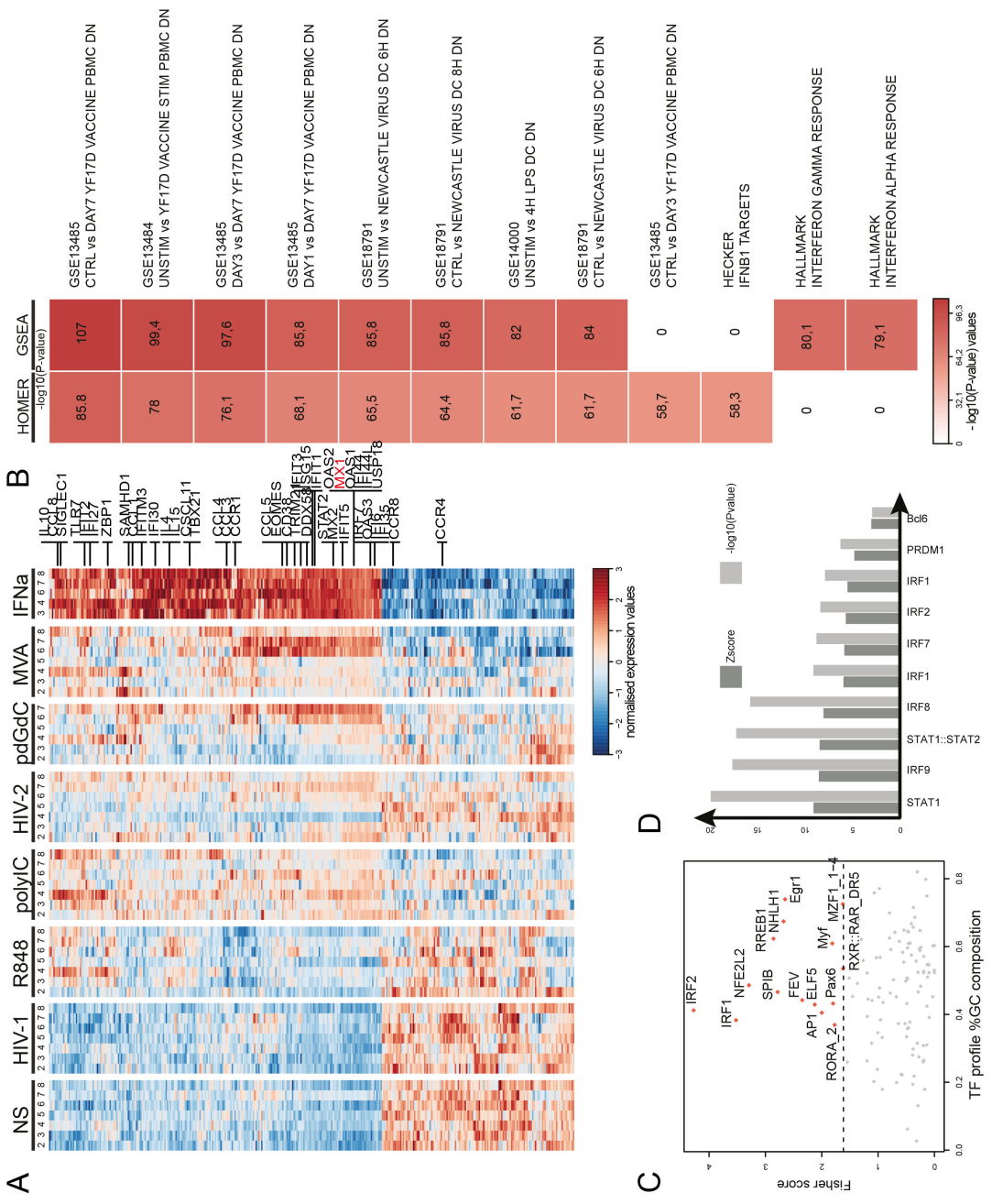
A
NS
HIV-1
R848
polyIC
HIV-2
pdGdC
MVA
IFNa
normalised expression values
B
HOMER -log10(P-value)
GSEA -log10(P-value)
GSE13485 CTRL vs DAY7 YF17D VACCINE PBMC DN
GSE13484 UNSTIM vs YF17D VACCINE STIM PBMC DN
GSE13485 DAY3 vs DAY7 YF17D VACCINE PBMC DN
GSE13485 DAY1 vs DAY7 YF17D VACCINE PBMC DN
GSE18791 UNSTIM vs NEWCASTLE VIRUS DC 6H DN
GSE18791 CTRL vs NEWCASTLE VIRUS DC 8H DN
GSE14000 UNSTIM vs 4H LPS DC DN
GSE18791 CTRL vs NEWCASTLE VIRUS DC 6H DN
GSE13485 CTRL vs DAY3 YF17D VACCINE PBMC DN
HECKER IFNB1 TARGETS
HALLMARK INTERFERON GAMMA RESPONSE
HALLMARK INTERFERON ALPHA RESPONSE
- log10(P-value) values
C
Fisher score
TF profile %GC composition
D
-log10(Pvalue)
Zscore

Fig.4 Module 1: IFN-I signature MX1 like-pattern of expression in CD4+ T cells

(A) Heat-map of the Z-score for normalised expression values of genes in module 1. Z-score is performed to improve the colour contrast of the normalised expression values due to the variation range of these values (genes are ordered by Pearson distance and Ward methodology).
(B) Representation of the 10 best GO terms for GSEA and HOMER tools, selected on P-value and represented -log10(P-values).

(C) Representation of the Transcription-Factors analysis for module 1 of WGCNA clustering on a distance of -2000 bp before the promoter region of the genes through oPOSSUM web-tool (The dashed line represents the threshold used to select significant transcription factors = mean + 1 standard deviation).
(D) Representation of the best 10 TFs for module 1 of WGCNA clustering on a distance of -500 bp before the promoter region of the genes through P-scan web-tool.

4.1.5 Identification of candidate resistance genes controlling CD4+ T cell susceptibility to infection

We hypothesized that some of the genes responsible for the increased resistance to HIV-infection (Fig.2A-C) following HIV-2 infection would be correlated at the gene expression level with MX1, and that we could thus generate a list of candidate resistance genes. We used multiple criteria (k-means occurrence clustering algorithm and correlation score to MX-1 patter of expression overall the stimuli) to generate a list of resistance candidate genes with an MX1 like expression profile (Fig.3A). Overall, we selected 386 genes as candidate resistance factors of which 47% are new candidates that do not appear in Schoggins's screen list (Fig.S4A) [112].

To determine which genes could be resistance factors of HIV infection, we moved to a siRNA-based, high-throughput screening approach. We individually silenced all 386 candidate resistance genes using 3 different siRNAs per gene in HIV-surrogate infected human RPE-1 target cells in presence or absence of IFN-α2a treatment. As readout for infection, GFP fluorescence intensity in the nucleus was measured. First we verified that RPE-1 cells treated with type I IFN become 10 time less susceptible to HIV infection demonstrating the suitability of using RPE-1 cells instead of primary CD4+ T cells for the screening approach (Fig.4A).

We proceeded by generating a heat-map of the number of nuclei for each well for each siRNA (Fig.4B). GFP intensities were then normalized for each well for all the plates in order to be able to compare them (Fig.4C). As expected, we found that GFP intensity, as measure of infection, was completely abrogated by silencing GFP expression with sieGFP (Fig.4C position A19, A20) and rescued by silencing type I IFN receptor expression with siIFNAR1 (Fig.4C position P15).
Calculating the mean value for the 3 siRNAs for each gene we could generate a final representation of the preliminary candidate genes sorted from high to low GFP intensity (Fig.4D). Focusing on the top 34 genes, we found expected resistance candidate genes, genes already present in Schoggins' list, and unexpected genes (Fig.4E). Further analyses are required to validate the identified, putative resistance genes one by one in primary CD4+ T cells.

FIGURE 5

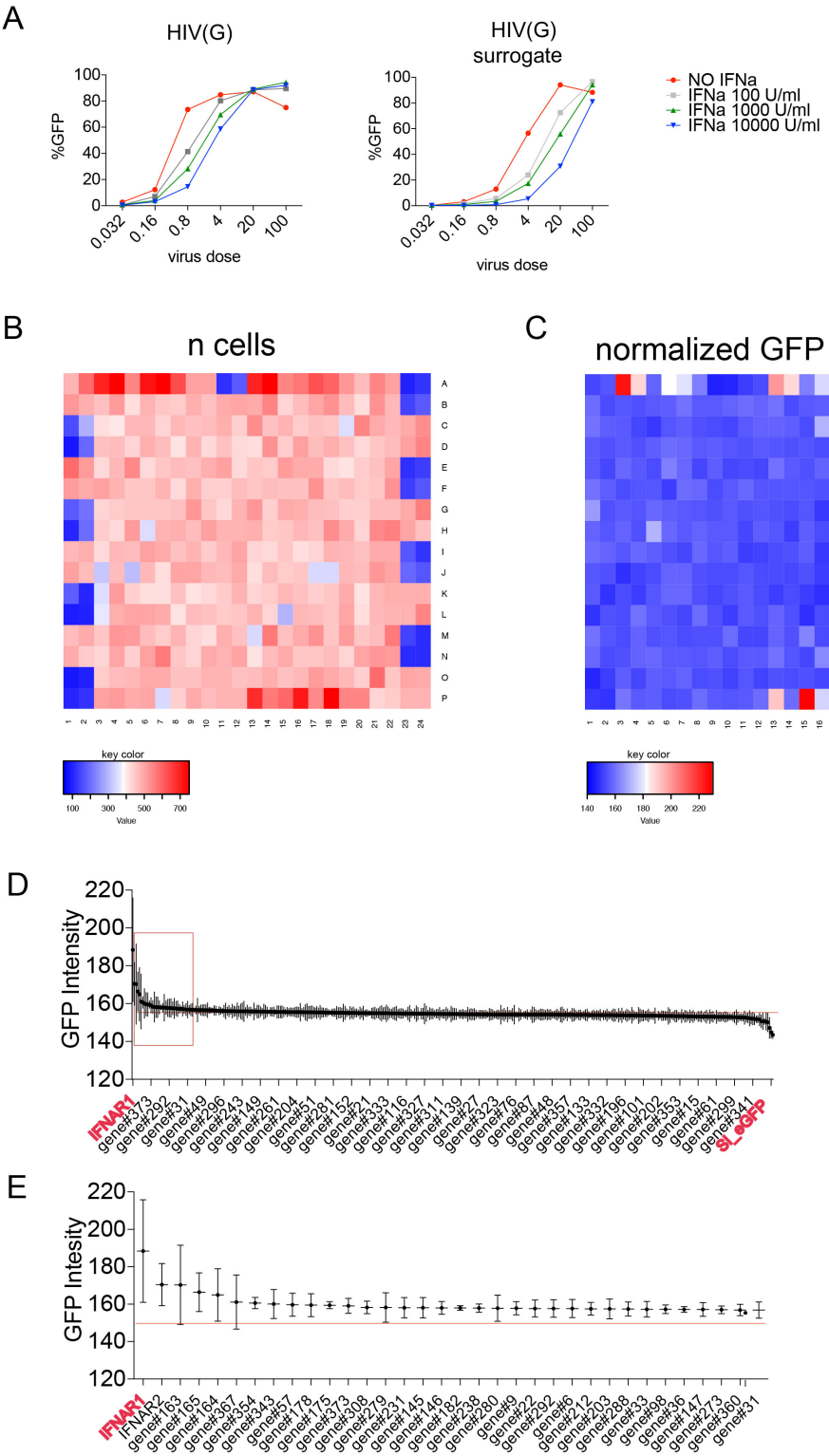
A
HIV(G)
HIV(G) surrogate
%GFP
virus dose
NO IFNa
IFNa 100 U/ml
IFNa 1000 U/ml
IFNa 10000 U/ml
B
n cells
key color
Value
C
normalized GFP intensity
key color
Value
D
GFP Intensity
IFNAR1
SL_eGFP
E
GFP Intesity
IFNAR1
IFNAR2

Fig.5 Candidate HIV resistance genes siRNA-based screening.

(A) Infection (%GFP) in RPE-1 cells 48hrs after challenge with HIVGFPenv-nef-(G) (right panel) or HIV-surrogate (left panel) when RPE-1 where treated with different doses of IFN-α2a 24hrs prior to HIV challenge (one representative experiment).
(B) Heat-map of the number of nuclei per condition in 386 wells/plate.
(C) Heat-map of the normalized GFP intensities calculated in the nuclei for each of the 386 siRNAs (one representative plate).
(D) Representation of mean GFP intensities of the 3 siRNA per gene (386 antiviral candidate genes in total) sorted from high (siIFNAR1 in red) to low (sieGFP in blue) GFP intensities.
(E) Representation of the mean GFP intensities of the first 34 genes based on the preliminary analysis.

FIGURE S1

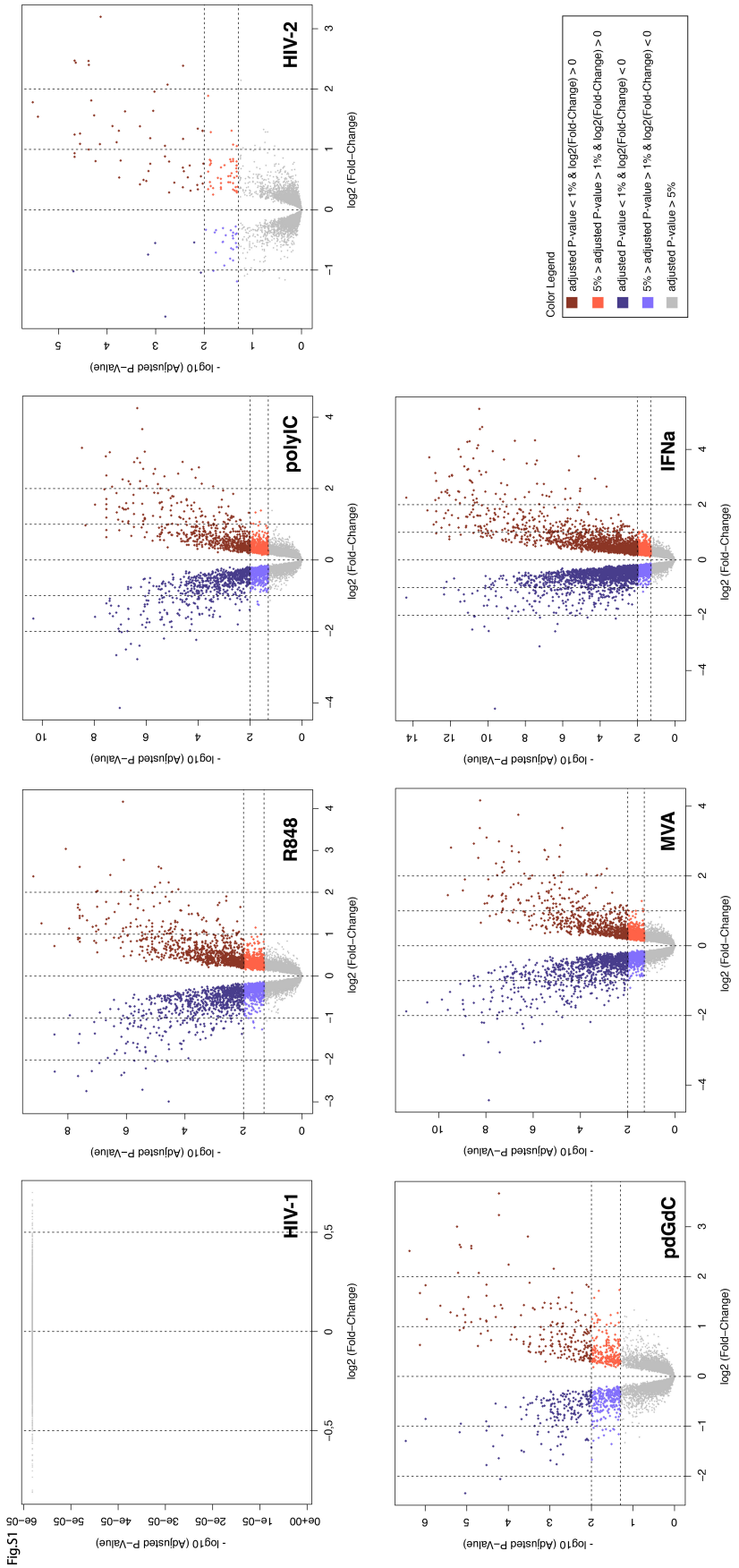

Fig.S1

Fig.S1 Volcano plot of distribution of differentially expressed genes between the experimental and NS condition in CD4+ T cells.

Each volcano-plot computed from the results of the differential expression analysis versus NS condition. Each dot coordinate corresponds to the log2(Fold-Change) and the - log10(Adjusted P-value) of a specific gene (all 43686 probes are represented). The most up-regulated genes located on the upper right corner of the volcano, with the highest positive Fold-Change and the lowest adjusted P-value; whereas the most down-regulated genes are on the upper left corner, with the highest negative Fold-Change and the lowest adjusted P-value.

FIGURE S2

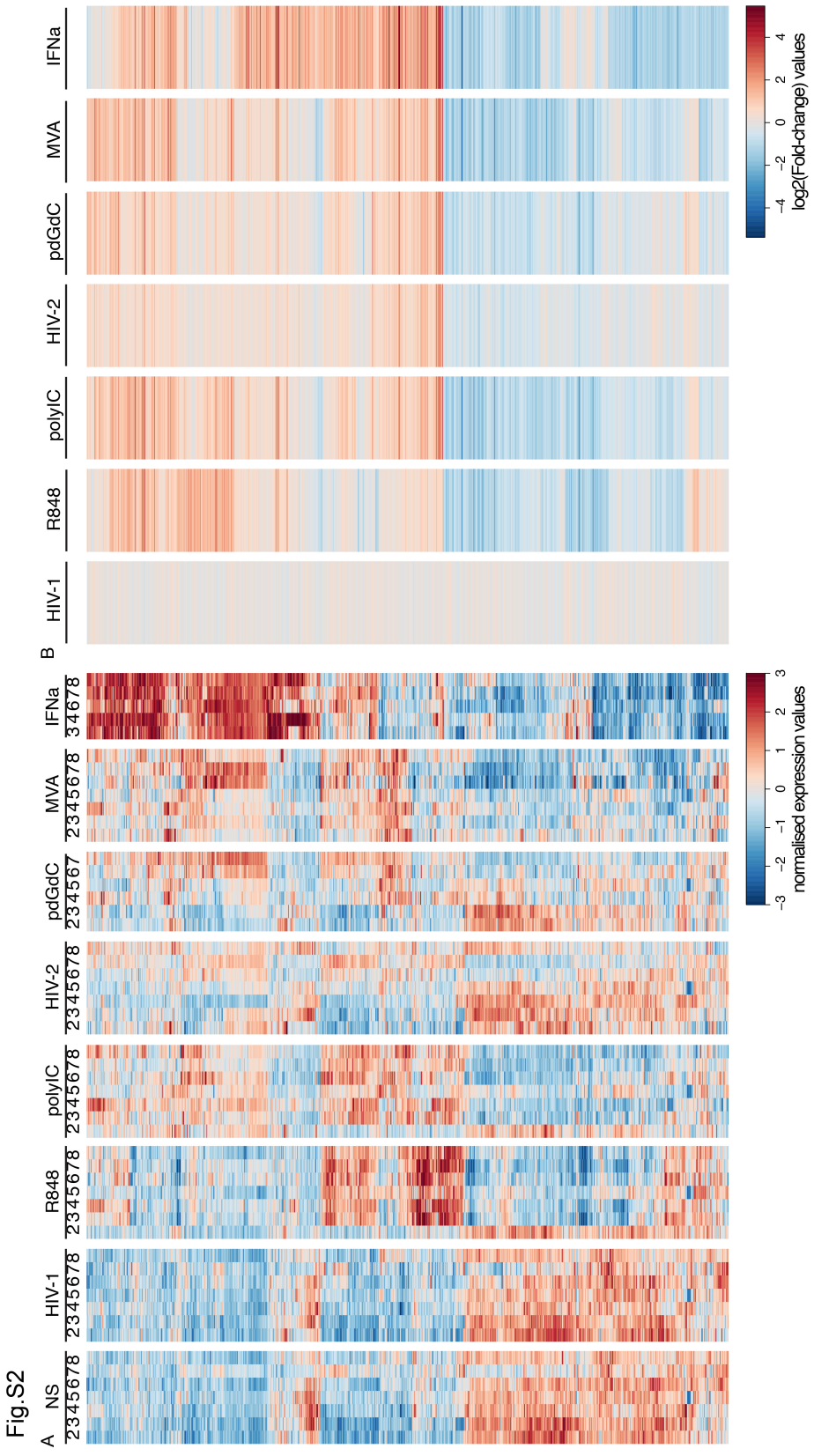

Fig.S2

Fig.S2 Heat-maps on the 943 differentially expressed genes (DE) versus NS condition.

DE selected with an adjusted P-value < 5% and a -1 > log2(Fold-Change) >1. Genes ordered by Pearson distance and Ward methodology. (A) Heat-map of the Z-score for normalised expression values of the genes (Z-score performed to improve the colour contrast of the normalised expression values due to the variation range of these values). (B) Heat-map of the log2(Fold-Change) of these genes, no Z-score is performed (red in the colour scale corresponds to up-regulated genes and blue to down-regulated genes).

FIGURE S3

Fig.S3

Fig.S3 Modules 0-5.

Enrichment of the Weighted Correlation Network Analysis clustering modules (0-5) by stimuli on the 1033 probes differentially expressed (ajusted P-value < 5% and -1 < log2(Fold-Change) > 1). The enrichment is separated for up and down-regulated responses (%).

FIGURE S4

A

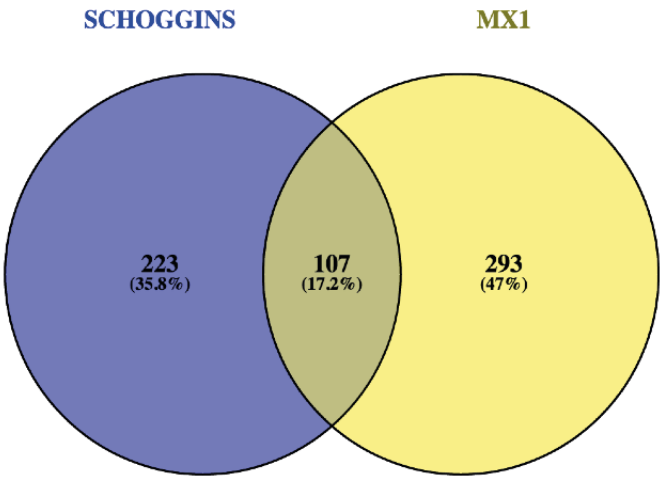

Fig.S4 Candidate HIV resistance genes in CD4+T cells.
(A) Vann-diagram of our list of candidate resistance factors and Schoggins's list.

4.1.6 Materials and Methods

Cells

293FT and HL116 were cultured as previously described [99]. Human peripheral blood mononuclear cells were isolated from buffy coats from normal human donors (approved by the Institut National de la Santé et de la Recherche Médicale ethics committee) using Ficoll-Paque PLUS (GE). Naïve CD4+ T cells enrichment was performed with EasySep Human Naive CD4 T cells Enrichment kit (STEM CELL #19155) prior to sort naive CD4 T cells ($CD4^+$, $CD27^+$, $CD45RO^-$, $CD25^-$, $CD8^-$, $CD14^-$, $CD16^-$, $CD19^-$, $CD123^-$) with MoFlo Astrios (Beckman Coulter). Sorted naïve $CD4^+$ T cells purity were superior to 98%. Cells were then labeled with CPD670 (eBioscience#65-0840-85), counted and resuspended at 10e6/ml in RPMI glutamax, 10% decomplemented FBS, 10 mM HEPES (Invitrogen), Penicillin-Streptomicin, Gentamicine 50 µg/ml (Invitrogen) and incubate at 37°C overnight. Monocytes were freshly isolated from blood of healthy donors and cultured as previously described [168].

Plasmids

Expression plasmids psPAX, CMV-VSV-G were previously described [329]. HIVGFPenv-nef- was derived from HIV-GFP. It encodes for Vpr+Vif+Vpu+. Env is mutated by insertion and GFP is in Nef. HIV2ROD9ΔenvΔnefGFP+ pseudotyped was kindly provided by Yamashita M. from Emerman M.'s lab. X4GFP (HIV-1NL4-3) is replicative competent nef-, replaced by GFP. pTRIP-SV40-GFP VSVG was used as HIV-surrogate in the siRNA-based screening.

Viral production in 293FT

293FT cells were transfected for virus production as previously described [99].

Allogeneic co-culture of MDDCs with naïve CD4+ T cells

At day 4 of MDDC differentiation, cells were harvested, counted, and resuspended in fresh media at 0,25 million/ml with 5 µg/ml polybrene and GM-CSF 5ng/ml, and 100 µl was aliquoted in round-bottomed 96-well plates. For infection, 100 µl of HIVGFPenv-nef- pseudotype VSVG (G) or HIV-2ROD9ΔenvΔnefGFP+ (G) were added. For control stimuli, 100µl of poly(IC) 1µg/ml (Invivogen#tlrl-pic), R848 1µg/ml (Invivogen#tlrl-r848), MVATG N33P 4x10e5 pfu/ml, poly(dG:dC) 600 ng/ml (Invivogen#tlrl-pgcn) or fresh media (NS= not stimulated) were used. MDDCs were infected or stimulated for 3hrs then cells were centrifugated, harvested and 100µl of X-VIVO 15 were added. Twenty-four hours after stimulation/infection of MDDCs, 50 10e4 resting CD4+ T cells were co-cultured with 25 10e4 heterologous infected/stimulated MDDCs in 96-well U bottom plates with AZT 10µM. IFN-α2a 1000 U/ml (Invitrogen) was added at the time of co-culture as independent condition. For microarray, 8 days after co-culture CD4+CD3+DCSIGN- cells were sorted in Aria (BD Bioscience). Cells were then centrifugated 5 minutes at 300g and the pellet used for RNA extraction (Quiagen#217087) to generate microarrays data. For cytokines intracellular expresson analysis, eight days after co-culture, cell were collected, counted and resuspended at 2 10e6/ml. 100µl of cells per condition were stimulated with PMA 50ng/ml (SIGMA#P8139), Ionomycin 500ng/ml (SIGMA#I0634) and Brefeldin A 5µg/ml (SIGMA#B7651) for 5 hours. For cytokines production in the supernatant, eight day after co-culture, cell were collected, counted and resuspended at 1 10e6/ml in fresh X-VIVO 15. 200µl of cells were stimulated

with dynabeads anti-CD3/anti-CD28 at cell:bead 2:1 ratio (Life Thecnologies#11161D) for 24 hrs. After 24 hrs, supernatant was collected for LUMINEX analysis.

Type I IFN neutralization

For type I IFN neutralization experiments, a cocktail of B18R (3µg/ml, eBioscience), anti-IFNß (2,5 µg/ml, eBioscience), anti-IFNα (1,2µg/ml, eBioscience), anti-IFNAR (0,6µg/ml, Millipore) was added in all the MDDCs conditions 1 hour before to start the co-culture with naïve CD4+ T cells, and maintained during the course of the experiment until day8 of co-culture.

CD4+ T cells challenge

Eight days after co-culture, CD4+ T cells were collected, counted and resuspended at 1 10e6/ml in X-VIVO 15. 100 µl of cells were plated in new 96-well U bottom and infected with 100µl of the indicated viruses with 8µg/ml of polybrene. 48 hours after infection, cells were stained and analyzed by flowcytometry.

Flow cytometry analysis of human $CD4^+$ T cells

For cytokines intracellular expression analysis, cells were centrigugated for 5 minutes at 300g and wash one time with 1x PBS (Gibco). Cells were then incubated in 50µl of 1x PBS were Aqua Dead cell staining was diluted (Fisher Scientific#L349557). Cell were incubated 30 minutes at RT. After one wash with 1x PBS, cells were fixed with 100µl/well of IC Fixation Buffer (eBioscience) for 30 minutes at room temperature and then permeabilized with 200µl of 1X Permeabilization Buffer (eBioscience) at room temperature. Cells were then centrifugated at 1700g for 3 minutes. Cells were incubated for 30 minutes at room temperature in 50µl of 1X Permeabilization Buffer were anti- human IFNg PE-Cy7 (clone 4S.B3, eBioscience), anti-human IL-21 PE (clone 3A3-N2.1, BD) or Isotype controls (PE-Cy7 eBioscience#25-4714; PE BD#551436) were diluted. Cells were washed in 200 µl of 1X Permeabilization Buffer and resuspended in FACS buffer prior to acquisition. For intracellular MX1 expression analysis, cells were fixed with 100µl/well of IC Fixation Buffer (eBioscience) for 30 minutes at room temperature and then permeabilized with 200µl of 1X Permeabilization Buffer (eBioscience) at room temperature. Cells were then centrifugated at 1700g for 3 minutes. Cells were incubated for 30 minutes at room temperature in 50µl of 1X Permeabilization Buffer were anti-MX1 antibodies (Abcam Ab95926) or Normal Rabbit IgG (Life Technologies) were diluted. Cells were washed in 200 µl of 1X Permeabilization Buffer and incubated for 30 minutes at room temperature with secondary antibody F(ab')2 Fragment Donkey Anti-Rabbit IgG (H+L) Phycoerythrin R-PE (Jackson Immuno Research). For challenge experiments, cells were centrigugated for 5 minutes at 300g and wash one time with 1x PBS (Gibco). Cells were then incubated in 50µl of 1x PBS where Aqua Dead cell staining was diluted. Cell were incubated 30 minutes at RT. Cells were washed and resuspended in FACS buffer before to be acquired on a FACSVerse (BD) flow cytometer and analyzed in FlowJo.

Flow cytometry for dendritic cells

Cell surface staining was performed in PBS, 1% BSA (Euromedex), 1mM EDTA (GIBCO), 0.01% NaN3 (AMRESCO). The antibody anti-human CD86 PE (clone IT2.2, eBioscience) was used to the cells for 15 minutes at 4°C, washed for two times

and fixed in 1% paraformaldehyde (Electron Microscopy Sciences). Data was acquired on a FACSVerse (BD) flow cytometer and analyzed in FlowJo.

Type I interferon and Cytokines quantification

For MDDCs, cytokines concentration was measured with a Human IP-10, IL-6, IL-12p70, IL-10, IL-1b or TNF cytometric assay (BD) according to the manufacturer's protocol. Data was acquired on a BD FACSVerse (BD) flow cytometer and analyzed in FCAP Array (BD). Type I IFN measurement was performed using the HL-116 as previously described [99]. For CD4+ T cells, cytokines concentration was measure with human Luminex Multiplex assay (HTH17MAG-14K-21 cytokines, Millipore) according to the manufacturer's protocol. Data was acquired and analyzed in Bioplex 200 LUMINEX (Biorad).

Microarrays

The data was obtained with Affymetrix® Human Gene 2.1 ST technology. The raw data files were collected for the 8 conditions (NS / HIV-1 / R848 / polyIC / HIV-2 / poly(dGdC) / MVA / IFNα) for 8 donors (= 64 samples). Microarray analyses were processed with R (version 3.0.0) using packages from *Bioconductor*. The quality control was performed using *ArrayQualityMetrics* [330] package detecting 3 samples as outliers (polydGdC for donor #8 / IFNα for donors #2 and #5). We also removed all the samples for donor #1 due to technical issues (total of 53 samples). Data was normalized using the Robust Multi-array Average algorithm from the *Oligo* [331] package. Annotation of the probes was done using the annotation updated file (2015/03/27) for Human Gene 2.1 ST Arrays from the Affymetrix website. To compare the responses between the samples we performed differential expression through *Limma* [332] package using NS (= non stimulated) as the control. A threshold of an adjusted P- value below 5% and a -1 > log2 (fold-change) > 1 for the differential expression was decided using volcano-plots (n = 1033 probes). For representation we selected the most variant probe when multiple probes were linked to the same gene (DE = 943 genes). We represented the summarized gene expression level and the log2(fold-change) of these genes using heat-maps with *Made4* [Ref4] package. A PCA was also done using the summarized gene expression level of these probes for all the stimuli with the function included in *Made4* [333] package. We performed a clustering on the differentially expressed probes using the WGCNA (= Weighted Correlation Network Analysis) from *WGCNA* [334] package. We identify 5 modules (module 0 = left over genes) on which we performed further analysis as gene-ontology enrichment and transcription factor motifs over-representation. To be able to compare results we used the web-tool GSEA [335] and HOMER software [336] for gene-ontology enrichment. In the same manner, we used for transcription factors motifs over-representation the web-tool oPOSSUM3 [337] and the web-tool Pscan [338].

siRNA-based screening

CELL CULTURE: RPE-1 cells were cultured in DMEM-F12 (Gibco Life Technologies); supplemented with 10% fetal bovine serum (Life Technologies), 0.01 mg/ml Hygromycin, 1% L-Glutamin and 1% Penicillin/Streptomycin (Life Technologies), at 37°C and 5% CO2. For cell passages, cells were washed once with PBS and detached with trypsin-EDTA (Life Technologies) for 5 minutes at 37°C.

Cells were found to be mycoplasma negative by biochemical assay detection using MycoAlertTM Mycoplasma Detection Kit (Lonza). For replicate experiments, cells were thawed 5 days before seeding and passed once. The same batch of cryopreserved cells was used for both replicates. Cells were counted with a T4 Cellometer cell counter (Nexcelom).

PIPELINE STEPS VALIDATION: We optimized the siRNA transfection conditions using 2 different types of custom pre-designed siRNAs (Select and Silencer Select) from Ambion (Thermo Fisher Scientific) and a reference from Eurogentec. Transfections were performed using control siRNAs (10 nM final concentration) that targeted KIF11 (kinesine family member 11) and GM130 to assess efficacy and toxicity. Controls also included transfection mix (OptiMEM + Interferin) without siRNA. Cell viability and GM130 silencing was determined 72 hrs after transfection using DAPI and GM130 staining. The optimal transfection conditions were defined within the siRNA type that gave the best efficiency versus toxicity ratio in several independent experiments. Assay design and optimization also included virus titration (in GHOSTX4R5 cell line), optimization (maximal infection frequency) and the antiviral activity induced by IFNα2a titration. All the assay steps have been miniaturized in 384-well plates, including pipetting volumes calibration and solutions preparation to adapt the set up assay to a larger scale experiment. Robotics scripts have been developed and calibrated in order to allow a fully automated screening pipeline. Several experiments have been made to ensure that robotic handling for each experiment step was not affecting cell adhesion and giving coherent results as compared to experiments that have been previously performed in a bench-like process.

SCREENING WORKFLOW:

1. Cell seeding (morning). Cells were plated in 384-well plates (Viewplate-384 Black, 6007460 Perkin Elmer) at a density of 600 cells/well using MultiDrop combi (Thermo Fisher Scientific), in 40µl of media.
2. siRNAs transfection (afternoon). RPE-1 cells were transfected with a single 10nM siRNA (Ambion) diluted in a mix of 20µl of OptiMEM (Life Technologies) and 0.05µl of Interferin reagent (Polyplus Transfection). A total of 1,158 siRNAs have been transfected using an Evo 150 with MCA384 (Tecan). siKIF11, siSel_NC1 and siGL2 were used as transfection controls and were present in columns 1, 2, 23, 24 of each screen plates and in an additional control plate where they were meshed (Eurogentec).
3. Interferon treatment: 24 hrs after transfection cells were induced with IFN-α2a at a final concentration of 10000U/ml (ImmunoTools, Cat.n° 11343504, Lot. 353970). Interferon was diluted into media and 30µl of the mix was transferred to each well with the MCA384 head (Tecan).
4. HIV-surrogate infection: 24 hrs after interferon treatment, media was removed and 60µl of the HIV surrogate (pTRIP-SV40A-GFP-psPAX2 (G)), diluted 1.24X and then 1:2 into media with 8µg/ml protamine, was added to the plates with the MCA384 head (Tecan). HIV surrogate titer was 8,8.105 i.u./ml and measured in GHOSTX4R5 as previously described in [99]. Cells were then incubated 48 hrs prior to fixation.
5. DAPI staining and image acquisition. Cells were fixed with 4% of formaldehyde (Sigma-Aldrich) for 15 minutes and nuclei were stained with

0.2µg/ml DAPI. Images of DAPI and GFP channels (4 fields per well) were acquired with an INCell 2000 automated wide-field system (GE Healthcare) at 10x magnification (Nikon 10X/0.45, Plan Apo, CFI/60), leading to 15,360 tiff images per replicate experiment. Two independent experiments were performed for each treatment.

QUALITY CONTROL: Transfection quality control was performed on controls of all plates for each replicate. Cell count feature, quantified with the IN Cell Analyzer workstation 3.7 software, was used for assessing transfection efficiency. For each plate a beta factor was calculated to assess for the differential effect of the 2 control siRNA populations (KIF11 and siSel_NC1 / siGL2) on cell proliferation (Cell count measurement was used). A beta score above 3 indicates a good separation between the 2 populations hence good transfection efficiency.

For all plates of the two replicates, the transfection efficiency was assessed with the statistical parameter defined as Beta factor (β) that is computed as the dynamic range of the assay (i.e. the absolute difference between mean cell phenotype for a given negative control and positive control) divided by the sum of the covariance between the two groups as defined:

$$Beta\ factor = \frac{abs(\mu(X) - \mu(Y)}{\sqrt{\frac{n_X - 1}{n_X}\sigma^2(X) + \frac{n_Y - 1}{n_Y}\sigma^2(Y)}}$$

β was computed using siKIF11 as positive population and siSel_NC1 (for library plates) and siGL2 (for BFX external control plate. A β close to 3.0 is considered as a good transfection efficiency, which is the case of the screening), performed.

ANALYSIS: Image analysis was performed using Fiji software. For each field in each well, nuclei were segmented using auto-threshold (Triangle method) after background subtraction (20 px radius). Then corresponding intensities were measured for each nucleus on the GFP image.
Plates analysis was then achieved using R software. First, heat-map of the number of cells per well was generated for each plate. Then, GFP intensities normalization was performed to allow comparison of data from different plates in the screen. Briefly, for each plate, the mean GFP intensity was computed and corrected to the mean value for all the plates. Finally we realized heat-map of the normalized intensities. We also performed heat-map of the percentage of GFP positive ("rescue") cells per well. To do so, an intensity value of 150 was used as threshold after normalization. This threshold value was determined according to the distribution of the GFP intensity in control conditions, in detail siIFNAR1 (P15 in 384 wells/plate) as positive "rescue" control and siSel_NC1 (A22 in 384 wells/plate) as a negative control.
As a final representation, mean of GFP intensity was plotted for each silenced gene, as the mean of 3 different siRNA per gene for 2 replicates.

4.2 Intrinsic anti-proliferative activity of the innate sensor STING in T lymphocytes

S. Cerboni[1,†], N. Jeremiah[1,†], M. Gentili[1], U. Gehrmann[1], C. Conrad[1], M. Stolzenberg[3], C. Picard[3], B. Neven[2,4], A. Fischer[2,4], S. Amigorena[1], F. Rieux-Laucat[2,*], N. Manel[1,*]

Affiliations:
[1]Immunity and Cancer Department, Institut Curie, PSL Research University, INSERM U932, 75005 Paris, France.
[2]Laboratory of Immunogenetics of Pediatric autoimmune Diseases, INSERM UMR 1163, Paris Descartes-Sorbonne Paris Cité University, Imagine Institute, 75015 Paris, France
[3]Center for Primary Immunodeficiencies, Hopital Necker Enfants-Malades, Assistance Publique-Hôpitaux de Paris, 75015 Paris France
[4] Pediatric Immunology Haematology and Rheumatology Unit, Necker Children's Hospital, Assistance Publique-Hôpitaux de Paris;
*Correspondence to: frederic.rieux-laucat@inserm.fr and nicolas.manel@curie.fr
†These authors contributed equally to the work.

Abstract:
Activation of the cyclic dinucleotide sensor, stimulator of interferon genes (STING), is critical for interferon and inflammatory gene expression during innate immune responses. The role of STING in adaptive immunity, however, is still unknown. Here, we show that STING activation reduces the proliferation of CD4+ T lymphocytes. This activity is independent of TBK1 and IRF3 recruitment and of type I interferon, and requires a distinct domain of innate activation in STING. Inhibition of cell proliferation by STING requires its re-localization to the Golgi apparatus and causes mitotic errors. CD4+ T lymphocytes from patients carrying constitutive active mutations in STING have impaired proliferation and reduced numbers of memory lymphocytes. Therefore, STING, a critical innate sensor, also functions intrinsically in cells of the adaptive immune system to inhibit proliferation.

Introduction

Innate control of adaptive immunity relies on the paradigm that activation of innate sensors in specialized cells leads to extrinsic signals, such as cytokines, that instruct lymphocytes for adaptive immunity [339]. However, innate sensors may adopt distinct activity when they function intrinsically in cells of adaptive immunity, such as T cells. The inflammasome receptor NLRP3 was recently identified as a transcription factor for Th2 cells, although this activity was not linked to the activation of NLRP3 [340]. Here, we examined the activity adopted by STING in CD4+ T cells.

STING is a receptor for cyclic di-nucleotides such as 2'3'-cGAMP produced by cGAS in response to cytosolic dsDNA [43, 55, 341]. STING activation induces its relocation from the endoplasmic reticulum to the Golgi [50]. During this process, STING recruits the non-canonical IκB kinase TBK1, which phoshorylates serine 366 in the C-terminal tail (CTT) of STING, generating a platform for IRF3 recruitment and phosphorylation by TBK1 [83]. STING also activates NF-κB through a poorly resolved mechanism, although TBK1 has also been implicated [68]. Phosphorylated IRF3 and NF-κB subsequently induce type I interferon and inflammatory gene expression. In dendritic cells (DCs), STING activation additionally induces expression of co-stimulatory molecules, leading to cell maturation and launching of adaptive immunity [342].

Monogenic immune dysregulation syndromes have been instrumental in the understanding of the contribution of individual proteins to immunity. Genetic defects in components of the innate nucleic acid sensing and signaling pathway leading to an increase in the production of type I interferons have been identified and grouped as interferonopathies [146]. The disease phenotypes associated are broad affecting several organ systems, and have been classified as auto-inflammation (*RNASEH2*, *ADAR*, *DDX58*, *TMEM173*), infection (*STAT1*-GOF, *C1Q*, *C1R*, *C1S*, *C4*, *CYBB*, *NCF1*, *NCF2*), autoimmunity (*TREX1*, *PSMB8*, *IFIH1*, *ACP5*), and malignancy (*SAMHD1*) [343].This suggests that the implicated proteins could have non-redundant functions distinct from their described role in type I interferon production and nucleic acid sensing.

Activating mutations in *TMEM173* (*STING*) have been described in humans leading to a severe early-onset inflammatory disease characterized by interstitial lung disease and vascular skin disease particularly targeting the extremities [103, 104]. The reported mutations lie in the dimerization domain and were proposed to mimic the effect of 2'3'-cGAMP binding. STING with activating mutation was reported to be localized in the Golgi at steady state in the absence of ligand stimulation and to induce constitutive type I interferon expression in cell lines. Accordingly, circulating type I interferon and inflammatory cytokines have been detected in these patients. Interestingly, alteration in the immunological phenotype such as lymphopenia and leukopenia in patients with STING activating mutations were also observed [103, 104]. Here, we show that patients carrying an active mutation in STING have a T cell imbalance, and we leverage this finding to show that STING adopts an anti-proliferative activity in $CD4^+$ T cells.

Results

Clinical parameter analysis of patients carrying activating *STING* mutations revealed a peripheral T cell compartment imbalance characterized by an increased fraction of naive CD4+ and CD8+ T cells and a reduced fraction of memory cells (**Fig. 1A, Supplementary Table 1**). This raised the possibility that STING may have activities in lymphocytes. We focused on CD4+ T lymphocytes obtained from healthy donors and examined the expression of STING and upstream sensors cGAS and IFI16 at the protein level. STING was expressed at similar levels in resting naive and central memory CD4+ T cells, while cGAS and IFI16 were more expressed in memory cells (**Fig. 1B**). We followed protein expression during activation of naive CD4+ T cells in vitro. STING expression was maintained overtime, while cGAS and IFI16 were induced during the first few days of activation (**Fig. 1C**). Thus STING, a sensor of innate immunity, is also expressed in cells of adaptive immunity. To examine the impact of wild-type (WT) and mutated active STING on CD4+ T cells, we developed an over-expression approach using BFP-2A lentivectors combined with cell proliferation profile analysis. CD4+ T cells transduced with control vector or STING WT steadily proliferated (**Fig. 1D, 1E**). In contrast, CD4+ T cells transduced with STING carrying the patients' activating mutation V155M showed reduced expansion (**Fig. 1D, 1E)**. Strikingly, the fraction of cells expressing the highest level of STING V155M gradually decayed at each cell cycle. Untransduced BFP-negative cells in the same well expanded normally, indicating that the effect required cell-intrinsic STING V155M activity (**Supplementary Fig. 1A**).

STING activation leads to the expression of type I interferon and TNF [59]. CD4+ T cells transduced with STING WT and STING V155M produced type I interferon and TNF (**Fig. 2A**). While proliferation of BFP-negative cells was not affected by STING V155M-expressing cells, autocrine TNF or IFN could be required in cells expressing STING to inhibit proliferation. We used neutralizing reagents to assess the role of these cytokines in the reduced expansion of STING V155M cells. To control for type I interferon neutralization, we measured the expression of MX1, an interferon-stimulated gene (ISG) (**Supplementary Fig. 2A**). MX1 was induced in STING V155M cells, and abrogated when type I interferon was neutralized (**Fig. 2B, 2C**). However, the STING V155M cells conserved their reduced expansion under type I interferon neutralization conditions (**Fig. 2B, 2C**). To assess the TNF neutralization, we used a NF-κB reporter in $CD4^+$ T cells. Recombinant TNF stimulated reporter expression, which was neutralized with anti-TNF/TNFR antibodies (**Supplementary Fig. 2B**). In contrast, parallel treatment of the STING V155M cells with anti-TNF/TNFR antibodies did not rescue the expansion of STING V155M cells (**Fig. 2D, Supplementary Fig. 2C**). Thus, inhibition of CD4+ T cells proliferation by STING V155M was independent from autocrine type I interferon and TNF signals. Activation of mouse STING by a synthetic agonist induces apoptosis of malignant murine B cells [344] and STING activation in endothelial cells was shown to induce apoptosis [103]. More than 90% of cells expressing STING V155M remained negative for Annexin V, indicating no overt induction of apoptosis (**Fig. 2E, 2F**). To determine if apoptosis was implicated in the reduced proliferation, we used the pan-caspase inhibitor Z-VAD-FMK. Z-VAD-FMK protected from etoposide-induced apoptosis in T cells, validating the approach (**Supplementary Fig. 2D**), but did not rescue the proliferation of cells expressing STING V155M (**Fig. 2G, 2H**).

Next, we sought to determine if the signaling activity of STING V155M was required to inhibit T cell proliferation. The natural polymorphism R71H-G230A-R293Q (HAQ) in STING WT has been proposed to inhibit its response to cyclic

dinucleotides [101, 102]. We hypothesized that HAQ could function as genetic inhibitors of STING signaling. We introduced the HAQ polymorphism in STING WT and STING V155M. The presence of HAQ in STING V155M abolished its constitutive activity in a reporter assay for type I interferon transcription (**Supplementary Fig. 3A, 3B**). STING HAQ V155M remained responsive to 2'3'-cGAMP stimulation, indicating that the protein only lost its constitutive activity and was not otherwise crippled by the mutations. While STING V155M localized to the Golgi, a hallmark of STING activation, STING HAQ V155M localized to the endoplasmic reticulum similar to unstimulated STING WT (**Fig. 3A**). In addition to type I interferon transcription through TBK1-IRF3, STING signaling also activates dendritic cells. To examine how the HAQ polymorphism would impact DC activation by STING, we developed a lentiviral transduction assay in DCs. STING V155M induced expressed of the ISG SIGLEC1 in DCs, but transduction was low, presumably due to the presence of type I interferon (**Supplementary Fig. 3C, 3D**). We combined STING lentivector transduction with type I interferon neutralization. Type I interferon neutralization abolished SIGLEC1 expression and efficient transduction was restored. Unexpectedly, STING V155M induced expression of CD86 when type I interferon was neutralized, indicating DC activation through STING signaling, independently of type I interferon (**Supplementary Fig. 3C, 3D**). In contrast, STING HAQ V155M also lost the ability to induce expression of CD86 and SIGLEC1 in DCs (**Supplementary Fig. 3E, 3F**). Overall, this validated that the HAQ polymorphism functionally inhibited STING signaling by the constitutive active mutant V155M. Strikingly, in CD4+ T cells, the presence of HAQ in STING V155M restored cell proliferation (**Fig. 3D, 3E**). Thus, STING activation is required to inhibit proliferation of T cells.

To determine if STING V155M required IRF3 binding and TBK1 binding to inhibit proliferation, we introduced the S366A mutation which prevents IRF3 recruitment after activation [83] or deleted the CTT of STING which was proposed to be required for TBK1 binding (Δ342) [67, 345], respectively (**Fig. 4A**). We validated that Δ342 in STING, but not S366A, prevented the interaction with TBK1 (**Fig. 4B**). The Δ342 mutation also abolished the localization of STING V155M to the Golgi (**Fig. 4C**). In T cells, both mutations abolished the production of type I interferon and the upregulation of MX1 (**Supplementary Fig. 4A, 4B**). However, only the Δ342 mutation abolished the anti-proliferative activity of STING (**Fig. 4D, 4E**). Thus, the anti-proliferative activity of STING requires the C-terminal tail but not the IRF3 binding site.

To determine if TBK1 binding was required for the anti-proliferative activity of STING, we introduced partial deletions (Δ354 and Δ368) in the CTT of STING V155M (**Fig. 5A**). Similar to Δ342, Δ354 and Δ368 lost the ability to bind TBK1 (**Fig 5B**) and to induce type I interferon and ISG expression (**Supplementary Fig. 5A, 5B**). Unexpectedly, STING V155M Δ354 and Δ368 localized to the Golgi (**Fig. 5C**) and were capable of inducing activation of DCs despite the lack of TBK1 binding (**Fig. 5D, 5E**). Strikingly, STING V155M Δ354 and Δ368 also conserved their anti-proliferative ability in T cells (**Fig. 5F, 5G**). We wished to establish that the identified CTT subdomain 343-354 is also a functional domain in wild-type STING. We examined cGAMP-induced IFN activation in THP-1 cells (**Supplementary Fig. 5C**). We noticed that in THP-1 cells, cGAMP stimulation induced cell death (**Fig. 5H**). cGAMP-induced IFN production and cell death were inhibited in STING KO THP-1 cells, and expression of STING WT in STING KO restored IFN expression and cell death induced by cGAMP (**Fig. 5H, Supplementary Fig. 5D**). STING Δ342, Δ354

Δ368 in STING KO cells did not restore IFN expression, in agreement with the lack of TBK1 recruitment, or cGAMP-induced cells death (**Supplementary Fig. 5D**). Interestingly, expression of STING Δ354 and Δ368 protected WT THP-1 from cGAMP-induced cell death, and STING Δ342 did not have such an effect (**Fig. 5H, 5I**). This indicate that the domain 343-354 is biologically active in STING WT. Overall, these findings define domain 343-354 as a minimal functional subdomain of the CTT in STING V155M and STING WT (miniCTT), independent of TBK1 and IRF3 binding, that mediates dendritic cell activation and inhibition of T cell proliferation.

To examine how STING V155M could inhibit T cell proliferation, we assessed DNA content during cell cycle. T cells expressing STING V155M displayed a shift in their G1 peak, and accumulated cells with >4n DNA (**Fig. 6A, 6B**), indicating mitotic errors [346]. We performed live imaging of primary T cells to examine mitosis, but cells were too motile to track mitotic events. We transduced STING V155M in an adherent human epithelial cell line and found that it recapitulated the anti-proliferative effect observed in T cells (data not shown). The duration of mitosis was increased in cells expressing STING V155M, with strikingly unstable and long metaphases, as compared to control cells (**Fig. 6C, 6D**).

Finally, we next sought to determine if endogenous STING could impact proliferation of T cells. We first examined STING-deficient mice (**Supplementary Figure 6A**). Spleen and lymph nodes of STING-deficient mice did not show defects in the proportion of T cell subsets (**Supplementary Figure 6B, 6C, 6D, 6E**). In contrast, stimulation of T cells revealed that STING-deficient cells had an increased proliferation capacity (**Fig. 7A, 7B**). Thus, endogenous STING is a negative regulator of T cell proliferation. Finally, we examined the ability of T cells from patients with activating *STING* mutations to undergo cell division. Using a moderate TCR stimulation, patient T cells exhibited a profound proliferation defect as compared to healthy controls (**Fig. 7C, 7D**).

Discussion

Overall, our findings show that in T cells, STING is a negative regulator of lymphocyte proliferation under normal and pathological conditions.

Stimulation of STING was previously shown to induce apoptosis, but we could not find any evidence of apoptosis in STING V155M expressing $CD4^+$ T cells. Instead, our results are consistent with a loss of proliferative capacity. The anti-proliferative activity of STING required STING localization to the Golgi and a sub-domain in the C-terminal domain, termed miniCTT, distinct from TBK1 and IRF3 recruitment domains. Using a THP-1 assay of 2'3'-cGAMP-induced cell death and IFN production, we found that STING comprising the miniCTT actually protected from 2'3'-cGAMP induced cell death. This evokes the possibility that IFN induction by TBK1 and IRF3 recruitment on one hand, and the anti-proliferative activity on the other hand, are competing activities of STING.

The anti-proliferative activity of STING in T cells mediated via the miniCTT paralleled STING's ability to induce DC activation. DC activation occurred in the absence of TBK1 and IRF3 recruiting determinants in STING. This shows that STING has an additional mode of innate stimulation, independent from TBK1 and IRF3 binding.

Similar to our findings in patients with STING activating mutation, patients with loss of function mutations in *IKBKB*, *CARD11*, *BCL10* and dominant gain of function mutations in *IKBA* show an imbalance in peripheral T cell subset characterized by an increase in naive and decrease in the memory subset [347-351]. Isolated T cells from these patients also show a defect in ex vivo T cell proliferation. T cell subset balance and proliferation is thus critically dependent on functional NF-κB signaling pathway. We thus propose that STING V155M interferes with NF-κB-related signals required for T cell proliferation. DC activation also typically requires NF-κB signaling [3]. Thus, the miniCTT of STING may converge on NF-κB signaling in T cells and dendritic cells. Interestingly, NF-κB activation has been previously implicated in the control of senescence [352]. In T cells, we envision that the NF-κB-stimulatory activity of STING intersects with anti-proliferative pathways associated with cell cycle arrest and senescence, consistent with the induction of mitotic errors by STING V155M.

The anti-proliferative activity of STING required its localization to the Golgi. This was observed independently by introducing the HAQ polymorphism in STING, or by deleting the CTT of STING. Golgi is a critical organelle for cell mitosis entry and progression [353], and it was also recently proposed to function as a signaling platform [354]. However, these properties remain poorly characterized and it will be important to study the interplay between STING and the Golgi in these processes. STING induced mitotic errors characterized by aberrant cellular DNA content, extended mitosis and unstable metaphases. Similar mitotic error and aberrant cellular DNA content has been reported in cell types that are dependent on TBK1 for mitosis, when TBK1 was inhibited or sequestered [346, 355]. We found that TBK1 binding to STING is not required for its anti-proliferative activity. Thus, distinct proteins involved in innate sensing may converge to induce mitotic errors.

We found that STING-deficient mouse T cells had a constitutive increased cell proliferation rate. In this setting, the nature of the STING activating signal remains unknown. We found cGAS to be induced upon T cell stimulation, which may hence contribute to endogenous STING anti-proliferative activity. Alternatively, we do not exclude that STING anti-proliferative activity may be triggered by yet unknown

cGAS-independent signals. Accordingly, STING V155M is active in the absence of ligand binding.

We find that STING plays a role in T cell proliferation of normal and STING-mutated cells. STING may impact T cell proliferation and T cell subset balance in other situations that implicate the cGAS-STING pathway, such as in HIV infection [99, 100, 150]. Since T cells undergo clonal expansion during immune responses, the intrinsic anti-proliferative activity of STING may be a primitive innate defense mechanism to limit pathogen replication in infected T cells. In summary, our results extend the paradigm of innate control of adaptive immunity by establishing that inhibition of proliferation is a lymphocyte-intrinsic activity for the innate sensor STING.

Online Methods

Cells

293FT and HL116 were cultured as previously described [99]. Human peripheral blood mononuclear cells were isolated from buffy coats from normal human donors (approved by the Institut National de la Santé et de la Recherche Médicale ethics committee) using Ficoll-Paque PLUS (GE). Naive CD4 T cells enrichment was performed with EasySep Human Naive CD4 T cells Enrichment kit (STEM CELL #19155) prior to sort naive CD4 T cells ($CD4^+$, $CD27^+$, $CD45RO^-$, $CD25^-$, $CD8^-$, $CD14^-$, $CD16^-$, $CD19^-$, $CD123^-$) with MoFlo Astrios (Beckman Coulter). Sorted naive $CD4^+$ T cells purity was superior to 98%. Cells were then labeled with carboxyfluorescein succinimidyl ester (CFSE) (eBioscience#85-0850-84) or CPD670 (eBioscience#65-0840-85), counted and resuspended at 10e6/ml in X-VIVO15 (Lonza), Penicillin-Streptomicin (Invitrogen), and incubate at 37°C overnight. The next day, $CD4^+$ T cells were cultured at 1 million per ml (200µl/well in round-bottomed 96-well plates) in X-VIVO15 (Lonza), Penicillin-Streptomicin and activated with the T Cell Activation/Expansion Kit (Miltenyi) (ratio 2 cells/bead). For immunoblots, total $CD4^+$ T cells were pre-enriched by a positive selection with anti-human CD4 magnetic beads (Miltenyi) prior to sorting of naive ($CD4^+$, $CD27^+$, $CD8^-$, $CD45RO^-$, $CD25^-$) and central memory ($CD4^+$, $CD8^-$, $CD45RO^+$, $CD27^+$, $CD25^-$). Sorted CD4+ T cells were directly lysed or activated with PHA-L (5µg/ml) (SIGMA - ALDRICH#61764) and IL-2 (1000 U/ml) (Novartis) in RPMI glutamax, 10% decomplemented FBS, 10 mM HEPES (Invitrogen), Penicillin-Streptomycin, Gentamicin 50 µg/ml (Invitrogen). 48h after activation, fresh media was added with IL-2 (1000 U/ml) and cells were resuspended at 10e6/ml. Cells were collected and counted from day0 to day6 post activation for immunoblot or cytometry analysis.

Plasmids

Expression plasmids psPAX, CMV-VSV-G and HXB2 envelope were previously described [329]. NF-kB reporter lentivector was pTRH1_NFkB_dscGFP (System Biosciences). pTRIP-SFFV-BFP-2A was generated from pTRIP-SFFV [329] by replacing GFP with mTagBFP (Evrogen) followed by the 2A peptide from porcine teschovirus-1 [356]. The STING WT and STING V155M coding sequence were previously described [104]. STING HAQ sequence was cloned by PCR from pUNO1-hSTING-HAQ (Invivogen). The V155M mutation was introduced by site directed mutagenesis. STING V155M S366A, STING V155M Δ342, STING V155M Δ354, STING V155M Δ368, STING Δ342, STING Δ354 and STING Δ368 were obtained by overlapping PCR mutagenesis and cloned in pTRIP-SFFV-tagBFP-2A. In immunoprecipitation experiments, pcDNA3.1-Hygro(+) (Invitrogen) and pEF-BOS huTBK1 Flag-His (Addgene # 27241) were used. STING WT, STING V155M, STING HAQ and STING HAQ V155M were cloned in pMSCV-Hygro used in type I Interferon reporter assay in 293FT. In all final constructs, the DNA fragments originating from the PCR and encompassing the restriction sites used for cloning were fully verified by sequencing.

Lentiviral transductions in human $CD4^+$ T cells

293FT cells were transfected for lentivectors production as previously described [329]. Ratio of plasmids for transfection was, per well of 6-well plate: 0.2µg HXB2 envelope expression plasmid, 0.2µg CMV-VSV-G, 1µg psPAX2 and 1.6 µg pTRIP lentivector. Sorted naive $CD4^+$ T cells were activated 24h of activation in 96-well plates as described above. 100µl of media was removed and 100µl of 293FT

supernatant containing indicated lentivectors with 8µg/ml of protamine was added to cells. Cells were spinoculated at 1200g, 2h at 25°C. At day 2 post-transduction (day 3 post-activation), cells were seeded at 0.5 million per ml and media was changed in presence of IL-2 1000 U/ml (Novartis). At day 4 post-transduction (day 5 post-activation), cells and supernatants were harvested for analyses.

Human CD4+ T cells treatments

For type I IFN neutralization experiments, a cocktail of B18R (3µg/ml, eBioscience), anti-IFNß (2,5 µg/ml, eBioscience), anti-IFNα (1,2µg/ml, eBioscience), anti-IFNAR (0,6µg/ml, Millipore) was added at the time of CD4+ T cells transduction, Reverse transcriptase inhibitors AZT (25µM) and NVP (10µM) were used to inhibit lenvitiral transduction as negative control. To inhibit caspases, Z-VAD-FMK (50µM, RnD) was added at the time of transduction and maintained during the course of the experiment. Etoposide (25µM, Sigma) was added for 24h at day 3 post-transduction. For TNF neutralization experiments, a cocktail of anti-human-TNFRI (10µg/ml, RnD), anti-human-TNFRII (10µg/ml, RnD) and anti-human-TNF (10µg/ml, RnD), was added at the time of CD4+ T cells transduction and maintained during the course of the experiment. Recombinant TNF (RnD) was added to $CD4^+$ T transduced with NF-kB reporter lentivector 24h before analysis.

Flow cytometry analysis of human $CD4^+$ T cells

Staining was performed in FACS Buffer composed of PBS, 1% BSA (Euromedex), 1mM EDTA (GIBCO). The antibodies used were anti-human-CD25 and anti-human-CD69. Cells were stained for 15 minutes at 4°C, washed for two times and fixed in 1% paraformaldehyde (Electron Microscopy Sciences). For intracellular MX1 expression analysis, cells were fixed with 100µl/well of IC Fixation Buffer (eBioscience) for 30 minutes at room temperature and then permeabilized with 200µl of 1X Permeabilization Buffer (eBioscience) at room temperature. Cells were then centrifugated at 1700g for 3 minutes. Cells were incubated for 30 minutes at room temperature in 50µl of 1X Permeabilization Buffer where anti-MX1 antibodies (Abcam Ab95926) or Normal Rabbit IgG (Life Technologies) were diluted. Cells were washed in 200 µl of 1X Permeabilization Buffer and incubated for 30 minutes at room temperature with secondary antibody F(ab')2 Fragment Donkey Anti-Rabbit IgG (H+L) Phycoerythrin R-PE (Jackson Immuno Research). Cells were washed and resuspended in FACS buffer. For Annexin-V and PI staining, cells were washed twice with cold PBS, resuspended with 50µl of 1x Annexin-V binding buffer (BD#51-66121E) and 5µl of Annexin-V FITC (Miltenyi#130-093-060). Cells were incubated at room temperature for 15 minutes. 150 µl of 1x binding buffer with PI (2µg/ml) was added prior to acquisition. Acquisition occurred within 15 minutes after PI addition to cells. Data was acquired on a FACSVerse (BD) flow cytometer and analyzed in FlowJo.

Western Blotting analysis of human $CD4^+$ T cells

1,5 million of sorted naive and central memory or activated $CD4^+$ T cells were lysed in sample buffer [4% SDS, 20% Glycerol, 0.1M Tris-HCl (pH6.8), 0.05% BPB, 0.1M DTT]. Cellular protein lysates were resolved on 4%- 20% Biorad precast SDS-PAGE gels and transferred on nitrocellulose membrane. Membrane was blocked in 1x TBS, 0.1% Tween20 (AMRESCO) and 5% BSA (Euromedex). Proteins were blotted with antibodies as follow: IFI16 (Santa Cruz 1G7), cGAS (SIGMA HPA031700), STING (Cell Signaling D2P2F), actin (Millipore C4) in 1x TBS, 0.1% Tween20

(AMRESCO) and 5% BSA (Euromedex). Membranes were washed 3 times in 1x PBS, 0.1% Tween20 (AMRESCO). ECL signal was recorded on the ChemiDoc XRS Biorad Imager. Data was analyzed and quantified with the Image Lab software (Biorad).

Type I interferon and TNF quantification

TNF concentration was measured with a Human TNF cytometric assay (BD) according to the manufacturer's protocol. Data was acquired on a BD FACSVerse (BD) flow cytometer and analyzed in FCAP Array (BD). Type I IFN measurement was performed using the HL116 as previously described [99].

Immunoprecipitations

0.8 million of 293FT were plated in 6-well plates and transfected as previously described [99] with 1.5 µg of pEF-BOS huTBK1 Flag-His or pcDNA3.1-Hygro(+) combined with 1.5 µg of empty pTRIP-SFFV-tagBFP-2A or pTRIP-SFFV-tagBFP-2A coding for STING. 24h later, supernatant was removed and 1ml of cold PBS was used to collect 3 wells/condition and transferred to an Eppendorf tube. Cells were then centrifuged at 240g for 5 minutes. Cells pellet was resuspended with cold PBS and centrifuged again. Cells were lysed in 500µl of cold Lysis Buffer [20mM Tris-HCl pH 7.5, 150mM NaCl, 0.5% NP40 as previously described [83] complemented with 1x EDTA-free protease inhibitors cocktail (Roche), 50mM NaF and 1mM sodium orthovanadate]. Lysis was performed on ice for 30 minutes, followed by centrifugation at 7000g for 7 minutes at 4°C. Supernatant was transferred into new Eppendorf tube and 10% of the total volume was removed and collected as input cell lysate prior to adding anti-FLAG M2 Affinity gel (SIGMA#A-2220). 40µl per sample of anti-FLAG M2 Affinity gel were washed once with 1ml of complemented Lysis Buffer and resuspended in 100µl of Lysis Buffer. 100µl of anti-FLAG M2 Affinity gel were added to 400µl of lysates and incubated at 18 rpm constant wheel rotation at 4 °C overnight. Immunoprecipitates were washed five times with 1ml of Lysis Buffer. Resulting 30µl immunoprecipitates were complemented with 30µl of 2x Laemmli Buffer and incubated at 95°C for 20 minutes. 15µl of input cell lysate and of immunoprecipitates were loaded and analyzed by western blot as described above.

Lentiviral transductions in dendritic cells

Lentiviral particles and SIVmac viral like particles were produced as previously described from 293FT cells[99].

Monocytes were freshly isolated from blood of healthy donors and cultured as previously described [168]. 50,000 freshly isolated monocytes were seeded in 96-well U bottom plates and infected in a final volume of 250µl (100µl of cells at $0.5x10^6$cells/ml, 100µl of freshly produced lentiviral particles, 50µl of freshly produced SIV-VLP) with Protamine (Sigma) at 8µg/ml in presence of human recombinant GM-CSF (Miltenyi) at 10ng/ml and IL-4 (Miltenyi) at 50ng/ml.

Type I interferon was inhibited using a combination of reagents consisting of of B18R carrier-free (eBioscience) at 3µg/ml, Anti-Human IFN-alpha antibody (clone EBI-1 – eBioscience) at 1.2µg/ml, Anti-Human IFN beta Functional Grade Purified (clone A1 – eBioscience) at 2.5µg/ml and Anti-Interferon-α/β Receptor Chain 2 Antibody (clone MMHAR-2 – Millipore) at 1.5µg/ml. The type I interferon blocking reagents were added to cells 1 to 2 hours prior to infection.

Confocal microscopy

293FT cells were plated on fibronectin (10µg/ml, Sigma) coated coverslips prior to transduction with STING or control BFP lentivectors. Two days post transduction cells were fixed with 4%PFA, quenched with PBS-Glycine and permeabilized with 0.1% Triton X-100. Cells were then blocked with PBS-2%BSA-10%goat serum (Sigma), incubated with primary antibodies STING (R&D MAB7169) and GM130 (BD 610823) in PBS-2%BSA followed by 5 washes and incubation with fluroscent-labeled secondary antibodies (Life technologies – A21242, A21121) in PBS-2%BSA followed by 4 washes. Fluromount-G (Clinisciences 0100-01) was used as the mounting solution, and slides were dried in 37°C chamber for 10mins. Images were acquired on Leica SP8 60X oil immersion objective. Image analysis was done on Fiji. For analysis of mitosis, 293FT cells transduced with pTRIP-SFFV (coding for GFP) were co-cultured with cells transduced with pTRIP-SFFV-BFP-2A-STING-V155M on fibronectin-coated fluordishes (WPI). Nuclear DNA was stained using SiR-DNA Kit (Spirochrome AG) 1 hour prior to acquisition. Live imaging was carried out in a temperature controlled CO_2 chamber with a Leica SP8 20x objective. Mitosis time was calculated from nucleus envelope breakdown to the appearance of daughter cells.

Interferon reporter assay in 293FT cells

The Interferon reporter assay in 293FT cells was performed as previously described [104, 168]. In brief, 45000 293FT cells were plated in a 24-well plate. The next day, cells were transfected with 500ng of total DNA comprising 200ng of IFNß-pGL3 and 300ng of the empty vector pMSCV-hygro or pMSCV-hygro encoding the STING variants with TransIT-293 (Mirus). The next day, medium was removed and 2'3'-cGAMP (InvivoGen) was delivered with Lipofectamine 2000 (Invitrogen) transfection (1µg 2'3'-cGAMP:1µl Lipofectamine 2000) in a final volume of 500µl (final concentrations: 4µg/ml, 1.3µg/ml, 0.4µg/ml). Fresh medium was added in the case of nonstimulated cells. After 24 hours cells were washed with PBS and lysed with Passive Lysis Buffer (Promega) and 10µl of the lysate were used to perform the Luciferase assay. Luciferase activity was measured using Luciferase Assay Reagent (Promega). Luminescence was acquired on a FLUOstar OPTIMA microplate reader (BMG labtech).

cGAMP stimulation assay in THP-1 cells

Lentiviral vectors were produced as described above. THP-1 WT and THP-1 STING KO were THP-1 cells transduced with pLentiCRISPRv2 and pLentiCRISPRv2-STING_gRNA3 (gRNA sequence: AGGTACCGGAGAGTGTGCTC), respectively, and selected with puromycin. Knockout efficiency was confirmed by western blotting and cells were maintained as bulk populations. 250,000 THP-1 WT or THP-1 STING KO cells were transduced with 1 ml of lentivector with 8µg/ml protamine and 1 ml of media in 6-well plate. Transduction rates were analyzed on a BD FACSVerse cytometer and were above 95% in all cases. For stimulation, 100,000 THP-1 WT or THP-1 STING KO cells were transfected with 2'3'-cGAMP (Invivogen) with Lipofectamine 2000 (1 µl of lipofectamine 2000 per µg of cGAMP). cGAMP final concentration in culture was 4 µg/ml. Two days after transfection, cells and supernatants were harvested. Cells were fixed in 4%PFA in FACS Buffer. Live cells were quantified on a BD FACSVerse cytometer using a FSC/SSC live cell gate. Supernatants were assayed for type I interferon activity with the HL116 cell line as described above.

Flow cytometry for dendritic cells

Cell surface staining was performed in PBS, 1% BSA (Euromedex), 1mM EDTA (GIBCO), 0.01% NaN3 (AMRESCO). The antibodies used were anti-human CD86 PE (clone IT2.2 – eBioscience) and anti-human CD169 (Siglec1) APC (clone 7-239 – Miltenyi). Cells were stained for 15 minutes at 4°C, washed for two times and fixed in 1% paraformaldehyde (Electron Microscopy Sciences). Data was acquired on a FACSVerse (BD) flow cytometer and analyzed in FlowJo.

Mouse *ex vivo* phenotyping and cell sorting

C57Bl/6 or *Tmem173*$^{gt/gt}$ mice (JAX) were sacrificed and spleens and lymph nodes collected. Tissues were homogenized and passed through 100µm cell strainers. Homogenates were counted using a MACSQuant analyzer (Miltenyi, Bergisch-Gladbach, Germany) and phenotyped using antibodies against CD4, CD8a, CD62L, CD44, CD25 (all BD Biosciences). T cell subpopulations were defined as follows: Naive CD4 T cells ($CD4^+$, $CD25^-$, $CD62L^{hi}$, $CD44^{lo}$), regulatory T cells ($CD4^+$, $CD25^+$), effector memory CD4 T cells ($CD4^+$, $CD25^-$, $CD62L^{lo}$, $CD44^{hi}$).
For sorting, splenocytes and lymphocytes were pooled and T cells enriched using a negative selection kit for mouse T cells (Life Technologies) according to the manufacturer's instructions. The enriched T cell fraction was stained with antibodies against CD4, CD8a, CD62L, CD44, CD25, CD69 (all BDBiosciences) and naive CD4 T cells ($CD4^+$, $CD25^-$, $CD69^-$, $CD62L^{hi}$, $CD44^{lo}$) were sorted using a FACSAria II (BD Biosciences).

In vitro stimulation of mouse $CD4^+$ T cell

Sorted naive $CD4^+$ T cells were stained with Cell Trace Violet (Life Technologies) according to the manufacturer's instructions and plated onto flat-bottomed 96-well plates coated with anti-CD3 (1 or 10µg/ml, pre-coated at 4°C overnight) and stimulated with 0.1 or 1µg/ml anti-CD28 (BD Biosciences) in complete medium [RPMI, 100mM Hepes, 2mM Glutamax, 50uM 2-mercaptoethanol, 100U/100µg/ml Penicillin/Streptomycin, 1X Non-essential amino acids, 1mM Sodium Pyruvate, (all Gibco, Thermo Fisher), 10% FCS (eurobio, Courtaboeuf, France)] at 37°C.
At the indicated time points, activated CD4+ T cells were stained with Fixable viability dye (Ebioscience) before being fixed using BD Cytofix/Cytoperm (BDBiosciences). Cells were acquired using a MACSQuant flow cytometer and data was analysed using FlowJo software (FlowJo LLC, Ashland, OR).

Ethics

Written informed consent (parental consent for minors) was obtained from all participants. The study and protocols conform to the 1975 Declaration of Helsinki and were approved by the Comité de protection des personnes Ile de France II and the French advisory committee on data processing in medical research.

Immunophenotyping of patient PBMCs

Leukocytes were counted in an automated hematological analyzer (ABXMicrosES60, Horiba Medical, Kyoto, Japan). Monoclonal antibodies (against CD3 (HIT3a), CD4 (OKT4), CD8 (RPA-T8), CD11a (2D7), CD14 (HCD14), CD15 (W6D3), CD19 (HIB19), CD27 (MT-271), CD31 (AC128), CD34 (8G12), CR45RA (HI100), CD45 (HI30), CD49d (9F10), CD56 (B159), CD57 (HNK-1), CD95 (DX2), CD178 (MFL3), HLADR (L243), IgM (G20-127), and IgD(IA6-2)), mouse IgM, IgG1k, IgG2a and IgG2b isotype controls, and 7- aminoactinomycin D (7AAD) were

obtained from BD Biosciences (San José, CA). Monoclonal CD183 (CXCR4, clone 12G5), CD197 (CCR7, clone 4B12) and CD304 (BDCA4, clone 12C2) antibodies were purchased from Biolegend (San Diego, CA).

Proliferation assay on patient cells

PBMCs were isolated from whole blood on Ficoll gradient. Cells were then stained with CFSE and immediately stimulated with coated anti-CD3 (eBioscience) and 1µg soluble anti-CD28 (SIGMA). Cells were acquired on BD Fortessa 4 days following stimulation and data was analyzed using FlowJo.

Statistics

Statistical analyses were performed in Prism 6 (GraphPad) as indicated in figure legends.

References:

1. Iwasaki, A. & Medzhitov, R. Control of adaptive immunity by the innate immune system. *Nat Immunol* **16**, 343-353 (2015).

2. Bruchard, M. *et al.* The receptor NLRP3 is a transcriptional regulator of TH2 differentiation. *Nat Immunol* **16**, 859-870 (2015).

3. Ishikawa, H. & Barber, G.N. STING is an endoplasmic reticulum adaptor that facilitates innate immune signalling. *Nature* **455**, 674-678 (2008).

4. Burdette, D.L. *et al.* STING is a direct innate immune sensor of cyclic di-GMP. *Nature* **478**, 515-518 (2011).

5. Wu, J. *et al.* Cyclic GMP-AMP Is an Endogenous Second Messenger in Innate Immune Signaling by Cytosolic DNA. *Science* (2012).

6. Ishikawa, H., Ma, Z. & Barber, G.N. STING regulates intracellular DNA-mediated, type I interferon-dependent innate immunity. *Nature* **461**, 788-792 (2009).

7. Liu, S. *et al.* Phosphorylation of innate immune adaptor proteins MAVS, STING, and TRIF induces IRF3 activation. *Science* **347**, aaa2630 (2015).

8. Abe, T. & Barber, G.N. Cytosolic-DNA-mediated, STING-dependent proinflammatory gene induction necessitates canonical NF-kappaB activation through TBK1. *J Virol* **88**, 5328-5341 (2014).

9. Li, X.D. *et al.* Pivotal roles of cGAS-cGAMP signaling in antiviral defense and immune adjuvant effects. *Science* **341**, 1390-1394 (2013).

10. Crow, Y.J. & Manel, N. Aicardi-Goutieres syndrome and the type I interferonopathies. *Nat Rev Immunol* **15**, 429-440 (2015).

11. Meyts, I. & Casanova, J.L. A human inborn error connects the alpha's. *Nat Immunol* **17**, 472-474 (2016).

12. Jeremiah, N. *et al.* Inherited STING-activating mutation underlies a familial inflammatory syndrome with lupus-like manifestations. *J Clin Invest* **124**, 5516-5520 (2014).

13. Liu, Y. *et al.* Activated STING in a vascular and pulmonary syndrome. *N Engl J Med* **371**, 507-518 (2014).

14. Sun, L., Wu, J., Du, F., Chen, X. & Chen, Z.J. Cyclic GMP-AMP synthase is a cytosolic DNA sensor that activates the type I interferon pathway. *Science* **339**, 786-791 (2013).

15. Tang, C.H. *et al.* Agonist-Mediated Activation of STING Induces Apoptosis in Malignant B Cells. *Cancer Res* **76**, 2137-2152 (2016).

16. Yi, G. *et al.* Single nucleotide polymorphisms of human STING can affect innate immune response to cyclic dinucleotides. *PLoS One* **8**, e77846 (2013).

17. Jin, L. *et al.* Identification and characterization of a loss-of-function human MPYS variant. *Genes Immun* **12**, 263-269 (2011).

18. Tanaka, Y. & Chen, Z.J. STING specifies IRF3 phosphorylation by TBK1 in the cytosolic DNA signaling pathway. *Sci Signal* **5**, ra20 (2012).

19. Kranzusch, P.J. *et al.* Ancient Origin of cGAS-STING Reveals Mechanism of Universal 2',3' cGAMP Signaling. *Mol Cell* **59**, 891-903 (2015).

20. Pillai, S. *et al.* Tank binding kinase 1 is a centrosome-associated kinase necessary for microtubule dynamics and mitosis. *Nat Commun* **6**, 10072 (2015).

21. Pannicke, U. *et al.* Deficiency of innate and acquired immunity caused by an IKBKB mutation. *N Engl J Med* **369**, 2504-2514 (2013).

22. Torres, J.M. *et al.* Inherited BCL10 deficiency impairs hematopoietic and nonhematopoietic immunity. *J Clin Invest* **124**, 5239-5248 (2014).

23. Courtois, G. *et al.* A hypermorphic IkappaBalpha mutation is associated with autosomal dominant anhidrotic ectodermal dysplasia and T cell immunodeficiency. *J Clin Invest* **112**, 1108-1115 (2003).

24. Greil, J. *et al.* Whole-exome sequencing links caspase recruitment domain 11 (CARD11) inactivation to severe combined immunodeficiency. *J Allergy Clin Immunol* **131**, 1376-1383 e1373 (2013).

25. Stepensky, P. *et al.* Deficiency of caspase recruitment domain family, member 11 (CARD11), causes profound combined immunodeficiency in human subjects. *J Allergy Clin Immunol* **131**, 477-485 e471 (2013).

26. Janeway, C.A., Jr. & Medzhitov, R. Innate immune recognition. *Annu Rev Immunol* **20**, 197-216 (2002).

27. Chien, Y. *et al.* Control of the senescence-associated secretory phenotype by NF-kappaB promotes senescence and enhances chemosensitivity. *Genes Dev* **25**, 2125-2136 (2011).

28. Colanzi, A. & Sutterlin, C. Signaling at the Golgi during mitosis. *Methods Cell Biol* **118**, 383-400 (2013).

29. Pourcelot, M. *et al.* The Golgi apparatus acts as a platform for TBK1 activation after viral RNA sensing. *BMC Biol* **14**, 69 (2016).

30. Onorati, M. *et al.* Zika Virus Disrupts Phospho-TBK1 Localization and Mitosis in Human Neuroepithelial Stem Cells and Radial Glia. *Cell Rep* **16**, 2576-2592 (2016).

31. Gao, D. *et al.* Cyclic GMP-AMP synthase is an innate immune sensor of HIV and other retroviruses. *Science* **341**, 903-906 (2013).

32. Yan, N., Regalado-Magdos, A.D., Stiggelbout, B., Lee-Kirsch, M.A. & Lieberman, J. The cytosolic exonuclease TREX1 inhibits the innate immune response to human immunodeficiency virus type 1. *Nat Immunol* **11**, 1005-1013 (2010).

33. Lahaye, X. *et al.* The capsids of HIV-1 and HIV-2 determine immune detection of the viral cDNA by the innate sensor cGAS in dendritic cells. *Immunity* **39**, 1132-1142 (2013).

34. Lahaye, X. *et al.* Nuclear Envelope Protein SUN2 Promotes Cyclophilin-A-Dependent Steps of HIV Replication. *Cell Rep* (2016).

35. Kim, J.H. *et al.* High cleavage efficiency of a 2A peptide derived from porcine teschovirus-1 in human cell lines, zebrafish and mice. *PLoS One* **6**, e18556 (2011).

36. Gentili, M. *et al.* Transmission of innate immune signaling by packaging of cGAMP in viral particles. *Science* **349**, 1232-1236 (2015).

Acknowledgments: Funding: SC was successively supported by Institut Curie and by Sidaction. NJ was successively supported by FRM grant FDT20140930816, by Institut Curie and by Agence Nationale de Recherche sur le Sida et les Hépatites Virales (ANRS). This work was supported by ATIP-Avenir program, ANRS (France REcherche Nord & Sud Sida-hiv Hépatites), Ville de Paris Emergence program, European FP7 Marie Curie Actions, LABEX VRI (ANR-10-LABX-77), LABEX DCBIOL (ANR-10-IDEX-0001-02 PSL* and ANR-11-LABX-0043), ACTERIA Foundation, Fondation Schlumberger pour l'Education et la Recherche (FSER) and European Research Council grant 309848 HIVINNATE for NM and by the National Research Agency (ANR-14-CE14-0026 Lumugène) and the Cancer national institute (INCa convention 2014-1-PL BIO-10-INSERM 5-1) for FRL.

FIGURE 1

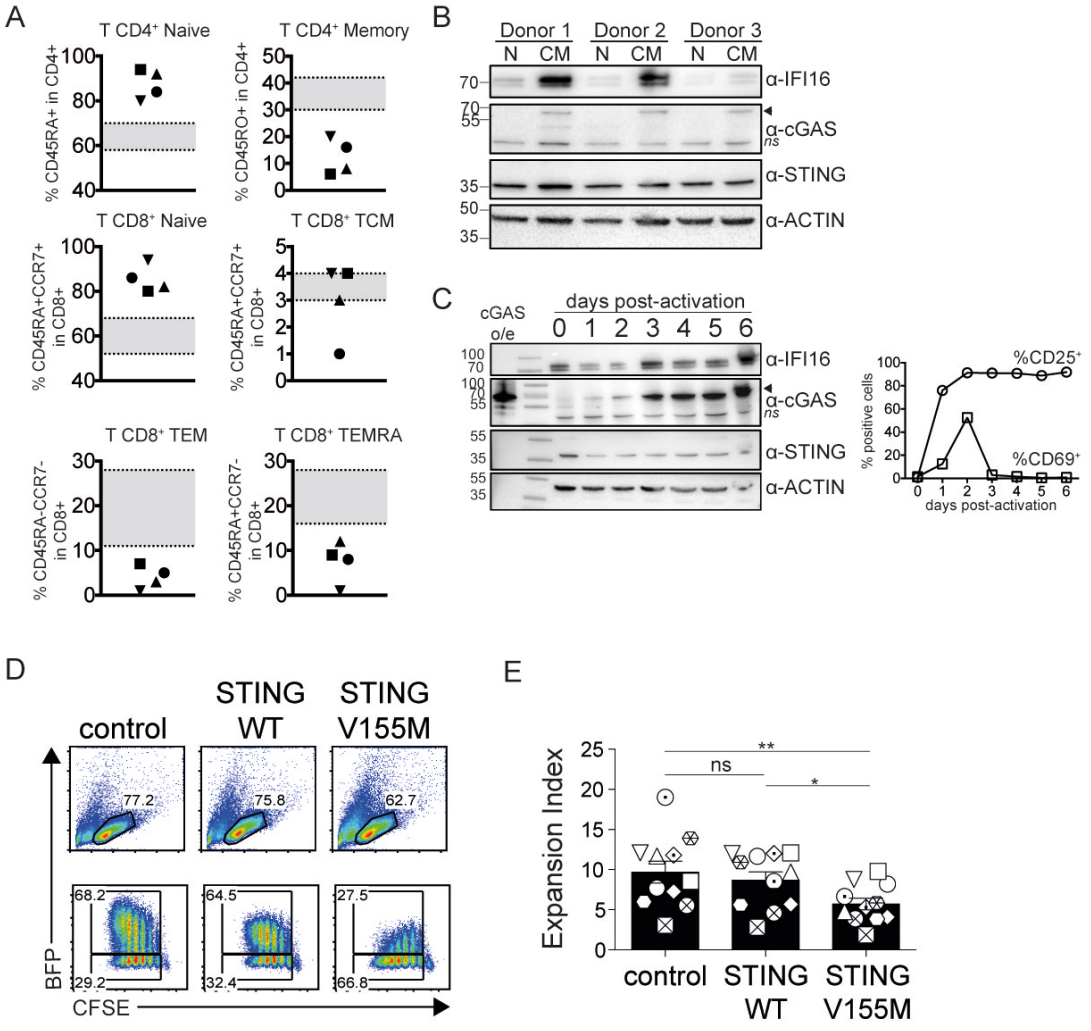
A
T CD4+ Naive
T CD4+ Memory
% CD45RA+ in CD4+
% CD45RO+ in CD4+
T CD8+ Naive
T CD8+ TCM
% CD45RA+CCR7+ in CD8+
T CD8+ TEM
T CD8+ TEMRA
% CD45RA-CCR7- in CD8+
% CD45RA+CCR7- in CD8+
B
Donor 1
Donor 2
Donor 3
N CM N CM N CM
α-IFI16
α-cGAS
ns
α-STING
α-ACTIN
C
cGAS o/e
days post-activation
0 1 2 3 4 5 6
%CD25+
%CD69+
% positive cells
D
control
STING WT
STING V155M
77.2
75.8
62.7
68.2
29.2
64.5
32.4
27.5
66.8
BFP
CFSE
E
Expansion Index
ns
control
STING WT
STING V155M

Figure 1 T cell imbalance induced by constitutive active STING.
(A) Frequency of naive and memory $CD4^+$ and $CD8^+$ T cell compartments in patients carrying activating TMEM173 mutations. TCM = T central memory; TEM = T effector memory; TEMRA = T effector memory CD45RA+. Age-matched expected values are indicated in grey.
(B) Immunoblot of cGAS, STING and IFI16 and actin expression in resting naive or central memory CD4+ T cells from blood of healthy donors (n=3 donors).
(C) Immunoblot of cGAS, STING, IFI16 and actin (left panel) and surface expression of CD25 and CD69 (right panel) in naive CD4 T cells from day 0 to day 6 after activation with PHA and IL-2 (representative of n=2 donors).
(D) Proliferation profile of naive $CD4^+$ T cells 4 days after transduction with BFP lentivectors coding for control, STING WT or STING V155M.
(E) Expansion index in BFP-positive and proliferating cells as in D (n=11 and mean ± sem, one-way ANOVA test, Tukey's correction; ns=not significant, *$p<0.05$ and **$p<0.01$).

FIGURE 2

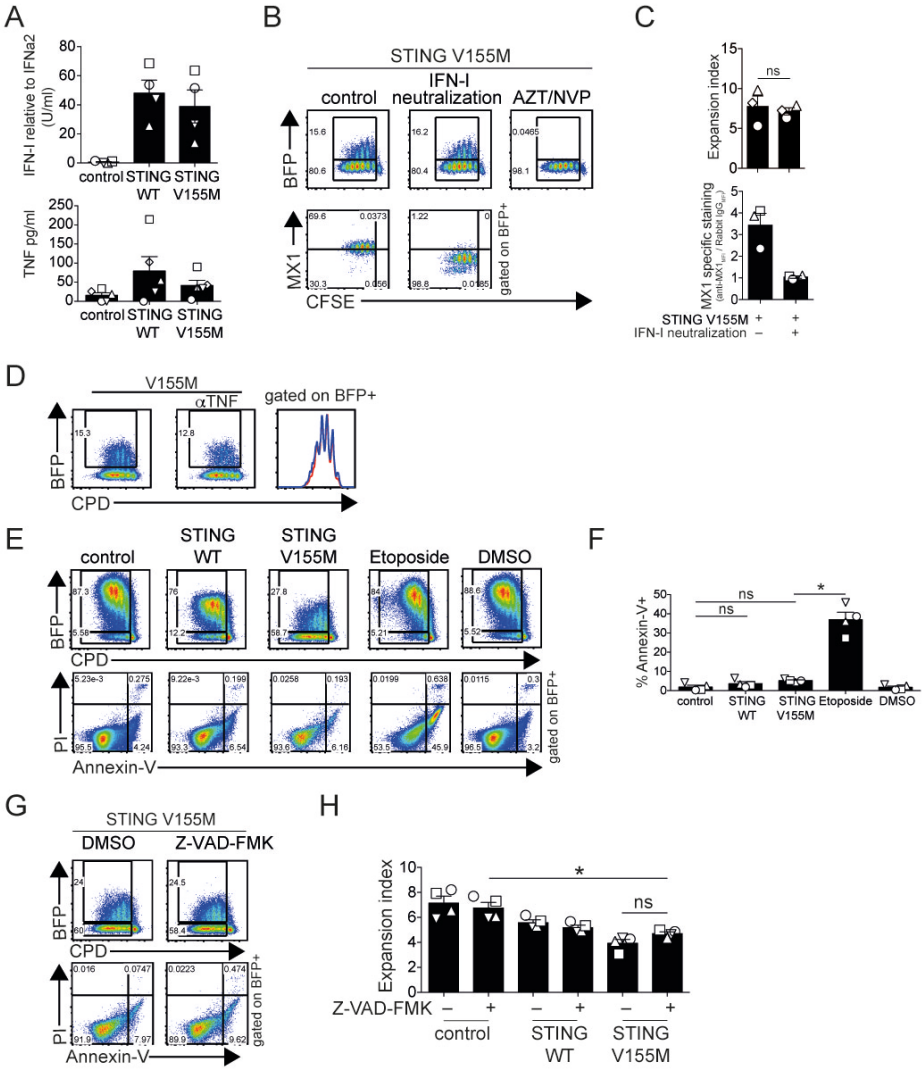
A
IFN-I relative to IFNa2 (U/ml)
control
STING WT
STING V155M
TNF pg/ml
B
STING V155M
control
IFN-I neutralization
AZT/NVP
BFP
MX1
CFSE
gated on BFP+
C
Expansion index
ns
MX1 specific staining
STING V155M
IFN-I neutralization
D
V155M
αTNF
gated on BFP+
BFP
CPD
E
control
STING WT
STING V155M
Etoposide
DMSO
BFP
CPD
PI
Annexin-V
gated on BFP+
F
% Annexin-V+
ns
*
control
STING WT
STING V155M
Etoposide
DMSO
G
STING V155M
DMSO
Z-VAD-FMK
BFP
CPD
PI
Annexin-V
gated on BFP+
H
Expansion index
*
ns
Z-VAD-FMK
control
STING WT
STING V155M

Figure 2 STING has an intrinsic anti-proliferative activity in T cells.
(A) Type I interferon activity (top panel; n=4 donors) and TNF concentration (bottom panel n=5 donors) in supernatants of naive $CD4^+$ T cells 4 days after transduction with control, STING WT, STING V155M BFP lentivectors.
(B) BFP and intracellular MX1 expression and proliferation profile (CFSE) after type I interferon neutralization or AZT/NVP treatment (BFP only) in naive $CD4^+$ T cells transduced with STING V155M BFP lentivectors.
(C) Expansion Index (top panel) and MX1 specific intracellular staining (bottom panel) in proliferating BFP-positive cells as in B (n=3 and mean ± sem, one-way ANOVA test, Tukey's correction, ns=not significant and *p<0.05).
(D) BFP expression and proliferation profile (CPD) after TNF neutralization in naive CD4+ T cells transduced with control, STING WT or STING V155M BFP lentivectors.
(E) Annexin-V and propidium iodide (PI) staining in naive $CD4^+$ T cells transduced with control, STING WT or STING V155M BFP lentivectors, or treated with etoposide (25μM) or DMSO.
(F) Frequency of Annexin-V-positive cells in BFP-positive cells as in E (n=4 and mean ± sem, one-way ANOVA test, Tukey's correction; ns= not significant, *p<0.05 and **p<0.01).
(G) BFP expression, proliferation profile, Annexin-V and PI staining in naive CD4+ T cells transduced with STING V155M BFP lentivectors after treatment with Z-VAD-FMK (50μM) or DMSO.
(H) Expansion index in BFP-positive naive CD4+ T transduced with control, STING WT or STING V155M BFP lentivectors after treatement with Z-VAD-FMK or DMSO (n=4 and mean ± sem, one-way ANOVA test, Tukey's correction, ns= not significant and *p<0.05).

FIGURE 3

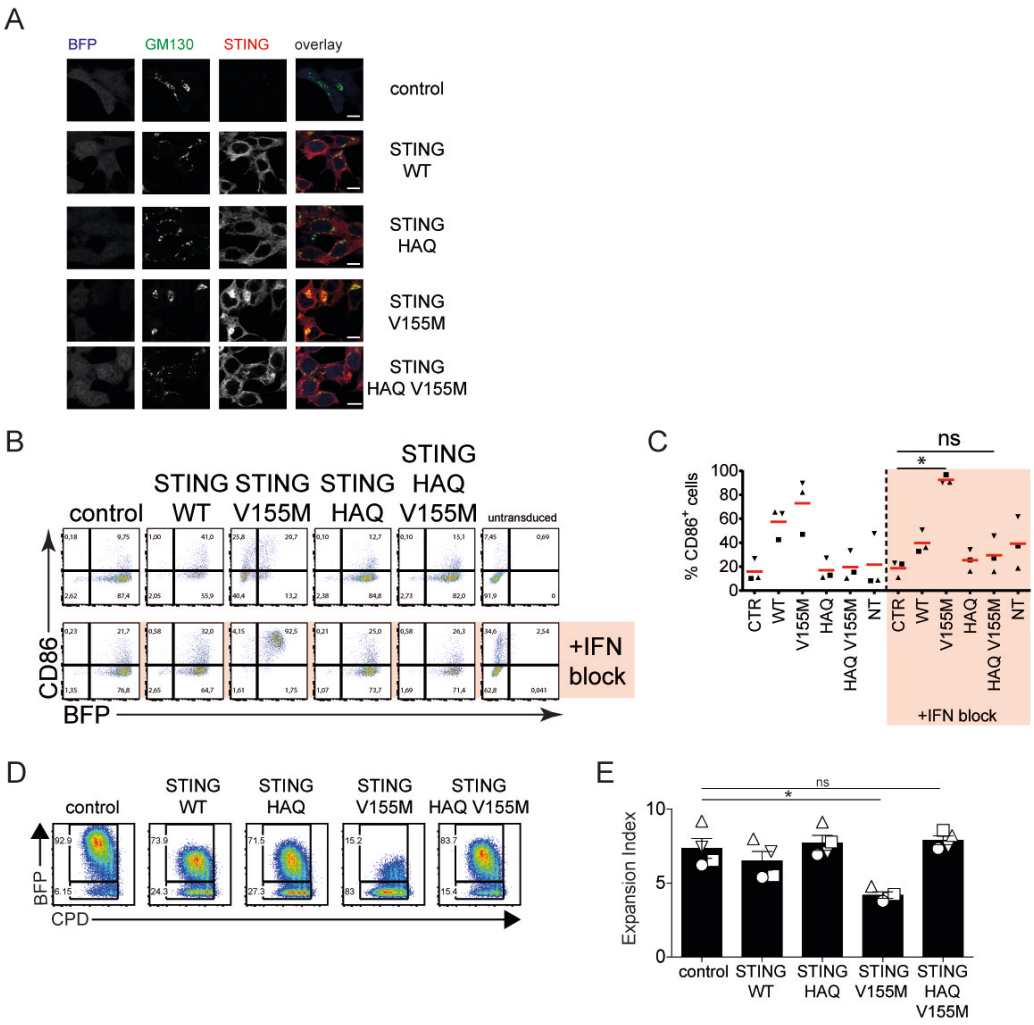
A
BFP
GM130
STING
overlay
control
STING WT
STING HAQ
STING V155M
STING HAQ V155M
B
control
STING WT
STING V155M
STING HAQ
STING HAQ V155M
untransduced
CD86
BFP
+IFN block
C
% CD86+ cells
ns
*
CTR
WT
V155M
HAQ
HAQ V155M
NT
+IFN block
D
control
STING WT
STING HAQ
STING V155M
STING HAQ V155M
BFP
CPD
E
Expansion Index
ns
*
control
STING WT
STING HAQ
STING V155M
STING HAQ V155M

Figure 3 STING signaling activity is required to inhibit T cell proliferation
(A) Staining for STING and GM130 and BFP expression in 293FT cells transduced with control, STING WT, STING HAQ, STING V155M or STING HAQ V155M lentivectors (portion of 1 field out of 4 fields, representative of 3 independent experiments, bar=10μM).
(B) BFP and CD86 expression in DCs 4 days after transduction with control, STING WT, STING HAQ, STING V155M or STING HAQ V155M BFP lentivectors and neutralization of type I IFN.
(C) CD86 expression as in B (n=3 independent donors combined from two experiments; one-way ANOVA with post-hoc Tukey test for stats; *$p < 0.05$, ns = not significant).
(D) Naive $CD4^+$ T cells proliferation profile (CPD) 4 days after transduction with BFP lentivectors coding for control, STING WT, STING HAQ, STING V155M or STING HAQ V155M.
(E) Expansion index in BFP-positive cells as in D (n=4 and mean ± sem, one-way ANOVA test, Dunnett's correction; ns= not significant, *$p<0.05$).

FIGURE 4

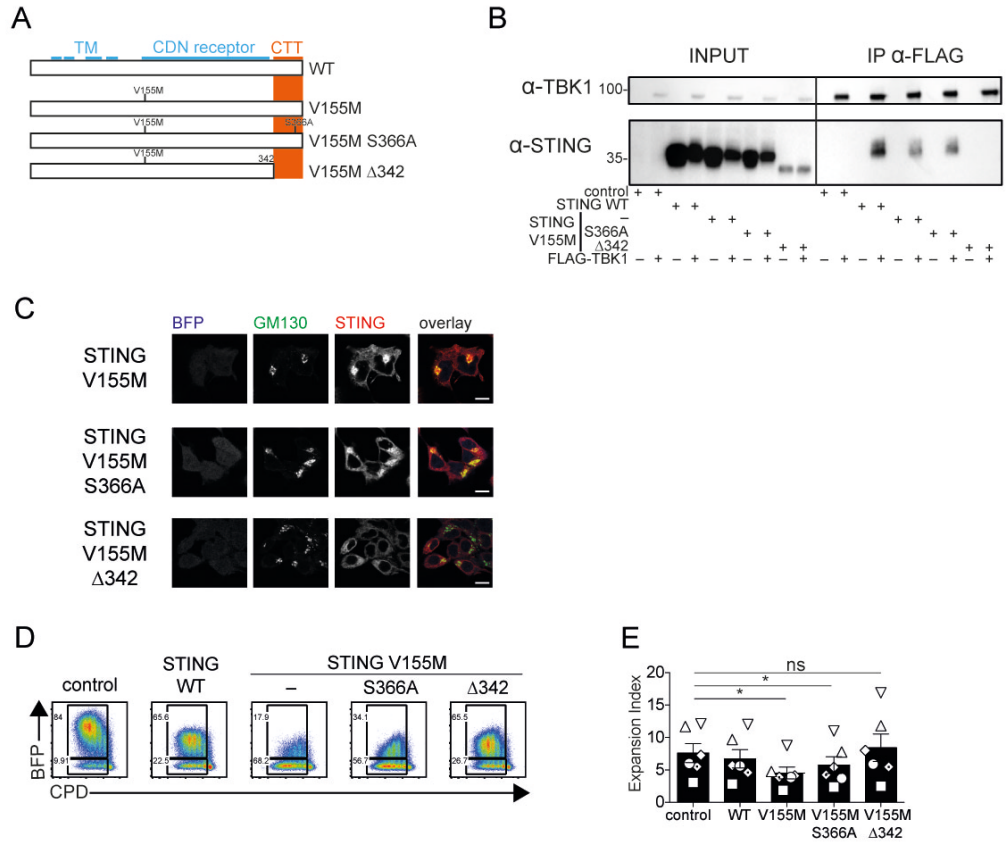
A
TM
CDN receptor
CTT
WT
V155M
V155M S366A
V155M Δ342
B
INPUT
IP α-FLAG
α-TBK1
α-STING
100
35
control
STING WT
STING V155M
S366A
Δ342
FLAG-TBK1
C
BFP
GM130
STING
overlay
STING V155M
STING V155M S366A
STING V155M Δ342
D
control
STING WT
STING V155M
–
S366A
Δ342
BFP
CPD
E
Expansion Index
ns
control
WT
V155M
V155M S366A
V155M Δ342

Figure 4 The anti-proliferative activity of STING requires the C-terminal tail but not the IRF3 binding site.
(A) Schematics of STING S366A and Δ342 mutants. TM denotes transmembrane domains, CDN denotes cyclic dinucleotide receptor domain, CTT denotes the C-terminal tail [345].
(B) Immunoprecipitation of STING mutants by TBK1. 293FT cells were transfected with control, STING WT, V155M, V155M S366A or V155M Δ342 plasmids for 24h. Cell lysates were prepared and immunoprecipitated with anti-FLAG beads. Input cell lysates and immunoprecipitates were analysed by western blot with indicated antibodies.
(C) Staining for STING and GM130 and BFP expression in 293FT cells transduced with STING V155M, V155M S366A or V155M Δ342 BFP lentivectors (portion of 1 field out of 4 fields, representative of 3 independent experiments, bar=10μM).
(D) Naive $CD4^+$ T cell proliferation profile (CPD) 4 days after transduction with control, STING WT, V155M, V155M S366A or V155M Δ342 BFP lentivectors.
(E) Expansion Index in BFP-positive cells naive CD4+ T cells as in D (n=6 and mean ± sem, one-way ANOVA test, Dunnett's correction; ns= not significant, *$p<0.05$).

FIGURE 5

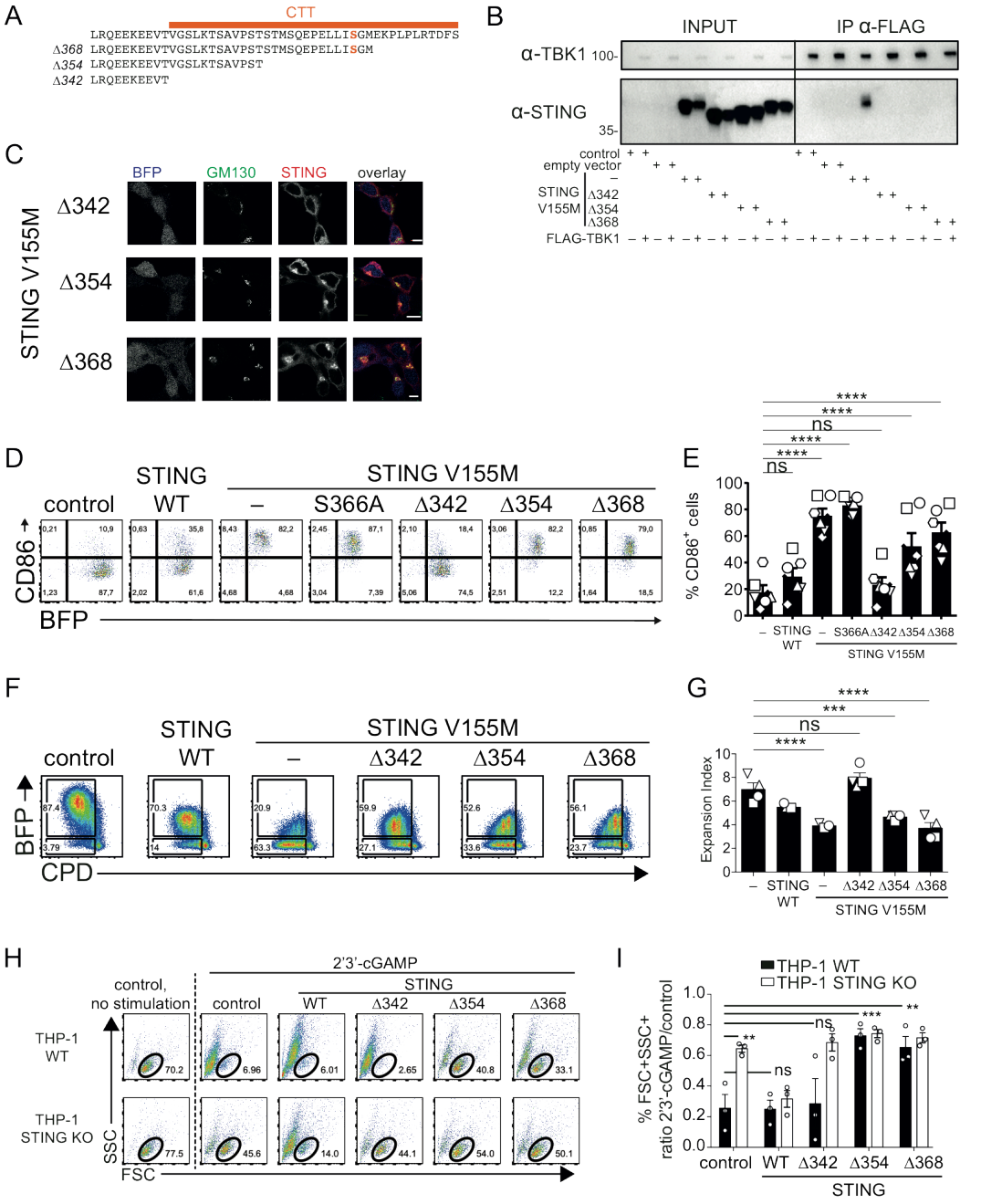
A
CTT
LRQEEKEEVTVGSLKTSAVPSTSTMSQEPELLISGMEKPLPLRTDFS
Δ368 LRQEEKEEVTVGSLKTSAVPSTSTMSQEPELLISGM
Δ354 LRQEEKEEVTVGSLKTSAVPST
Δ342 LRQEEKEEVT
B
INPUT
IP α-FLAG
α-TBK1 100-
α-STING
35-
control
empty vector
STING V155M
Δ342
Δ354
Δ368
FLAG-TBK1
C
BFP
GM130
STING
overlay
STING V155M
Δ342
Δ354
Δ368
D
control
STING WT
STING V155M
–
S366A
Δ342
Δ354
Δ368
CD86
BFP
E
% CD86+ cells
****
****
ns
****
****
ns
STING WT
S366A
Δ342
Δ354
Δ368
STING V155M
F
control
STING WT
STING V155M
–
Δ342
Δ354
Δ368
BFP
CPD
G
Expansion Index
****
***
ns
****
STING WT
Δ342
Δ354
Δ368
STING V155M
H
2'3'-cGAMP
STING
control, no stimulation
control
WT
Δ342
Δ354
Δ368
THP-1 WT
THP-1 STING KO
SSC
FSC
I
THP-1 WT
THP-1 STING KO
% FSC+SSC+ ratio 2'3'-cGAMP/control
ns
ns
control
WT
Δ342
Δ354
Δ368
STING

Figure 5 A distinct functional domain of STING inhibits T cell proliferation.
(A) Schematics of STING C-terminal tail deletion mutants Δ342, Δ354 and Δ368. Serine 366 is indicated in bold orange.
(B) Immunoprecipitation of STING mutants by TBK1. 293FT cells were transfected with control, STING V155M, V155M Δ342, V155M Δ354 or V155M Δ368 plasmids for 24h. Cell lysates were prepared and immunoprecipitated with anti-FLAG beads. Input cell lysates and immunoprecipitates were analysed by western blot with indicated antibodies.
(C) Staining for STING and GM130 and BFP expression in 293FT cells transduced with STING V155M Δ342, V155M Δ354 or V155M Δ368 BFP lentivectors (portion of 1 field out of 4 fields, bar=10μM).
(D) CD86 and BFP expression in dendritic cells transduced with control, STING WT, V155M,V155M S366A, V155M Δ342, V155M Δ354 and V155M Δ368 BFP lentivectors with type I interferon neutralization.
(E) CD86 and BFP expression as in D (n=6 independent donors combined from 3 independent experiments; One-Way ANOVA with Dunnett's multiple comparisons test, ****p<0.0001, ns: non-significant).
(F) Cell proliferation profile (CPD) in naive CD4+ T cells transduced with control, STING WT, V155M, V155M Δ342, V155M Δ354 or V155M Δ368 BFP lentivectors.
(G) Expansion Index in BFP-positive cells as in F (n=4 and mean ± sem, one-way ANOVA test, Dunnett's correction; ns= not significant, ***p<0.001 and ****p<0.0001).
(H) Induction of cell death by 2'3'-cGAMP with lipofactamin in THP-1 WT or THP-1 STING KO cells, transduced by the indicated BFP lentivector.
(I) Ratio of live cells (FSC^+SSC^+ live cell gate) after 2'3'-cGAMP stimulation vs. no stimulation is shown, as in H (n=3 independent experiments, One-Way ANOVA with Tukey's multiple comparisons test; ns= not significant, **p<0.01 and ***p<0.001).

FIGURE 6

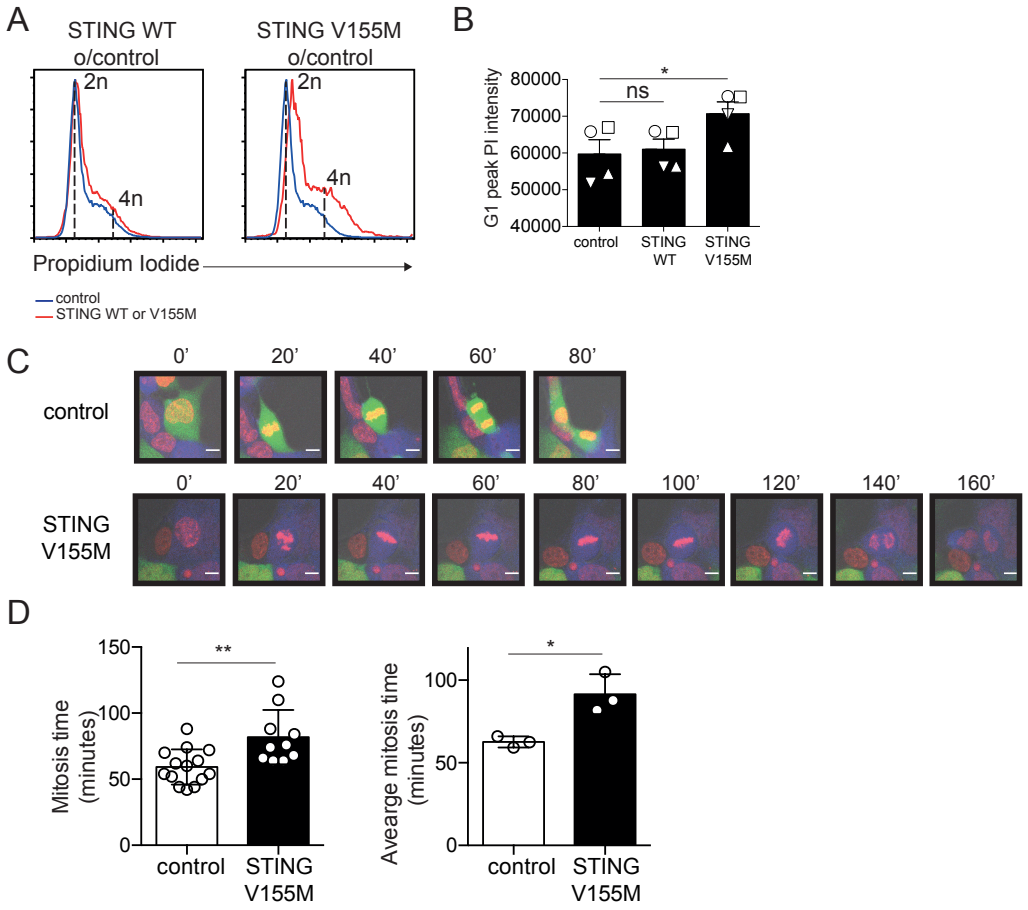
A
STING WT
o/control
STING V155M
o/control
2n
4n
2n
4n
Propidium Iodide
control
STING WT or V155M
B
G1 peak PI intensity
80000
70000
60000
50000
40000
*
ns
control
STING WT
STING V155M
C
0'
20'
40'
60'
80'
control
0'
20'
40'
60'
80'
100'
120'
140'
160'
STING V155M
D
Mitosis time (minutes)
150
100
50
0
**
control
STING V155M
Avearge mitosis time (minutes)
100
50
0
*
control
STING V155M

Figure 6 STING V155M induces mitotic errors.
(A) Propidium Iodide (PI) staining in naive CD4+ T cells 4 days after transduction with control, STING WT or STING V155M BFP lentivectors.
(B) PI intensity of G1 peak (Mode of linear PE) as in A (n=4 and mean ± sem, one-way ANOVA test, Dunnett's correction; ns= not significant, *p<0.05).
(C) Snapshots of a representative control cell expressing GFP (top) or STING V155M (bottom) and undergoing cell division. DNA (Red), BFP-2A-V155M (blue), control cells expressing GFP (green) (bar = 10μM).
(D) (Left) Mitosis time calculated in 293FT cells expressing STING V155M or control (GFP or untransduced). (Right) Average mitosis time from three independent experiments (n=3 and mean ± sd, unpaired t-test, *p<0.05, **p<0.005).

FIGURE 7

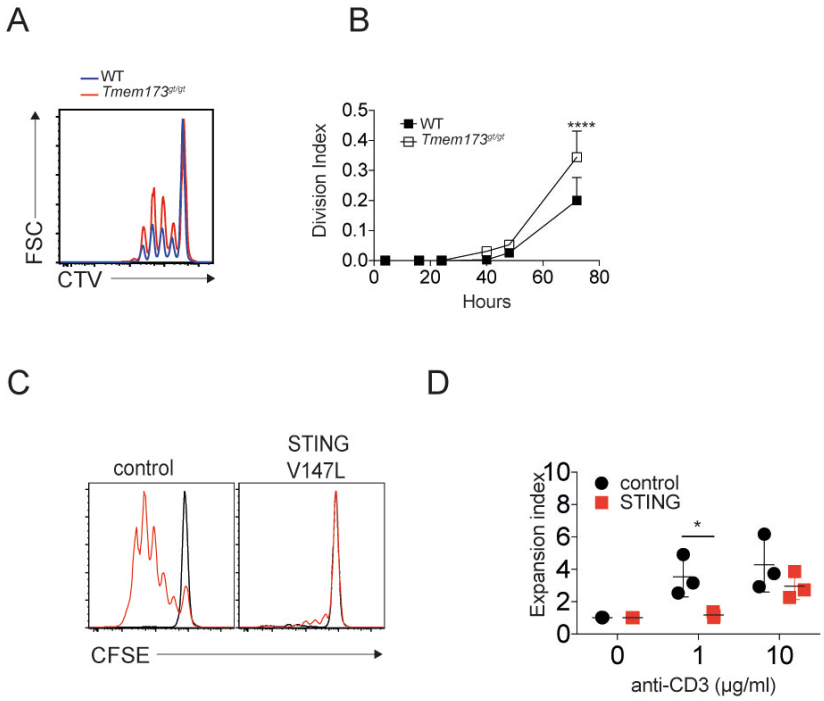
A
B
WT
Tmem173gt/gt
FSC
CTV
Division Index
0.5
0.4
0.3
0.2
0.1
0.0
0
20
40
60
80
Hours
****
C
D
control
STING
V147L
CFSE
Expansion index
10
8
6
4
2
0
control
STING
*
0
1
10
anti-CD3 (µg/ml)

Figure 7 STING inhibits T cell proliferation in normal and pathological conditions.
(A) Proliferation profile (CTV) of WT (blue) or *Tmem173*$^{gt/gt}$ (red) murine CD4^{+} T cells 72hrs after activation with 1µg/ml αCD3/αCD28.
(B) Division index as in A (n=4 mice combined from 2 independent experiments, mean +sem, two-Way ANOVA with Sidak's multiple comparison test, ****p<0.0001)**.**
(C) Proliferation profile (CFSE) of CD3^{+} T cells from a patient carrying an activating *STING* mutation (V147L) or from a healthy control upon PBMC stimulation with anti-CD3 (1µg/ml) and anti-CD28 (1µg/ml) for 4 days. Black peaks indicate unstimulated cells and red peaks correspond to the stimulated condition.
(D) Expansion index as in C for two patients carrying the V155M mutation and one patient carrying the V147L mutation in STING (n=3 donors, mean ± sem, two-Way ANOVA with Sidak's multiple comparison test, *p<0.05).

FIGURE S1

A

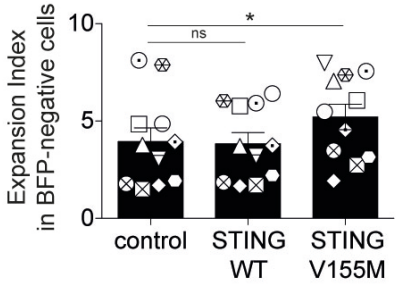
Expansion Index
in BFP-negative cells
10
5
0
ns
*
control
STING
WT
STING
V155M

Supplementary Figure 1 T cell imbalance induced by constitutive active STING, related to figure 1.
(A) Expansion index in BFP-negative and proliferating cells as in figure 1D (n=11 and mean ± sem, one-way ANOVA test, Tukey's correction; ns= not significant, *p<0.05 and **p<0.01).

FIGURE S2

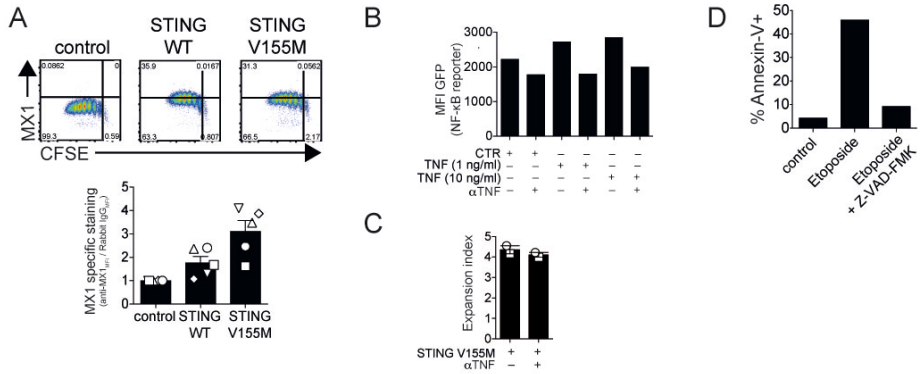
A
control
STING WT
STING V155M
MX1
CFSE
MX1 specific staining
control
STING WT
STING V155M
B
MFI GFP (NF-κB reporter)
CTR
TNF (1 ng/ml)
TNF (10 ng/ml)
αTNF
C
Expansion index
STING V155M
αTNF
D
% Annexin-V+
control
Etoposide
Etoposide + Z-VAD-FMK

Supplementary Figure 2 STING has an intrinsic anti-proliferative activity in T cells, related to figure 2.
(A) Intracellular MX1 expression and proliferation profile (CFSE) in naive $CD4^+$ T cells transduced with control, STING WT, STING V155M BFP lentivectors (n=5 donors).
(B) GFP expression in naive $CD4^+$ T cells transduced with a lentivector coding for GFP under the control of a NF-κB reporter promoter, after treatment with recombinant TNF or neutralizing anti-TNF antibody.
(C) Expansion index as in figure 2D (n=2).
(D) Annexin-V staining in naive CD4+ T cells as in figure 2E, after treatment with etoposide (25μM) or etoposide with Z-VAD-FMK (50μM).

FIGURE S3

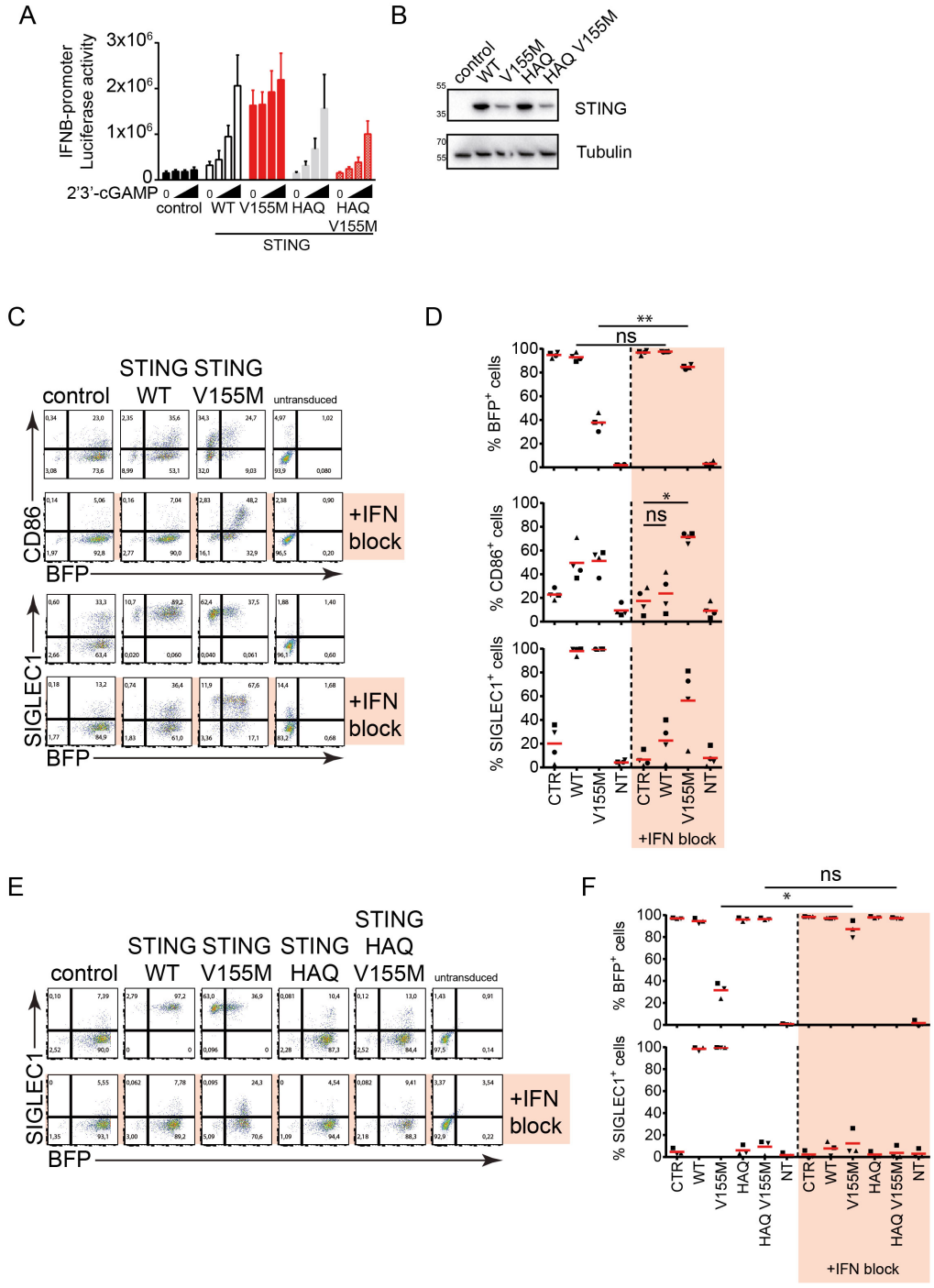
A
IFNB-promoter Luciferase activity
3x10^6
2x10^6
1x10^6
0
2'3'-cGAMP
control WT V155M HAQ HAQ V155M
STING
B
control WT V155M HAQ HAQ V155M
STING
Tubulin
C
STING STING
control WT V155M untransduced
CD86
BFP
+IFN block
SIGLEC1
BFP
+IFN block
D
% BFP+ cells
% CD86+ cells
% SIGLEC1+ cells
ns
*
**
CTR WT V155M NT CTR WT V155M NT
+IFN block
E
STING STING STING STING
control WT V155M HAQ V155M untransduced
SIGLEC1
BFP
+IFN block
F
% BFP+ cells
% SIGLEC1+ cells
ns
*
CTR WT V155M HAQ HAQ V155M NT CTR WT V155M HAQ HAQ V155M NT
+IFN block

Supplementary Figure 3 STING signaling activity is required to inhibit T cell proliferation, related to figure 3.
(A) Luciferase activity in 293FT cells co-transfected with empty vector, STING variants and a Luciferase-coding plasmid under control of the human IFNB promoter, stimulated with increasing amounts of synthetic 2'3' cGAMP (top dose 4μg/ml - three fold dilutions) (n=3 independent experiments, mean and sem plotted).
(B) Immunoblot of STING and actin expression in 293FT transfected cells as in A.
(C) Neutralization of type I IFN enables lentiviral transduction of DCs with STING V155M, revealing the ability of STING V155M to activate DCs. BFP, CD86 and SIGLEC1 expression in DCs 4 days after transduction with control, STING WT or STING V155M BFP lentivectors and neutralization of type I IFN.
(D) BFP, CD86 and SIGLEC1 expression as in C (n=4 independent donors combined from two experiments; one-way ANOVA with post-hoc Tukey test for stats; *$p < 0.05$, ns = not significant).
(E) BFP and SIGLEC1 expression in DCs 4 days after transduction with control, STING WT, STING HAQ, STING V155M or STING HAQ V155M BFP lentivectors and neutralization of type I IFN.
(F) BFP and SIGLEC1 expression as in E (n=3 independent donors combined from two experiments; one-way ANOVA with post-hoc Tukey test for stats; *$p < 0.05$, ns = not significant).

FIGURE S4

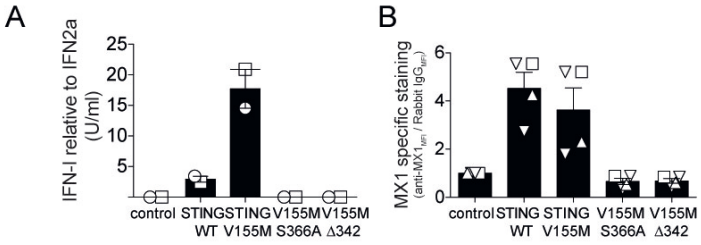
A
IFN-I relative to IFN2a (U/ml)
25
20
15
10
5
control
STING WT
STING V155M
V155M S366A
V155M Δ342
B
MX1 specific staining
6
4
2
0
control
STING WT
STING V155M
V155M S366A
V155M Δ342

Supplementary Figure 4 The anti-proliferative activity of STING requires the C-terminal tail but not the IRF3 binding site, related to figure 4.
(A) Type I interferon activity in supernatants of naive $CD4^+$ T cells 4 days after transduction with control, STING WT, V155M, V155M S366A or V155M Δ342 BFP lentivectors (n=2 independent donors).
(B) Specific intracellular MX1 staining in naive $CD4^+$ T cells 4 days after transduction with control, STING WT, V155M, V155M S366A or V155M Δ342 BFP lentivectors (n=2).

FIGURE S5

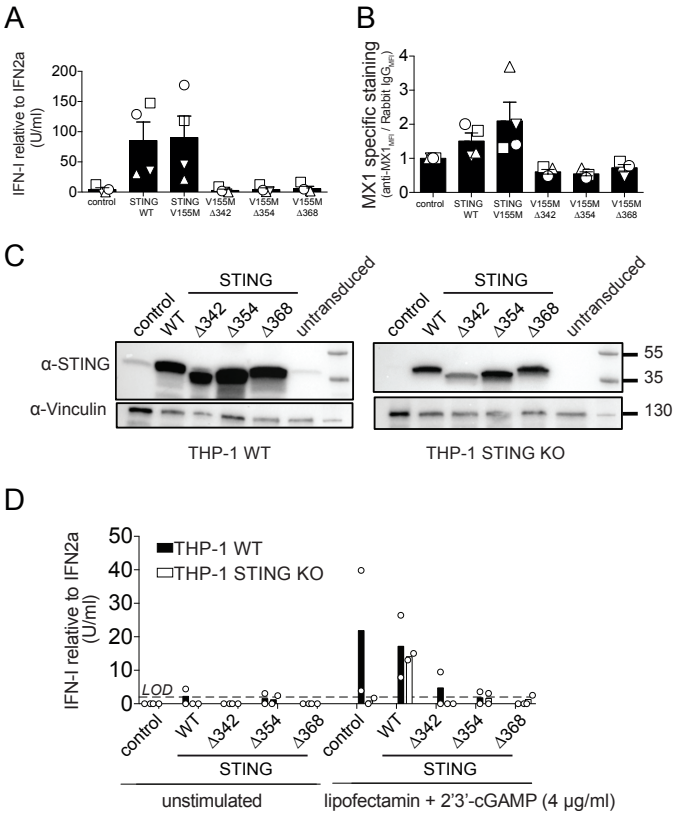
A
IFN-I relative to IFN2a (U/ml)
200
150
100
50
0
control
STING WT
STING V155M
V155M Δ342
V155M Δ354
V155M Δ368
B
MX1 specific staining
(anti-MX1 / Rabbit IgG)
4
3
2
1
0
control
STING WT
STING V155M
V155M Δ342
V155M Δ354
V155M Δ368
C
STING
control
WT
Δ342
Δ354
Δ368
untransduced
α-STING
α-Vinculin
55
35
130
THP-1 WT
THP-1 STING KO
D
IFN-I relative to IFN2a (U/ml)
THP-1 WT
THP-1 STING KO
50
40
30
20
10
0
LOD
control
WT
Δ342
Δ354
Δ368
STING
unstimulated
lipofectamin + 2'3'-cGAMP (4 µg/ml)

Supplementary Figure 5 A distinct functional domain of STING inhibits T cell proliferation, related to figure 5.
(A) Type I interferon activity in supernatants of naive $CD4^+$ T cells 4 days after transduction with control, STING WT, V155M, V155M Δ342, V155M Δ354 or V155M Δ368 BFP lentivectors (n=2 independent donors).
(B) Intracellular staining of MX1 in naive $CD4^+$ T cells 4 days after transduction with control, STING WT, V155M, V155M Δ342, V155M Δ354 or V155M Δ368 BFP lentivectors (n=2 independent donors).
(C) Immunoblot of STING and vinculin in THP-1 WT and THP-1 STING KO cells transduced with the indicated BFP lentivectors.
(D) Type I interferon activity in supernatants of THP-1 WT and THP-1 STING KO cells transduced with the indicated BFP lentivectors, after no stimulation or stimulation with 2'3'-cGAMP-lipofectamin (n=2 independent experiments).

FIGURE S6

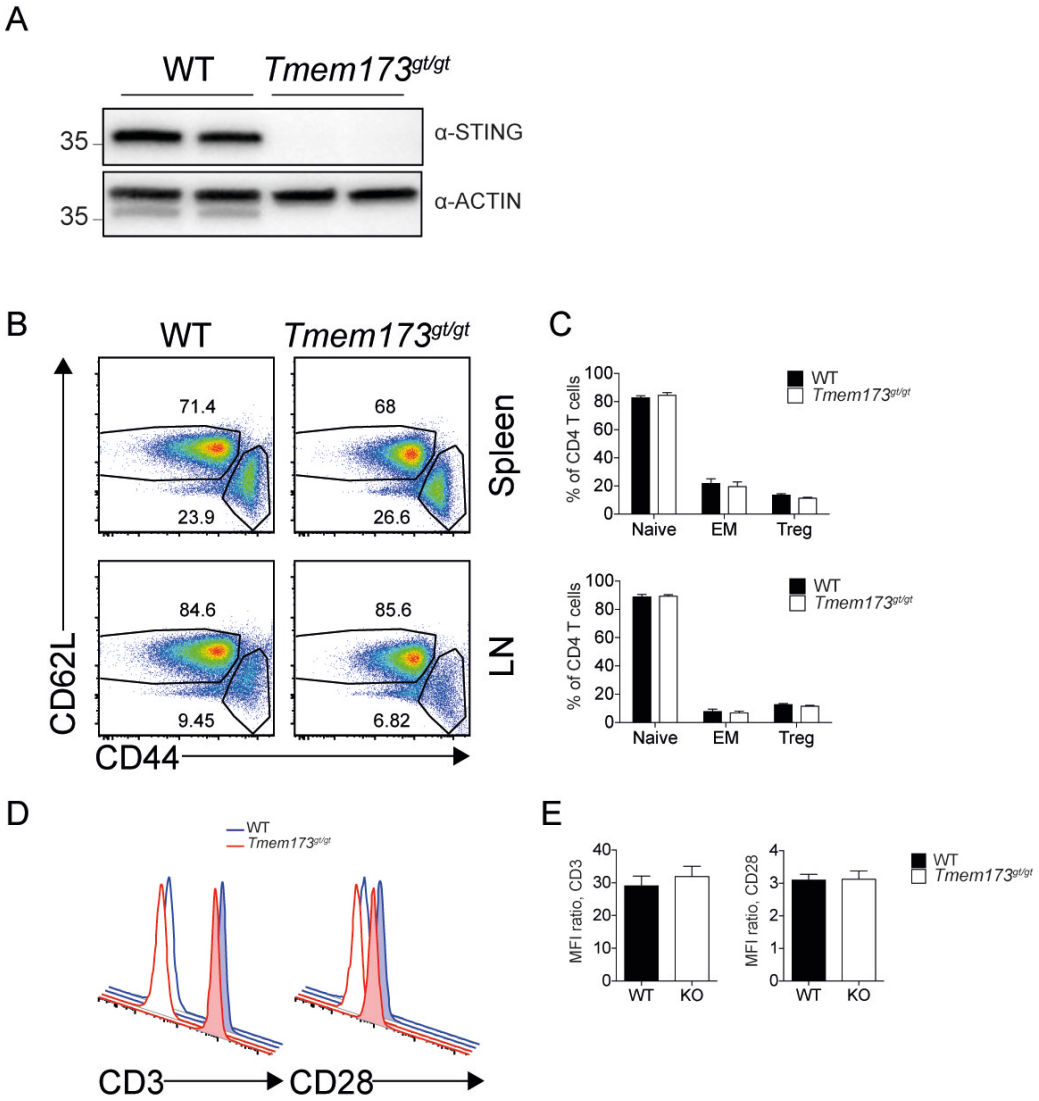
A
WT
Tmem173gt/gt
35
α-STING
35
α-ACTIN
B
WT
Tmem173gt/gt
71.4
23.9
68
26.6
Spleen
84.6
9.45
85.6
6.82
LN
CD62L
CD44
C
% of CD4 T cells
WT
Tmem173gt/gt
Naive
EM
Treg
D
WT
Tmem173gt/gt
CD3
CD28
E
MFI ratio, CD3
MFI ratio, CD28
WT
KO

Supplementary Figure 6. STING inhibits T cell proliferation in normal and pathological conditions, related to figure 7.
(A) Immunoblot of STING and actin expression in CD8+ T cells pooled from spleen and lymph nodes of WT and *Tmem173*$^{gt/gt}$ mice (n=2).
(B) Representative dot plots of CD4+ T cell subpopulations in spleens (upper panel) or peripheral lymph nodes (LN, lower panel) of WT or *Tmem173*$^{gt/gt}$ mice.
(C) Quantification of CD4^{+} T cell subpopulations in spleens (upper panel) or LN (lower panel) of WT or *Tmem173*$^{gt/gt}$ mice (n=4 mice from 2 independent experiments, mean+sem).
(D) Representative histogram plots showing expression of CD3 and CD28 surface expression in naive CD4^{+} T cells from WT or *Tmem173*$^{gt/gt}$ mice. Solid color filling indicates specific antibody, white filling indicates isotype control staining.
(E) Quantification of CD3 and CD28 expression on naive CD4^{+} T cells from WT or *Tmem173*$^{gt/gt}$ mice (n=4 mice from 2 independent experiments, mean+sem).

Table S1 Clinical immunophenotype of patients carrying an activating STING mutation.

	Age group1		Age group2				Age group3	
	P1	Expected values	P5	P7	P11	Expected values	P10	Expected values
TMEM173 mutation	V155M		V155M	V147L	V154S		V155M	
Age at analysis	2		11	8	7		14	
Absolute counts								
CD3+	3060	1400-3700	1782	1560	1444	1200-2600	**558**	1200-2600
CD4+	1935	700-2200	999	960	819	650-1500	**270**	650-1500
CD8+	945	490-1300	729	560	566	370-1100	**270**	370-1100
CD19+	1170	390-1400	621	380	410	270-860	**1206**	110-570
CD16+CD56+	225	130-720	270	**60**	**98**	100-480	**36**	70-480
Percentage								
T cells								
CD3+%	68	56-75	66	**78**	74	60-76	**31**	56-84
CD4+%	43	28-47	37	**48**	42	31-47	**15**	31-52
CD8+%	21	16-30	27	28	29	18-35	**15**	18-35
CD45RO+CD4+%	**10**	14-27	**16**	**6**	**8**	30-42	**20**	30-42
CD45RA+CD4+%	**90**	73-86	**84**	**94**	**92**	58-70	**80**	58-70
CD31+CD45RA+/CD4+%	**74**	57-65	**65**	51	**47**	43-55	55	43-55
CCR7+CD45RA+/CD8+%	**88**	52-68	**86**	**80**	**82**	52-68	**94**	52-68
CCR7+CD45RA-/CD8+%	**1**	3-4	**1**	4	3	3-4	4	3-4
CCR7-CD45RA-/CD8+%	**3**	11-20	**5**	**7**	**3**	11-20	**1**	11-20
CCR7-CD45RA+/CD8+%	**8**	16-28	**8**	**9**	**12**	16-28	**1**	16-28
CD19+%	30	14-33	23	19	21	13-27	**67**	6-23
CD27+/ CD19+%	**1.8**	>10	–	**4**	–	14.7-25.8	**0.7**	12.6-25.2
CD16+CD56+%	5	4-17	10	3	5	4-17	**2**	3-22

5 Discussion

The innate immune system acts in concert with the adaptive immune system to clear viral and bacterial infections. For a virus and many bacteria to be infectious, they need to access the cytosol of a host to start their replication cycle. Cells of the innate immune system mount a fast antiviral response upon DNA detection in the cytosol among others through the cGAS-STING axis [329]. The importance of STING-dependent innate immune sensing, especially in DCs, is illustrated by the differences in infectivity and immunopathology between HIV-2 and HIV-1. To-date, it is believed that the ability of HIV-2-infected patients to better control the infection and to progress slower to AIDS, relies mainly on innate immune sensing of viral cDNA by cGAS-STING axis. However, how innate HIV sensing contributes impacts naïve CD4 T cells is not yet known. Importantly, while STING activity is well described in innate cells, it is unknown what role STING has in adaptive immune cells. In a recent genetic screen, focused on the identification of new mutations involved in the onset of autoimmune disease, it was observed that the mutant STING-V155M correlated with reduced numbers of memory and increased numbers of naive T cells, compared to age-matched controls [104].

Based on these findings, we decided to study the intrinsic and extrinsic effects of STING on CD4+ T cells. First we examined the extrinsic effect by focusing on how HIV sensing by DCs primes naïve CD4+ T cells. In the second project, we investigated the cell intrinsic activity of the innate sensor STING in CD4+ T lymphocytes. The two projects are discussed separately below and a final model will be proposed.

5.1 Regulation of adaptive immunity by HIV sensing in dendritic cells

To examine the extrinsic role of STING, we used MDDCs infected with HIV-1, HIV-2 or MVA or stimulated with other control stimuli in an *in vitro* model for naïve CD4+ T cell priming and subsequent HIV challenge. We found that HIV-2 sensing by MDDCs leads to the acquisition of a partial resistance to HIV infection in the primed naive $CD4^+$ T cells. This resistance correlates with the induction of an ISG signature. We have also found that the T_{HIV-2} profile is characterized by IFNγ production, reminiscent of a Th1 profile. We have performed an exploratory analysis on the differentially expressed genes from microarray analysis and have generated a list of candidate resistance factors in CD4+ T cells.

5.1.1 HIV-2, but not HIV-1, induces activation and type I IFN production in MDDC

Innate immune sensing induces maturation and cytokine production in DCs, required for activation and differentiation of naïve CD4+ T into effector cells [5]. We have chosen different ligands of nucleic acids sensors to study the effect of HIV determinants sensed by DCs that shape the T cell response and compared their effect

to that of HIV-1 or -2. First, we verified the activation state of MDDCs in our model, and we confirmed that all control stimuli and HIV-2, but not HIV-1, induce CD86 expression 48hrs after stimulation or infection. Sensing of nucleic acids induces type I IFN production [50]. We found that poly(IC), poly(dG:dC) and MVA induce production of type I IFN already at 24hrs and it accumulates at 48 hrs. Induction of type I IFN occurs at later time with HIV-2, possibly due to different kinetics between sensing of slowly accumulating viral cDNA as a result of HIV-infection and synthetic ligands added in high doses. All the condition in which type I IFN was produced at 48hrs also induced IP-10 production. However, IP-10 can be induced by other, IFN-I independent signalling pathways [357]. Importantly, as expected HIV-1 did not infect and mature MDDCs, as previously reported [99, 247]. We also showed that R848 strongly activates MDDCs and IL-6, IL-12 and TNF production as previously reported [358], but type I IFN was detected in minute amounts in our model. While R848 has been used in trials for its antiviral and antitumor properties [359], another study has shown that the MDDCs from healthy donors could behave as "low" rather than "high" responders when compared to *e.g.* pDCs [360]. Also, it is possible that the low amounts of type I IFN induced by R848 are due to pDCs contamination in MDDCs or differences between our human model and the already published data, mainly based on mouse models. Also dose effects could impact on R848-dependent release of type I IFN. Although we used a dose that induces full maturation of MDDCs in our system, R848 could be tested at higher dose to clarify the antiviral activity of R848 in our model. Whatever the reason for the lack of IFN-I response, our data show that R848 did not confer resistance to infection to primed CD4+ T cells highlighting the importance for IFN in inducing the antiviral state in CD4+ T cells.

5.1.2 HIV-2-infected MDDC protect CD4+ T cells from subsequent HIV infection

One of the main striking differences between HIV-1 and HIV-2 is the ability of HIV-2 to be sensed by and to infect DCs. We found that THIV-2 but not THIV-1 acquired a partial resistance to subsequent HIV infection which correlated with the acquisition of an ISG signature. Block of type I IFN reduced MX-1 expression to basal levels in all conditions, highlighting the central role of type I IFN in inducing antiviral state in naïve CD4+ T cells. An indirect confirmation that type I IFN is the main driver of the observed Tantiviral is the observation that R848 or poly(I:C) stimulated MDDCs are fully activate and produce comparable amounts of IL-6 and IL-12 , however TR848 are significantly more susceptible to HIV infection than Tpoly(I:C). Here, the most striking difference between the two stimuli is the type I IFN production, which is almost absent in R848 stimulated MDDCs. It would be important to validate the central role of type I IFN for Tantiviral priming, by performing a challenge experiment in the same DC:T system in the presence of neutralizing antibodies against type I IFN alone or in combination with IL-6, IL-12 and TNF neutralizing antibodies.

5.1.3 T helper cell profile of CD4+ T cells

The impact of IFN-I on the quality of the resulting CD4+ T cell response is less clear than its direct antiviral effect. We wondered whether the susceptibility of CD4+ T

cells to HIV-infection correlated with a bias in effector T cell differentiation. We found that CD4+ T cells produced IFNg after co-culture with MDDC from all stimulation conditions. In vitro generated, unstimulated MDDCs bias naive CD4 T cells towards Th1 differentiation with almost 40% of CD4+ TNS being IFNg+. However, we also showed a further increase in IFNg in conditions where stimulation or infection of MDDCs induced high type I IFN production. Type I IFN positively contributes to lymphocyte activation survival and differentiation in a STAT-4 dependent signalling [309, 310] when it provides a third signal in simultaneously to TCR engagement and antigen presentation. Adding recombinant IFNa was sufficient to induce higher IFNg in the DC:T cell culture. Type I IFN autocrine signalling also induces IL-12 production by DCs [6, 361], further contributing to Th1 differentiation. However, IL-12 was not detected in the supernatant of HIV-2 infected MDDCs after 48hrs. It is possible that type I IFN autocrine loop requires longer time to induce IL-12 secretion in vitro, or that CBA is too insensitive to detect small amounts of IL12. Overall, it seems that type I IFN production promoted naïve CD4+T cell differentiation towards Th1 cells.

We also found that IL-21 was only produced by TR848, suggesting that HIV-2 does not induce Tfh polarization in our system. However, IL-21 is an interesting cytokine in HIV infection. IL-21 is under investigation for its potential antiviral activity. In fact, IL-21 can enhance natural killer cells, cytotoxic CD8+ T cells [271, 362, 363] and it can induce the antiviral miRNA29 in CD4+ T cells, demonstrating an intrinsic resistance to HIV-1 infection [364, 365]. The production of IL-21 in SIV-infected macaques also correlated with a better immune activation and decrease in latent viral reservoir [366, 367]. However, the generation of IL-21-producing CD4+ T cells requires high amount of IL-12, as shown for T cells co-cultured with LPS-stimulated DCs in vitro [368]. As already discussed above, we do not detect IL-12 production in HIV-2-infected MDDCs in our model.

5.1.4 Resistance to HIV infection in CD4+ T cells is associated with the induction of type I IFN regulated genes

We generated unbiased transcription profiles of CD4+ T cells, in order to identify candidate genes responsible for the acquired antiviral resistance of THIV-2 to HIV infection. 943 genes were differentially expressed in one or more of the tested conditions using an adjusted p-value < 5% and -1 < log2 (Fold-Change) > 1, which clustered in 5 modules using the WGCNA algorithm. We proceeded with an exploratory functional analysis to study the gene enrichment in the different modules. We found that genes in module 2 and 5 showed a similar pattern of regulation but were found to be unchanged in the HIV-2 condition, while module 3 and 4 were specific to regulation in response to R848 or IFNa, respectively. Indeed, the Tfh-associated genes IL-21, ASCL1, IL-23R clustered in module 3 confirming the suggested role of R848 in the differentiation of CD4+ T cells into Tfh cells [369]. In module 4 we found genes that were specifically induced by type I IFN that conferred the biggest resistance to HIV-infection. Among the interesting genes present in module 4 are CD40 and IL-10. CD4+ T lymphocytes express CD40 in autoimmune mouse model [370] and CD3/CD40L mediated co-stimulation increased T cell activation and induced IL-10, TNF-a and IFN-γ production. However, early CD40-mediated activation was followed by apoptosis of the activated CD4+ T cells,

preventing the formation of an adaptive memory population [371]. Further, IL-10 downmodulates effector adaptive immunity by reducing the ability of APCs to promote CD4+ T cell differentiation and proliferation. Thus, it is conceivable that cells expressing module 4 genes would quickly die if challenged by HIV. In fact, copious amounts of type I IFN in absence or prior to antigen-presentation has a detrimental effect on CD4+ T cells [321]. In vitro, IFN-I dependent STAT-1 signalling can occur in absence of TCR engagement and induce pro-apoptotic signals during lymphocytes differentiation. Constant and abundant type I IFN stimulation induced a state of exhaustion in lymphocytes [311, 312]. This may be part of the mechanism through which HIV-1-mediated immune activation exhausts the capacity of the immune system.

Given that most DE genes in THIV-2 clustered in module 1 and not in module 4 as TIFN, we thought that HIV-2-induced resistance in CD4+ T cells is more than a pure type I IFN signalling, even though type I IFN seems to play a major role in shaping TANTIVIRAL profile. Indeed, a recent study has shown that HIV-2 induces pDC maturation towards antigen-presenting cells rather than IFN-I producing cells [372]. It has been suggested that when type I IFN is coupled with other signals it contributes to a protective adaptive immune response rather than IFN-mediated T cell exhaustion and loss of CD4+ T cells, as observed during progression to AIDS [319, 320].

In our DC:T system we have chosen to use in vitro differentiated monocytes since the innate sensing of HIV-2 was first demonstrated in this cell type. However, the physiological relevance of our results still needs to be addressed in vivo. In the lab we have also generated data that justify the use of MDDC as a relevant model for HIV studies. We analysed the tolerance of different blood DC subsets to become infected with HIV. We found that CD1+ DCs (also known as BDCA1+ DC subset) become infected with HI, while pDCs were poorly infected compare to CD1+DCs. However, pDCs produced type I IFN and IP-10 and turned into weak antigen-presenting cells (Silvin et al., manuscript in revision). CD1+ blood dendritic cells however, behaved like MDDCs (during HIV infection). While they were capable of restricting HIV-1 infection, which can be reverted by Vpx, they were permissive to HIV-2 infection. Here, cGAS and SAMHD1, like for MDDCs [247, 329] are implicated in viral cDNA sensing and viral restriction (Silvin et al., manuscript in revision). Given these results, it would be interesting to set up a co-culture system with blood DC subsets and naïve CD4+ T cells to validate our in vitro findings and to integrate the contribution of different subsets to HIV-2 induced resistance in CD4+ T cells.

5.1.5 Identification of candidate resistance genes controlling CD4+ T cell susceptibility to infection

To identify HIV-2 induced candidate resistance genes, we focused on module 1 of the Affymetrix profile since it contained genes that are differentially regulated in all stimuli associated with HIV-infection resistance including HIV-2. Functional analysis of genes in module 1 revealed an association with genes involved in the immune response, the response to virus, antiviral defense and cytokine activity.

MX-1 is not antiviral against HIV [133], but in our system the susceptibility to HIV infection correlates with MX1 expression. We thus generated a list of antiviral candidate genes among all probes that correlate with MX-1 expression in all the stimuli that confer protection from HIV infection. The rational of selecting antiviral candidates from all the probes rather than only in module 1, is to not miss false negative genes that did not appear in the selected DE due to the stringency criteria of the bioinformatic analysis. Indeed, such stringent parameters were selected due to the subtle changes in gene expression values in CD4+ T cells during the allogeneic co-culture. Within the generated list we found genes that had already been described as HIV restriction factors such as several ISGs. We found involved in the block of HIV viral fusion at the cell membrane [135-137], proteins such as IFITM2, involved in the restriction of replication such as ISG15 and proteins such as tetherin that interfere with the diffusion of viral particles after budding [138]. We finally selected 386 candidate genes, 47% of which were new, previously undescribed candidate genes to be tested in a high-throughput screening approach. Our list of candidates is significantly different from those selected in the screening approach adopted by Schoggins for the identification of antiviral ISGs against a broad group of viruses, based on overexpression of a cDNA library [112]. The main limit for conventional cDNA screening is the ability to control the expression level of the selected candidate. In fact, cDNA libraries are often expressed at high level that may raise questions of physiological relevance of the observed phenotype. On the other hand a genome-wide, loss of function, siRNA-based screen for the identification of genes involved in viral restriction allows for the identification of genes which expression is regulated by the virus at RNA level. In fact, siRNA are important for the host to suppress the expression of genes encoded for by an invading virus. The main criticism to this approach is the variability due to possible incomplete silencing, or off-target knockdown effects. However, at the time of the screening, more sophisticated techniques such as genome editing were not available in our facility yet. Thus we decided to optimize the screening strategy by including 3 siRNAs per gene, each targeting a different part of the gene.

We proceeded to adapt our HIV challenge experiment to the human RPE-1 cell line commonly used in siRNA-based screening approaches in our facility. As screening had to be performed in under L2 safety conditions, we optimised the protocol using a HIV-1 surrogate, GFP-expressing lentivirus as measure of infection. Also, we found that the cells become less susceptible to HIV infection when treated with IFN-a2a. Overall this preliminary setting demonstrates the suitability of using RPE-1 cells for the screening alternatively to primary CD4+ T cells and HIV-1 surrogate for infection. However, we do not exclude that type I IFN in RPE-1 could induce different sets of ISGs than in primary CD4+ T cells, which can be seen as a limitation to our system.

Using a GFP-encoding lentivirus allowed us to use GFP expression intensity as a measure of infection and to determine the capacity of the tested siRNAs to rescue infection. We decided to normalize the GFP intensities for all siRNA conditions, to be able to compare the results for both replicates. As negative controls, siRNAs targeting KF11, an essential gene for cell division, and eGFP completely block cells proliferation and GFP expression, respecitively. As positive control, GFP expression, and thus infection, was rescued by silencing type I IFN receptor expression with siIFNAR1. However, we also noticed some variability in GFP intensity between the 3

siRNAs for our internal control siIFNAR1. In fact, while siIFNAR1 #1 and #2 gave the highest GFP intensity overall the screening, siIFNAR1 #3 was less efficient in blocking infection. Based on this, we propose to proceed comparing both 1) the efficiency of each of the three siRNA per gene, and 2) the reproducibility between the two replicates. We intend to apply several parameters before considering a gene as a true positive hit. First, at least two of the three independent siRNA per gene should produce the same phenotype. Second, to validate selected hits, we could combine all siRNAs to induce a more efficient silencing.

Overall, we have shown the results of a preliminary analysis that has generated an intriguing list of candidate target genes. As expected, our positive control (siIFNAR) and negative control (sieGFP) are the first and the last genes in the list, respectively. Thus, we conclude that the screening technically succeeded; however we need to perform an in-depth analysis to reach further conclusions. We intend to calculate the statistical relevance of the phenotype observed for each silenced gene. Finally, each hit will be validated in primary CD4+ T cells performing overexpression and silencing experiments using HIV for virus challenge. These analyses may contribute to the identification of new antiviral ISGs responsible for lymphocytes resistance acquired after HIV-2 sensing by innate immune response. The identification of new, restriction factors in CD4+ T cells could contribute to the intricate host-HIV interaction understanding. Indeed, pharmacological mobilization of new restriction factors would be an attractive approach for the development of new antivirals.

5.2 Intrinsic anti-proliferative activity of the innate sensor STING in lymphocytes

To assess STING activity in lymphocytes, we developed an *in vitro* model of $CD4^+$ T cells transduced with STING WT or other STING mutants. We have found that STING adopts an anti-proliferative activity in $CD4^+$ T lymphocytes under normal and pathological conditions. This activity was independent of TBK1 and IRF3 recruitment and of type I interferon, but it activated DCs. Inhibition of cell proliferation by STING required also its localization to the Golgi and induced mitotic errors. Altogether, our findings revealed the intrinsic anti-proliferative activity of an innate sensor in cells of the adaptive immune system.

In order to determine the mechanism responsible for block of proliferation in T cells, we first determined Annexin-V expression in STING-V155M T cells, since stimulation of STING was previously shown to induce apoptosis [344]. We did not find any evidence of apoptosis in STING V155M expressing $CD4^+$ T cells. In this previous study, STING activity was assessed in mouse normal and human malignant B cells, suggesting a different activity of STING in human CD4+ T cells, possibly due to differences in structure between mouse and human. Indeed, it was shown that chemical compounds such as DMXAA or CMA activate STING only in mouse, while no activity was detected in human cells and tissue [65, 66]. The V155M mutation is also predicted to induce a change in STING conformation, reminiscent of a ligand-dependent activation, inducing permanent localization of STING to the Golgi and constitutive signaling activation. We then showed that the anti-proliferative activity of STING required STING localization to the Golgi and a sub-region in the C-terminal domain, termed miniCTT. Using a THP-1 assay of 2'3'-cGAMP-induced cell death

and IFN production, we found that STING comprising the miniCTT actually protected from 2'3'-cGAMP induced cell death. Amino acid sequence alignment of the miniCTT of mouse and human STING revealed the presence of a proline at position 345 absent in the human sequence that is present in mouse STING (data not shown). The generation of a 345P mutant in human STING could determine if this residue is involved in STING-dependent apoptosis observed in mouse. The antiproliferative activity of STING mediated by the miniCTT paralleled STING's ability to induce DC activation. DC activation occurred in the absence of TBK1 and IRF3 recruiting determinants in STING. This shows that STING has an additional mode of innate stimulation, independent from TBK1 and IRF3 binding. It is possible that mouse STING interacts with a molecule, which converges STING-signaling to a unique antiviral and pro-apoptotic immune response. Contrary, human STING might activate two different pathways in relation to the nature (quantity/persistence) of a danger signal. On one hand, human STING antiviral activity is induced by the recruitment of TBK1 and IRF3. STING is quickly degraded by ULK-mediated autophagy after activation [84], preventing the detrimental effect of persistent type I IFN expression. On the other hand, we can envision a pathological situation where STING-mediated antiviral activity is not sufficient to counteract an infection. While activated STING persists at the Golgi and increases autophagy (data not shown), it may recruit yet unknown immune regulator/s to inhibit pathogen spreading by blocking lymphocyte proliferation. By boosting autophagy, e.g. using rapamycin, we could investigate whether STING persistence at the Golgi is the limiting factor to trigger the anti-proliferative signal. The Golgi apparatus is a critical organelle for entry and progression of cell mitosis [353], and acts as a signaling platform [354]. However, these properties remain poorly characterized and it will be essential to examine the interplay between STING and the Golgi in these processes. An interesting candidate protein involved in the regulation of STING in the Golgi is optinuerin. Optineurin is a cytosolic protein mainly located in the perinuclear area close to the Golgi. Optineurin interacts with proteins involved in cytoskeleton organization and it has been proposed to contribute to the maintenance of Golgi structure by orchestrating the microtubule organization in its proximity [373]. Recently, it was found that optinuerin is involved in targeting of TBK-1 to the Golgi upon innate sensing [354]. Since, optinuerin is also found to bind LC-3 during autophagosome formation, we propose to investigate whether persistent STING signaling interferes with optinuerin and its functions in relation to autophagy, Golgi and Nf-κB pathways impairment. Of note, optineurin has a strong homology with NEMO (IKK-γ), and its overexpression impairs NF-κB functions, suggesting competition between optineurin and NEMO. The relevance of NF-κB in our phenotype is also suggested by genetic studies. Similar to our findings in patients with constitutively active STING, patients with loss of function mutations in the NF-kB associated molecules IKKB, CARD11, BCL10 and dominant gain of function mutations in IκBα show an imbalance in peripheral T cell subset characterized by an increase in naive and decrease in the memory subset [347-350]. Isolated T cells from these patients also show a defect in *ex vivo* T cell proliferation. T cell subset balance and proliferation is thus critically dependent on a functional NF-κB signaling pathway. We thus propose that STING V155M interferes with NF-κB-related signals required for T cell proliferation. Interestingly, DC activation typically requires NF-κB signaling [3]. The miniCTT of STING may converge on NF-κB signaling in T cells and dendritic cells. At steady state NF-kB is localized in the cytosol in a inhibitory complex composed by IkBα, IkBβ and IkBε. After TCR engagement, downstream

signaling induces the activation of IKKs (IKKα, IKKβ and IKKγ), which in turn counteract NF-κB inhibition, allowing its translocation into the nucleus. We found that T cells from patients have an impaired proliferation when weakly stimulated in vitro, while the proliferation is almost rescued at higher dose of OKT3. Interestingly STING was found to interact with LAT [374], an important adaptor molecule that interconnects proximal and distal signaling events after TCR activation. Thereby, it is possible that STING activation interferes with NF-κB signaling through its sequestration in sub-vesicular compartment from the Golgi. By performing immunoprecipitation of STING-V155M with IKKα, IKKβ or IKKε or IκBα we can determine if STING interacts with any of these proteins, suggesting an involvement of NF-κB in our phenotype. Using Imagestream, we can investigate whether NF-κB translocates into the nucleus in STING WT or V155M overexpressing primary CD4+ T cells. Impairment of NF-κB signaling would result in reduction of cytokine production. TNF production is reduced in STING-V155M overexpressing CD4+ T cells compare to STING-WT as assessed by CBA. Although we cannot exclude that this is due to differences in cell number. Intracellular cytokine staining for TNF will clarify whether NF-κB is involved in the block of proliferation observed in V155M CD4+ T cells.

The anti-proliferative activity of STING required its localization to the Golgi. This was observed independently by introducing the HAQ polymorphism in STING, or by deleting the CTT of STING. STING induced mitotic errors characterized by aberrant cellular DNA content, extended mitosis and unstable metaphases. Similar mitotic error and aberrant cellular DNA content has been reported in cell types that are dependent on TBK1 for mitosis, when TBK1 was inhibited or sequestered [346, 355]. We excluded the importance of TBK1 binding to STING for its antiproliferative activity, suggesting that several innate sensing signaling pathways may converge to induce mitotic errors. Interestingly, NF-κB activation has been previously implicated in the control of senescence [352]. In T cells, we envision that the NF-κB-stimulatory activity of STING intersects with anti-proliferative pathways associated with cell cycle arrest and senescence, consistent with the induction of mitotic errors by STING V155M.

Using a mouse model we found that STING-deficient mouse T cells had a constitutive increased cell proliferation rate. In this setting, the nature of the STING activating signal remain unknown. Both, patients and STING-deficient mice T cells poorly proliferate when stimulated by low dose of anti-CD3, while the proliferation was improved at higher dose. NF-κB could be sequestered by STING-LAT and impairment of its signaling could impact the differentiation and development of memory T cells. Indeed preliminary results indicate that effector Th1, Th2 or Th17 cells generated from STING-deficient naive CD4 T cells have an increased production of the respective effector cytokine early after differentiation (data not shown). To investigate the relevance of STING in the development of effector T cell responses we will compare naive to STING-KO CD4 T cells in a transfer colitis model.

In regard to the nature of the physiological STING stimulus we found cGAS to be induced upon T cell stimulation, which could hence contribute to endogenous STING anti-proliferative activity. Alternatively, we do not exclude that STING anti-proliferative activity may be triggered by yet unknown ligand-independent signals.

Accordingly STING V155M is active in the absence of ligand binding. We find that STING plays a role in T cell proliferation of normal and STING-mutated cells. STING may impact T cell proliferation and T cell subset balance in other situations implicating the cGAS-STING pathway, such as in HIV infection [99, 100, 150]. In summary, our results extend the paradigm of innate control of adaptive immunity by establishing that inhibition of proliferation is a lymphocyte-intrinsic activity for the innate sensor STING.

5.3 MODEL: extrinsic and intrinsic functions of STING adapted by the immune system to eradicate HIV infection

The innate and adaptive immune responses are a defense mechanism of the host to protect itself against viral infection. They are a result of millions of years of coevolution of host and pathogen. Here, a virus develops several strategies to circumvent the host's defense strategies and to improve fitness and survival within the host. Viral adaptation infers pressure on the host to develop new antiviral defense mechanisms. The efforts made to understand the roles of viral accessory proteins during viral replication within host cells, shed light on the evolution of restriction factors in the host.

All viruses, including HIV-1, need to enter the cell to start the replication of their viral genome. HIV-1 preferentially infects CD4+ expressing cells such as T cells and macrophages [375, 376], but has weak tropism for other cell types such as dendritic cells. DCs are a heterogeneous population of cells, categorized into several subsets with different ability in the generation of adaptive immune response (Aymeric Silvin *et al.*, manuscript in revision). HIV-infection of DCs is a crucial step in HIV pathogenesis as it decides about the efficiency of infection of the CD4+ T cell pool [99, 255]. Upon primary infection, HIV needs to reverse transcribe its viral genome before it can be integrated into the nucleus. To ensure reverse transcription, HIV-2 carries Vpx, which inhibits the restriction factor SAMHD1 and allows HIV to access the cytosolic pool of dNTPs [251]. HIV-1, which does not express Vpx, must have evolved not yet entirely understood strategies, such as higher affinity for dNTPs or other viral protein adapted to overcome host restriction of reverse transcription (*e.g.* Vpr) such as for African green monkeys (SIVagm) [377]. The high rate of genome mutagenesis in HIV-1 leads to the speculation, that it develops alternative mechanisms to bypass one host restriction during the course of an infection.

DCs are innate immune cells encoding for another class of host restriction factors: pattern recognition receptors responsible for detecting of viral PAMPs. One of the most potent PAMPs is the presence of DNA in the cytosol. Experiments in MDDCs demonstrated that the ability of HIV-2 to overcome SAMHD1 restriction, leads to cytosolic dsDNA sensing by cGAS [99]. Thus, the absence of Vpx in HIV-1, corresponding to its inability to infect DCs leads to the hypothesis that HIV-1, in contrast to HIV-2, has evolved strategies of immune evasion. This is further illustrated by the finding that HIV-1 takes advantages of the enzymatic activity of TREX-1 to degrade viral and non-self dsDNA in order to escape an antiviral response in the cytosol [150]. STING is the central adaptor for nucleic acids sensing in the cytosol. STING downstream signaling leads to the release of IFN-I [50], which induces several ISGs, the main class of host restriction factors [112, 127]. The most

striking difference between HIV-1 and HIV-2 during initial DCs infection is their ability to induce STING dependent activation and maturation. It is a crucial difference that affects the infectivity of the CD4+ T cell pool, the major viral reservoir. We found that DCs that have been activated through innate viral sensing can confer resistance to CD4+ T cells in a fashion that strongly correlates with DC production of antiviral IFN-I. Thus during HIV-2 infection, it is likely that CD4+ T lymphocytes benefit from innate sensing of HIV by DCs in two ways: 1) Maturation of DCs in the presence of viral antigen leads to the development of polyfunctional effector lymphocytes that are able to better control the infection; 2) DC-derived IFN-I confers better resistance to CD4+ T cells to HIV infection than DCs that are "infected" by HIV-1. Since the CD4+ T cell count is a prediction parameter for AIDS progression [162, 260], HIV infection might lead to slower loss of CD4+ T cells, which is observed in HIV-2 infected patients. Thus the ability of HIV-1 to circumvent STING-mediated innate sensing in DCs might be a major reason for the more severe pathogenicity of HIV-1 compared to HIV-2 infections.

Another, although largely unexplored, level of host restriction to HIV infection is the innate sensing in adaptive immune cells. While, peripheral naïve CD4+ T cells are “deeply” resistant to HIV-1 infection due to SAMHD1 restriction [289, 290], lymphoid tissue naïve CD4+ T cells are more permissive due to the richer surrounding environment. Still, in most T cells HIV-1 infection is abortive as reverse transcription can be sensed by IFI16, which leads to inflammatory apoptosis in CD4+T cells, also known as pyroptosis [39]. However, this mechanism is not sufficient to explain the massive cell death and loss of CD4+ T cells during HIV chronic infection. Based on our results, we propose that STING may directly contribute to viral cDNA sensing in CD4+ T cells. In activated CD4+ T cells SAMHD1 restriction is inefficient, as the cell needs access to the nucleotide pool for its own replication enabling viruses to rapidly replicate under these conditions. Thus, other mechanisms such as the delivery of exosome-packaged cGAMP from the infected cells into the cytosol of CD4+ T cells could directly activate STING and induce its translocation to the Golgi. Here, it either triggers an antiviral and/or an anti-proliferative pathway in an attempt to stop the virus infection. This intrinsic function of STING may lead to an abortive infection and thereby potently limit HIV spreading in CD4+ T cells. Thus we propose that an intrinsic STING activity in T cells is a third, desperate attempt by the immune system to block HIV infection in CD4+ T cells.

6 References

1. Murphy, K., *Janeway's Immunobiology*. 8th ed. Immunobiology 8th edition2012, London and New York: Garland Science.
2. Medzhitov, R. and C.A. Janeway, Jr., *Innate immunity: the virtues of a nonclonal system of recognition.* Cell, 1997. **91**(3): p. 295-8.
3. Janeway, C.A., Jr. and R. Medzhitov, *Innate immune recognition.* Annu Rev Immunol, 2002. **20**: p. 197-216.
4. Matzinger, P., *The danger model: a renewed sense of self.* Science, 2002. **296**(5566): p. 301-5.
5. Tao, X., et al., *Strength of TCR signal determines the costimulatory requirements for Th1 and Th2 CD4+ T cell differentiation.* J Immunol, 1997. **159**(12): p. 5956-63.
6. Korthals, M., et al., *Monocyte derived dendritic cells generated by IFN-alpha acquire mature dendritic and natural killer cell properties as shown by gene expression analysis.* J Transl Med, 2007. **5**: p. 46.
7. Raphael, I., et al., *T cell subsets and their signature cytokines in autoimmune and inflammatory diseases.* Cytokine, 2015. **74**(1): p. 5-17.
8. Hammarlund, E., et al., *Duration of antiviral immunity after smallpox vaccination.* Nat Med, 2003. **9**(9): p. 1131-7.
9. Kawai, T. and S. Akira, *The role of pattern-recognition receptors in innate immunity: update on Toll-like receptors.* Nat Immunol, 2010. **11**(5): p. 373-84.
10. Kumar, H., T. Kawai, and S. Akira, *Pathogen recognition by the innate immune system.* Int Rev Immunol, 2011. **30**(1): p. 16-34.
11. Newton, K. and V.M. Dixit, *Signaling in innate immunity and inflammation.* Cold Spring Harb Perspect Biol, 2012. **4**(3).
12. Alexopoulou, L., et al., *Recognition of double-stranded RNA and activation of NF-kappaB by Toll-like receptor 3.* Nature, 2001. **413**(6857): p. 732-8.
13. Kumagai, Y. and S. Akira, *Identification and functions of pattern-recognition receptors.* J Allergy Clin Immunol, 2010. **125**(5): p. 985-92.
14. Izaguirre, A., et al., *Comparative analysis of IRF and IFN-alpha expression in human plasmacytoid and monocyte-derived dendritic cells.* J Leukoc Biol, 2003. **74**(6): p. 1125-38.
15. Lepelley, A., et al., *Innate sensing of HIV-infected cells.* PLoS Pathog, 2011. **7**(2): p. e1001284.
16. Beignon, A.S., et al., *Endocytosis of HIV-1 activates plasmacytoid dendritic cells via Toll-like receptor-viral RNA interactions.* J Clin Invest, 2005. **115**(11): p. 3265-75.
17. Diebold, S.S., et al., *Viral infection switches non-plasmacytoid dendritic cells into high interferon producers.* Nature, 2003. **424**(6946): p. 324-8.
18. Wu, J. and Z.J. Chen, *Innate immune sensing and signaling of cytosolic nucleic acids.* Annu Rev Immunol, 2014. **32**: p. 461-88.
19. Hou, F., et al., *MAVS forms functional prion-like aggregates to activate and propagate antiviral innate immune response.* Cell, 2011. **146**(3): p. 448-61.
20. Goubau, D., S. Deddouche, and C. Reis e Sousa, *Cytosolic sensing of viruses.* Immunity, 2013. **38**(5): p. 855-69.
21. Takeuchi, O. and S. Akira, *Pattern recognition receptors and inflammation.* Cell, 2010. **140**(6): p. 805-20.

22. Yoo, J.S., H. Kato, and T. Fujita, *Sensing viral invasion by RIG-I like receptors.* Curr Opin Microbiol, 2014. **20**: p. 131-8.
23. Kuchta, K., et al., *Comprehensive classification of nucleotidyltransferase fold proteins: identification of novel families and their representatives in human.* Nucleic Acids Res, 2009. **37**(22): p. 7701-14.
24. Malathi, K., et al., *Small self-RNA generated by RNase L amplifies antiviral innate immunity.* Nature, 2007. **448**(7155): p. 816-9.
25. Malathi, K., et al., *RNase L releases a small RNA from HCV RNA that refolds into a potent PAMP.* RNA, 2010. **16**(11): p. 2108-19.
26. Chakrabarti, A., B.K. Jha, and R.H. Silverman, *New insights into the role of RNase L in innate immunity.* J Interferon Cytokine Res, 2011. **31**(1): p. 49-57.
27. Hovanessian, A.G., R.E. Brown, and I.M. Kerr, *Synthesis of low molecular weight inhibitor of protein synthesis with enzyme from interferon-treated cells.* Nature, 1977. **268**(5620): p. 537-40.
28. Kristiansen, H., et al., *The oligoadenylate synthetase family: an ancient protein family with multiple antiviral activities.* J Interferon Cytokine Res, 2011. **31**(1): p. 41-7.
29. Silverman, R.H., *Viral encounters with 2',5'-oligoadenylate synthetase and RNase L during the interferon antiviral response.* J Virol, 2007. **81**(23): p. 12720-9.
30. Williams, B.R., *Signal integration via PKR.* Sci STKE, 2001. **2001**(89): p. re2.
31. Rathinam, V.A., et al., *The AIM2 inflammasome is essential for host defense against cytosolic bacteria and DNA viruses.* Nat Immunol, 2010. **11**(5): p. 395-402.
32. Hornung, V., et al., *AIM2 recognizes cytosolic dsDNA and forms a caspase-1-activating inflammasome with ASC.* Nature, 2009. **458**(7237): p. 514-8.
33. Roberts, T.L., et al., *HIN-200 proteins regulate caspase activation in response to foreign cytoplasmic DNA.* Science, 2009. **323**(5917): p. 1057-60.
34. Chiu, Y.H., J.B. Macmillan, and Z.J. Chen, *RNA polymerase III detects cytosolic DNA and induces type I interferons through the RIG-I pathway.* Cell, 2009. **138**(3): p. 576-91.
35. Ablasser, A., et al., *RIG-I-dependent sensing of poly(dA:dT) through the induction of an RNA polymerase III-transcribed RNA intermediate.* Nat Immunol, 2009. **10**(10): p. 1065-72.
36. Parvatiyar, K., et al., *The helicase DDX41 recognizes the bacterial secondary messengers cyclic di-GMP and cyclic di-AMP to activate a type I interferon immune response.* Nat Immunol, 2012. **13**(12): p. 1155-61.
37. Gray, E.E., et al., *The AIM2-like Receptors Are Dispensable for the Interferon Response to Intracellular DNA.* Immunity, 2016. **45**(2): p. 255-66.
38. Unterholzner, L., et al., *IFI16 is an innate immune sensor for intracellular DNA.* Nat Immunol, 2010. **11**(11): p. 997-1004.
39. Doitsh, G., et al., *Cell death by pyroptosis drives CD4 T-cell depletion in HIV-1 infection.* Nature, 2014. **505**(7484): p. 509-14.
40. Monroe, K.M., et al., *IFI16 DNA sensor is required for death of lymphoid CD4 T cells abortively infected with HIV.* Science, 2014. **343**(6169): p. 428-32.
41. Rathinam, V.A. and K.A. Fitzgerald, *Innate immune sensing of DNA viruses.* Virology, 2011. **411**(2): p. 153-62.

42. Kanneganti, T.D., et al., *Critical role for Cryopyrin/Nalp3 in activation of caspase-1 in response to viral infection and double-stranded RNA.* J Biol Chem, 2006. **281**(48): p. 36560-8.
43. Ishikawa, H. and G.N. Barber, *STING is an endoplasmic reticulum adaptor that facilitates innate immune signalling.* Nature, 2008. **455**(7213): p. 674-8.
44. Ouyang, S., et al., *Structural analysis of the STING adaptor protein reveals a hydrophobic dimer interface and mode of cyclic di-GMP binding.* Immunity, 2012. **36**(6): p. 1073-86.
45. Dobbs, N., et al., *STING Activation by Translocation from the ER Is Associated with Infection and Autoinflammatory Disease.* Cell Host Microbe, 2015. **18**(2): p. 157-68.
46. Wu, X., et al., *Molecular evolutionary and structural analysis of the cytosolic DNA sensor cGAS and STING.* Nucleic Acids Res, 2014. **42**(13): p. 8243-57.
47. Jin, L., et al., *MPYS, a novel membrane tetraspanner, is associated with major histocompatibility complex class II and mediates transduction of apoptotic signals.* Mol Cell Biol, 2008. **28**(16): p. 5014-26.
48. Sun, W., et al., *ERIS, an endoplasmic reticulum IFN stimulator, activates innate immune signaling through dimerization.* Proc Natl Acad Sci U S A, 2009. **106**(21): p. 8653-8.
49. Zhong, B., et al., *The adaptor protein MITA links virus-sensing receptors to IRF3 transcription factor activation.* Immunity, 2008. **29**(4): p. 538-50.
50. Ishikawa, H., Z. Ma, and G.N. Barber, *STING regulates intracellular DNA-mediated, type I interferon-dependent innate immunity.* Nature, 2009. **461**(7265): p. 788-92.
51. Romling, U., M.Y. Galperin, and M. Gomelsky, *Cyclic di-GMP: the first 25 years of a universal bacterial second messenger.* Microbiol Mol Biol Rev, 2013. **77**(1): p. 1-52.
52. Witte, G., et al., *Structural biochemistry of a bacterial checkpoint protein reveals diadenylate cyclase activity regulated by DNA recombination intermediates.* Mol Cell, 2008. **30**(2): p. 167-78.
53. Davies, B.W., et al., *Coordinated regulation of accessory genetic elements produces cyclic di-nucleotides for V. cholerae virulence.* Cell, 2012. **149**(2): p. 358-70.
54. Woodward, J.J., A.T. Iavarone, and D.A. Portnoy, *c-di-AMP secreted by intracellular Listeria monocytogenes activates a host type I interferon response.* Science, 2010. **328**(5986): p. 1703-5.
55. Burdette, D.L., et al., *STING is a direct innate immune sensor of cyclic di-GMP.* Nature, 2011. **478**(7370): p. 515-8.
56. Shang, G., et al., *Crystal structures of STING protein reveal basis for recognition of cyclic di-GMP.* Nat Struct Mol Biol, 2012. **19**(7): p. 725-7.
57. Shu, C., et al., *Structure of STING bound to cyclic di-GMP reveals the mechanism of cyclic dinucleotide recognition by the immune system.* Nat Struct Mol Biol, 2012. **19**(7): p. 722-4.
58. Yin, Q., et al., *Cyclic di-GMP sensing via the innate immune signaling protein STING.* Mol Cell, 2012. **46**(6): p. 735-45.
59. Sun, L., et al., *Cyclic GMP-AMP synthase is a cytosolic DNA sensor that activates the type I interferon pathway.* Science, 2013. **339**(6121): p. 786-91.
60. Ablasser, A., et al., *cGAS produces a 2'-5'-linked cyclic dinucleotide second messenger that activates STING.* Nature, 2013. **498**(7454): p. 380-4.

61. Diner, E.J., et al., *The innate immune DNA sensor cGAS produces a noncanonical cyclic dinucleotide that activates human STING.* Cell Rep, 2013. **3**(5): p. 1355-61.
62. Gao, P., et al., *Cyclic [G(2',5')pA(3',5')p] is the metazoan second messenger produced by DNA-activated cyclic GMP-AMP synthase.* Cell, 2013. **153**(5): p. 1094-107.
63. Zhang, X., et al., *Cyclic GMP-AMP containing mixed phosphodiester linkages is an endogenous high-affinity ligand for STING.* Mol Cell, 2013. **51**(2): p. 226-35.
64. Gao, P., et al., *Structure-function analysis of STING activation by c[G(2',5')pA(3',5')p] and targeting by antiviral DMXAA.* Cell, 2013. **154**(4): p. 748-62.
65. Conlon, J., et al., *Mouse, but not human STING, binds and signals in response to the vascular disrupting agent 5,6-dimethylxanthenone-4-acetic acid.* J Immunol, 2013. **190**(10): p. 5216-25.
66. Cavlar, T., et al., *Species-specific detection of the antiviral small-molecule compound CMA by STING.* EMBO J, 2013. **32**(10): p. 1440-50.
67. Tanaka, Y. and Z.J. Chen, *STING specifies IRF3 phosphorylation by TBK1 in the cytosolic DNA signaling pathway.* Sci Signal, 2012. **5**(214): p. ra20.
68. Abe, T. and G.N. Barber, *Cytosolic-DNA-mediated, STING-dependent proinflammatory gene induction necessitates canonical NF-kappaB activation through TBK1.* J Virol, 2014. **88**(10): p. 5328-41.
69. Chen, H., et al., *Activation of STAT6 by STING is critical for antiviral innate immunity.* Cell, 2011. **147**(2): p. 436-46.
70. Tsuchida, T., et al., *The ubiquitin ligase TRIM56 regulates innate immune responses to intracellular double-stranded DNA.* Immunity, 2010. **33**(5): p. 765-76.
71. Zhang, J., et al., *TRIM32 protein modulates type I interferon induction and cellular antiviral response by targeting MITA/STING protein for K63-linked ubiquitination.* J Biol Chem, 2012. **287**(34): p. 28646-55.
72. Yilmaz, F., et al., *Epidemiologic and clinical characteristics and outcomes of scorpion sting in the southeastern region of Turkey.* Ulus Travma Acil Cerrahi Derg, 2013. **19**(5): p. 417-22.
73. Zhong, B., et al., *The ubiquitin ligase RNF5 regulates antiviral responses by mediating degradation of the adaptor protein MITA.* Immunity, 2009. **30**(3): p. 397-407.
74. Qin, Y., et al., *RNF26 temporally regulates virus-triggered type I interferon induction by two distinct mechanisms.* PLoS Pathog, 2014. **10**(9): p. e1004358.
75. Wang, Q., et al., *The E3 ubiquitin ligase AMFR and INSIG1 bridge the activation of TBK1 kinase by modifying the adaptor STING.* Immunity, 2014. **41**(6): p. 919-33.
76. Tsai, Y.C., et al., *Differential regulation of HMG-CoA reductase and Insig-1 by enzymes of the ubiquitin-proteasome system.* Mol Biol Cell, 2012. **23**(23): p. 4484-94.
77. Luo, W.W., et al., *iRhom2 is essential for innate immunity to DNA viruses by mediating trafficking and stability of the adaptor STING.* Nat Immunol, 2016. **17**(9): p. 1057-66.
78. Mukai, K., et al., *Activation of STING requires palmitoylation at the Golgi.* Nat Commun, 2016. **7**: p. 11932.

79. Zhou, Q., et al., *The ER-associated protein ZDHHC1 is a positive regulator of DNA virus-triggered, MITA/STING-dependent innate immune signaling.* Cell Host Microbe, 2014. **16**(4): p. 450-61.
80. Oku, S., et al., *In silico screening for palmitoyl substrates reveals a role for DHHC1/3/10 (zDHHC1/3/11)-mediated neurochondrin palmitoylation in its targeting to Rab5-positive endosomes.* J Biol Chem, 2013. **288**(27): p. 19816-29.
81. Zhang, L., et al., *NLRC3, a member of the NLR family of proteins, is a negative regulator of innate immune signaling induced by the DNA sensor STING.* Immunity, 2014. **40**(3): p. 329-41.
82. Saitoh, T., et al., *Atg9a controls dsDNA-driven dynamic translocation of STING and the innate immune response.* Proc Natl Acad Sci U S A, 2009. **106**(49): p. 20842-6.
83. Liu, S., et al., *Phosphorylation of innate immune adaptor proteins MAVS, STING, and TRIF induces IRF3 activation.* Science, 2015. **347**(6227): p. aaa2630.
84. Konno, H., K. Konno, and G.N. Barber, *Cyclic dinucleotides trigger ULK1 (ATG1) phosphorylation of STING to prevent sustained innate immune signaling.* Cell, 2013. **155**(3): p. 688-98.
85. Liang, Q., et al., *Crosstalk between the cGAS DNA sensor and Beclin-1 autophagy protein shapes innate antimicrobial immune responses.* Cell Host Microbe, 2014. **15**(2): p. 228-38.
86. Seo, G.J., et al., *Akt Kinase-Mediated Checkpoint of cGAS DNA Sensing Pathway.* Cell Rep, 2015. **13**(2): p. 440-9.
87. Schoggins, J.W., et al., *Pan-viral specificity of IFN-induced genes reveals new roles for cGAS in innate immunity.* Nature, 2014. **505**(7485): p. 691-5.
88. Sauer, J.D., et al., *The N-ethyl-N-nitrosourea-induced Goldenticket mouse mutant reveals an essential function of Sting in the in vivo interferon response to Listeria monocytogenes and cyclic dinucleotides.* Infect Immun, 2011. **79**(2): p. 688-94.
89. Archer, K.A., J. Durack, and D.A. Portnoy, *STING-dependent type I IFN production inhibits cell-mediated immunity to Listeria monocytogenes.* PLoS Pathog, 2014. **10**(1): p. e1003861.
90. Jin, L., et al., *STING/MPYS mediates host defense against Listeria monocytogenes infection by regulating Ly6C(hi) monocyte migration.* J Immunol, 2013. **190**(6): p. 2835-43.
91. Aguirre, S., et al., *DENV inhibits type I IFN production in infected cells by cleaving human STING.* PLoS Pathog, 2012. **8**(10): p. e1002934.
92. Yu, C.Y., et al., *Dengue virus targets the adaptor protein MITA to subvert host innate immunity.* PLoS Pathog, 2012. **8**(6): p. e1002780.
93. Ding, Q., et al., *Hepatitis C virus NS4B blocks the interaction of STING and TBK1 to evade host innate immunity.* J Hepatol, 2013. **59**(1): p. 52-8.
94. Nitta, S., et al., *Hepatitis C virus NS4B protein targets STING and abrogates RIG-I-mediated type I interferon-dependent innate immunity.* Hepatology, 2013. **57**(1): p. 46-58.
95. Sun, L., et al., *Coronavirus papain-like proteases negatively regulate antiviral innate immune response through disruption of STING-mediated signaling.* PLoS One, 2012. **7**(2): p. e30802.

96. Kalamvoki, M. and B. Roizman, *HSV-1 degrades, stabilizes, requires, or is stung by STING depending on ICP0, the US3 protein kinase, and cell derivation.* Proc Natl Acad Sci U S A, 2014. **111**(5): p. E611-7.
97. Sunthamala, N., et al., *E2 proteins of high risk human papillomaviruses down-modulate STING and IFN-kappa transcription in keratinocytes.* PLoS One, 2014. **9**(3): p. e91473.
98. Lau, L., et al., *DNA tumor virus oncogenes antagonize the cGAS-STING DNA-sensing pathway.* Science, 2015. **350**(6260): p. 568-71.
99. Lahaye, X., et al., *The capsids of HIV-1 and HIV-2 determine immune detection of the viral cDNA by the innate sensor cGAS in dendritic cells.* Immunity, 2013. **39**(6): p. 1132-42.
100. Gao, D., et al., *Cyclic GMP-AMP synthase is an innate immune sensor of HIV and other retroviruses.* Science, 2013. **341**(6148): p. 903-6.
101. Jin, L., et al., *Identification and characterization of a loss-of-function human MPYS variant.* Genes Immun, 2011. **12**(4): p. 263-9.
102. Yi, G., et al., *Single nucleotide polymorphisms of human STING can affect innate immune response to cyclic dinucleotides.* PLoS One, 2013. **8**(10): p. e77846.
103. Liu, Y., et al., *Activated STING in a vascular and pulmonary syndrome.* N Engl J Med, 2014. **371**(6): p. 507-18.
104. Jeremiah, N., et al., *Inherited STING-activating mutation underlies a familial inflammatory syndrome with lupus-like manifestations.* J Clin Invest, 2014. **124**(12): p. 5516-20.
105. Isaacs, A., J. Lindenmann, and R.C. Valentine, *Virus interference. II. Some properties of interferon.* Proc R Soc Lond B Biol Sci, 1957. **147**(927): p. 268-73.
106. Nagano, Y. and Y. Kojima, *[Interference of the inactive vaccinia virus with infection of skin by the active homologous virus].* C R Seances Soc Biol Fil, 1958. **152**(2): p. 372-4.
107. Pestka, S., C.D. Krause, and M.R. Walter, *Interferons, interferon-like cytokines, and their receptors.* Immunol Rev, 2004. **202**: p. 8-32.
108. Farrar, M.A. and R.D. Schreiber, *The molecular cell biology of interferon-gamma and its receptor.* Annu Rev Immunol, 1993. **11**: p. 571-611.
109. Muller, I., et al., *Expansion of gamma interferon-producing CD8+ T cells following secondary infection of mice immune to Leishmania major.* Infect Immun, 1994. **62**(6): p. 2575-81.
110. Stark, G.R. and J.E. Darnell, Jr., *The JAK-STAT pathway at twenty.* Immunity, 2012. **36**(4): p. 503-14.
111. MacMicking, J.D., *Interferon-inducible effector mechanisms in cell-autonomous immunity.* Nat Rev Immunol, 2012. **12**(5): p. 367-82.
112. Schoggins, J.W., et al., *A diverse range of gene products are effectors of the type I interferon antiviral response.* Nature, 2011. **472**(7344): p. 481-5.
113. Rusinova, I., et al., *Interferome v2.0: an updated database of annotated interferon-regulated genes.* Nucleic Acids Res, 2013. **41**(Database issue): p. D1040-6.
114. van Boxel-Dezaire, A.H., M.R. Rani, and G.R. Stark, *Complex modulation of cell type-specific signaling in response to type I interferons.* Immunity, 2006. **25**(3): p. 361-72.

115. Nielsen, R. and Z. Yang, *Likelihood models for detecting positively selected amino acid sites and applications to the HIV-1 envelope gene.* Genetics, 1998. **148**(3): p. 929-36.
116. Grossman, S.R., et al., *A composite of multiple signals distinguishes causal variants in regions of positive selection.* Science, 2010. **327**(5967): p. 883-6.
117. Laguette, N., et al., *SAMHD1 is the dendritic- and myeloid-cell-specific HIV-1 restriction factor counteracted by Vpx.* Nature, 2011. **474**(7353): p. 654-7.
118. Hrecka, K., et al., *Vpx relieves inhibition of HIV-1 infection of macrophages mediated by the SAMHD1 protein.* Nature, 2011. **474**(7353): p. 658-61.
119. Yu, X., et al., *Induction of APOBEC3G ubiquitination and degradation by an HIV-1 Vif-Cul5-SCF complex.* Science, 2003. **302**(5647): p. 1056-60.
120. Mehle, A., et al., *Phosphorylation of a novel SOCS-box regulates assembly of the HIV-1 Vif-Cul5 complex that promotes APOBEC3G degradation.* Genes Dev, 2004. **18**(23): p. 2861-6.
121. Elde, N.C. and H.S. Malik, *The evolutionary conundrum of pathogen mimicry.* Nat Rev Microbiol, 2009. **7**(11): p. 787-97.
122. Kueck, T. and S.J. Neil, *A cytoplasmic tail determinant in HIV-1 Vpu mediates targeting of tetherin for endosomal degradation and counteracts interferon-induced restriction.* PLoS Pathog, 2012. **8**(3): p. e1002609.
123. Schmidt, S., et al., *HIV-1 Vpu blocks recycling and biosynthetic transport of the intrinsic immunity factor CD317/tetherin to overcome the virion release restriction.* MBio, 2011. **2**(3): p. e00036-11.
124. Refsland, E.W., et al., *Quantitative profiling of the full APOBEC3 mRNA repertoire in lymphocytes and tissues: implications for HIV-1 restriction.* Nucleic Acids Res, 2010. **38**(13): p. 4274-84.
125. Koning, F.A., et al., *Defining APOBEC3 expression patterns in human tissues and hematopoietic cell subsets.* J Virol, 2009. **83**(18): p. 9474-85.
126. Iwasaki, A., *A virological view of innate immune recognition.* Annu Rev Microbiol, 2012. **66**: p. 177-96.
127. Liu, S.Y., et al., *Systematic identification of type I and type II interferon-induced antiviral factors.* Proc Natl Acad Sci U S A, 2012. **109**(11): p. 4239-44.
128. Haller, O. and G. Kochs, *Human MxA protein: an interferon-induced dynamin-like GTPase with broad antiviral activity.* J Interferon Cytokine Res, 2011. **31**(1): p. 79-87.
129. Sadler, A.J. and B.R. Williams, *Interferon-inducible antiviral effectors.* Nat Rev Immunol, 2008. **8**(7): p. 559-68.
130. Kane, M., et al., *MX2 is an interferon-induced inhibitor of HIV-1 infection.* Nature, 2013. **502**(7472): p. 563-6.
131. Goujon, C., et al., *Human MX2 is an interferon-induced post-entry inhibitor of HIV-1 infection.* Nature, 2013. **502**(7472): p. 559-62.
132. Liu, Z., et al., *The interferon-inducible MxB protein inhibits HIV-1 infection.* Cell Host Microbe, 2013. **14**(4): p. 398-410.
133. Goujon, C., et al., *Transfer of the amino-terminal nuclear envelope targeting domain of human MX2 converts MX1 into an HIV-1 resistance factor.* J Virol, 2014. **88**(16): p. 9017-26.
134. Liu, Z., et al., *The highly polymorphic cyclophilin A-binding loop in HIV-1 capsid modulates viral resistance to MxB.* Retrovirology, 2015. **12**: p. 1.
135. Lu, J., et al., *The IFITM proteins inhibit HIV-1 infection.* J Virol, 2011. **85**(5): p. 2126-37.

136. Li, K., et al., *IFITM proteins restrict viral membrane hemifusion.* PLoS Pathog, 2013. **9**(1): p. e1003124.
137. Tartour, K., et al., *IFITM proteins are incorporated onto HIV-1 virion particles and negatively imprint their infectivity.* Retrovirology, 2014. **11**: p. 103.
138. Neil, S.J., T. Zang, and P.D. Bieniasz, *Tetherin inhibits retrovirus release and is antagonized by HIV-1 Vpu.* Nature, 2008. **451**(7177): p. 425-30.
139. Li, M., et al., *TIM-family proteins inhibit HIV-1 release.* Proc Natl Acad Sci U S A, 2014. **111**(35): p. E3699-707.
140. Chiu, Y.L., et al., *Cellular APOBEC3G restricts HIV-1 infection in resting CD4+ T cells.* Nature, 2005. **435**(7038): p. 108-14.
141. Stremlau, M., et al., *The cytoplasmic body component TRIM5alpha restricts HIV-1 infection in Old World monkeys.* Nature, 2004. **427**(6977): p. 848-53.
142. Sayah, D.M., et al., *Cyclophilin A retrotransposition into TRIM5 explains owl monkey resistance to HIV-1.* Nature, 2004. **430**(6999): p. 569-73.
143. Okumura, A., et al., *Innate antiviral response targets HIV-1 release by the induction of ubiquitin-like protein ISG15.* Proc Natl Acad Sci U S A, 2006. **103**(5): p. 1440-5.
144. Gresser, I., et al., *Interferon-induced disease in mice and rats.* Ann N Y Acad Sci, 1980. **350**: p. 12-20.
145. Crow, Y.J., *Type I interferonopathies: a novel set of inborn errors of immunity.* Ann N Y Acad Sci, 2011. **1238**: p. 91-8.
146. Crow, Y.J. and N. Manel, *Aicardi-Goutieres syndrome and the type I interferonopathies.* Nat Rev Immunol, 2015. **15**(7): p. 429-40.
147. Vogt, J., et al., *Striking intrafamilial phenotypic variability in Aicardi-Goutieres syndrome associated with the recurrent Asian founder mutation in RNASEH2C.* Am J Med Genet A, 2013. **161A**(2): p. 338-42.
148. Baltimore, D., *RNA-dependent DNA polymerase in virions of RNA tumour viruses.* Nature, 1970. **226**(5252): p. 1209-11.
149. Bowerman, B., et al., *A nucleoprotein complex mediates the integration of retroviral DNA.* Genes Dev, 1989. **3**(4): p. 469-78.
150. Yan, N., et al., *The cytosolic exonuclease TREX1 inhibits the innate immune response to human immunodeficiency virus type 1.* Nat Immunol, 2010. **11**(11): p. 1005-13.
151. Barre-Sinoussi, F., et al., *Isolation of a T-lymphotropic retrovirus from a patient at risk for acquired immune deficiency syndrome (AIDS).* Science, 1983. **220**(4599): p. 868-71.
152. Fauci, A.S., *The acquired immune deficiency syndrome. The ever-broadening clinical spectrum.* JAMA, 1983. **249**(17): p. 2375-6.
153. Quinn, T.C., *Population migration and the spread of types 1 and 2 human immunodeficiency viruses.* Proc Natl Acad Sci U S A, 1994. **91**(7): p. 2407-14.
154. Clavel, F., et al., *[LAV type II: a second retrovirus associated with AIDS in West Africa].* C R Acad Sci III, 1986. **302**(13): p. 485-8.
155. Barre-Sinoussi, F., et al., *Isolation of a T-lymphotropic retrovirus from a patient at risk for acquired immune deficiency syndrome (AIDS). 1983.* Rev Invest Clin, 2004. **56**(2): p. 126-9.
156. Rowland-Jones, S.L. and H.C. Whittle, *Out of Africa: what can we learn from HIV-2 about protective immunity to HIV-1?* Nat Immunol, 2007. **8**(4): p. 329-31.

157. Sharp, P.M. and B.H. Hahn, *Origins of HIV and the AIDS pandemic.* Cold Spring Harb Perspect Med, 2011. **1**(1): p. a006841.
158. van der Loeff, M.F., et al., *Undetectable plasma viral load predicts normal survival in HIV-2-infected people in a West African village.* Retrovirology, 2010. **7**: p. 46.
159. Marlink, R., et al., *Reduced rate of disease development after HIV-2 infection as compared to HIV-1.* Science, 1994. **265**(5178): p. 1587-90.
160. Martinez-Steele, E., et al., *Is HIV-2- induced AIDS different from HIV-1-associated AIDS? Data from a West African clinic.* AIDS, 2007. **21**(3): p. 317-24.
161. Gottlieb, G.S., et al., *Lower levels of HIV RNA in semen in HIV-2 compared with HIV-1 infection: implications for differences in transmission.* AIDS, 2006. **20**(6): p. 895-900.
162. Duvall, M.G., et al., *Maintenance of HIV-specific CD4+ T cell help distinguishes HIV-2 from HIV-1 infection.* J Immunol, 2006. **176**(11): p. 6973-81.
163. de Silva, T.I., M. Cotten, and S.L. Rowland-Jones, *HIV-2: the forgotten AIDS virus.* Trends Microbiol, 2008. **16**(12): p. 588-95.
164. Hodges-Mameletzis, I., G.J. De Bree, and S.L. Rowland-Jones, *An underestimated lentivirus model: what can HIV-2 research contribute to the development of an effective HIV-1 vaccine?* Expert Rev Anti Infect Ther, 2011. **9**(2): p. 195-206.
165. Esbjornsson, J., et al., *Inhibition of HIV-1 disease progression by contemporaneous HIV-2 infection.* N Engl J Med, 2012. **367**(3): p. 224-32.
166. Coffin, J.M., S.H. Hughes, and H.E. Varmus, *The Interactions of Retroviruses and their Hosts.* 1997.
167. Brelot, A. and M. Alizon, *HIV-1 entry and how to block it.* AIDS, 2001. **15 Suppl 5**: p. S3-11.
168. Gentili, M., et al., *Transmission of innate immune signaling by packaging of cGAMP in viral particles.* Science, 2015. **349**(6253): p. 1232-6.
169. Rey, M.A., et al., *Characterization of human immunodeficiency virus type 2 envelope glycoproteins: dimerization of the glycoprotein precursor during processing.* J Virol, 1989. **63**(2): p. 647-58.
170. Bahraoui, E., et al., *Study of the interaction of HIV-1 and HIV-2 envelope glycoproteins with the CD4 receptor and role of N-glycans.* AIDS Res Hum Retroviruses, 1992. **8**(5): p. 565-73.
171. Mitchell, R.S., et al., *Retroviral DNA integration: ASLV, HIV, and MLV show distinct target site preferences.* PLoS Biol, 2004. **2**(8): p. E234.
172. Schroder, A.R., et al., *HIV-1 integration in the human genome favors active genes and local hotspots.* Cell, 2002. **110**(4): p. 521-9.
173. Marini, B., et al., *Nuclear architecture dictates HIV-1 integration site selection.* Nature, 2015. **521**(7551): p. 227-31.
174. Coffin, J.M., S.H. Hughes, and H.E. Varmus, *The Interactions of Retroviruses and their Hosts*, in *Retroviruses*, J.M. Coffin, S.H. Hughes, and H.E. Varmus, Editors. 1997: Cold Spring Harbor (NY).
175. Gupta, S. and D. Mitra, *Human immunodeficiency virus-1 Tat protein: immunological facets of a transcriptional activator.* Indian J Biochem Biophys, 2007. **44**(5): p. 269-75.
176. Yu, Z., et al., *The cellular HIV-1 Rev cofactor hRIP is required for viral replication.* Proc Natl Acad Sci U S A, 2005. **102**(11): p. 4027-32.

177. Garcia, F., et al., *[Absence of HIV infection among the mentally retarded]*. Enferm Infecc Microbiol Clin, 1991. **9**(8): p. 516.
178. Schwartz, O., et al., *Endocytosis of major histocompatibility complex class I molecules is induced by the HIV-1 Nef protein.* Nat Med, 1996. **2**(3): p. 338-42.
179. Stumptner-Cuvelette, P., et al., *HIV-1 Nef impairs MHC class II antigen presentation and surface expression.* Proc Natl Acad Sci U S A, 2001. **98**(21): p. 12144-9.
180. Thoulouze, M.I., et al., *Human immunodeficiency virus type-1 infection impairs the formation of the immunological synapse.* Immunity, 2006. **24**(5): p. 547-61.
181. Sheehy, A.M., et al., *Isolation of a human gene that inhibits HIV-1 infection and is suppressed by the viral Vif protein.* Nature, 2002. **418**(6898): p. 646-50.
182. Willey, R.L., et al., *Human immunodeficiency virus type 1 Vpu protein regulates the formation of intracellular gp160-CD4 complexes.* J Virol, 1992. **66**(1): p. 226-34.
183. Balliet, J.W., et al., *Distinct effects in primary macrophages and lymphocytes of the human immunodeficiency virus type 1 accessory genes vpr, vpu, and nef: mutational analysis of a primary HIV-1 isolate.* Virology, 1994. **200**(2): p. 623-31.
184. Connor, R.I., et al., *Vpr is required for efficient replication of human immunodeficiency virus type-1 in mononuclear phagocytes.* Virology, 1995. **206**(2): p. 935-44.
185. Heinzinger, N.K., et al., *The Vpr protein of human immunodeficiency virus type 1 influences nuclear localization of viral nucleic acids in nondividing host cells.* Proc Natl Acad Sci U S A, 1994. **91**(15): p. 7311-5.
186. Jowett, J.B., et al., *The human immunodeficiency virus type 1 vpr gene arrests infected T cells in the G2 + M phase of the cell cycle.* J Virol, 1995. **69**(10): p. 6304-13.
187. Laguette, N., et al., *Premature activation of the SLX4 complex by Vpr promotes G2/M arrest and escape from innate immune sensing.* Cell, 2014. **156**(1-2): p. 134-45.
188. Shibata, D., et al., *Human T-cell lymphotropic virus type I (HTLV-I)-associated adult T-cell leukemia-lymphoma in a patient infected with human immunodeficiency virus type 1 (HIV-1).* Ann Intern Med, 1989. **111**(11): p. 871-5.
189. Briz, V., E. Poveda, and V. Soriano, *HIV entry inhibitors: mechanisms of action and resistance pathways.* J Antimicrob Chemother, 2006. **57**(4): p. 619-27.
190. Moore, J.P. and J. Binley, *HIV. Envelope's letters boxed into shape.* Nature, 1998. **393**(6686): p. 630-1.
191. Poveda, E., et al., *Enfuvirtide is active against HIV type 1 group O.* AIDS Res Hum Retroviruses, 2005. **21**(6): p. 583-5.
192. Fassati, A. and S.P. Goff, *Characterization of intracellular reverse transcription complexes of human immunodeficiency virus type 1.* J Virol, 2001. **75**(8): p. 3626-35.
193. Miller, M.D., C.M. Farnet, and F.D. Bushman, *Human immunodeficiency virus type 1 preintegration complexes: studies of organization and composition.* J Virol, 1997. **71**(7): p. 5382-90.

194. Bukrinsky, M.I., et al., *Association of integrase, matrix, and reverse transcriptase antigens of human immunodeficiency virus type 1 with viral nucleic acids following acute infection.* Proc Natl Acad Sci U S A, 1993. **90**(13): p. 6125-9.
195. Bukrinsky, M.I., et al., *A nuclear localization signal within HIV-1 matrix protein that governs infection of non-dividing cells.* Nature, 1993. **365**(6447): p. 666-9.
196. Nisole, S. and A. Saib, *Early steps of retrovirus replicative cycle.* Retrovirology, 2004. **1**: p. 9.
197. Sundquist, W.I. and H.G. Krausslich, *HIV-1 assembly, budding, and maturation.* Cold Spring Harb Perspect Med, 2012. **2**(7): p. a006924.
198. Alabi, A.S., et al., *Plasma viral load, CD4 cell percentage, HLA and survival of HIV-1, HIV-2, and dually infected Gambian patients.* AIDS, 2003. **17**(10): p. 1513-20.
199. Andersson, S., et al., *Plasma viral load in HIV-1 and HIV-2 singly and dually infected individuals in Guinea-Bissau, West Africa: significantly lower plasma virus set point in HIV-2 infection than in HIV-1 infection.* Arch Intern Med, 2000. **160**(21): p. 3286-93.
200. Popper, S.J., et al., *Low plasma human immunodeficiency virus type 2 viral load is independent of proviral load: low virus production in vivo.* J Virol, 2000. **74**(3): p. 1554-7.
201. Popper, S.J., et al., *Lower human immunodeficiency virus (HIV) type 2 viral load reflects the difference in pathogenicity of HIV-1 and HIV-2.* J Infect Dis, 1999. **180**(4): p. 1116-21.
202. Simon, F., et al., *Cellular and plasma viral load in patients infected with HIV-2.* AIDS, 1993. **7**(11): p. 1411-7.
203. Reeves, J.D., et al., *CD4-independent infection by HIV-2 (ROD/B): use of the 7-transmembrane receptors CXCR-4, CCR-3, and V28 for entry.* Virology, 1997. **231**(1): p. 130-4.
204. Guillon, C., et al., *Coreceptor usage of human immunodeficiency virus type 2 primary isolates and biological clones is broad and does not correlate with their syncytium-inducing capacities.* J Virol, 1998. **72**(7): p. 6260-3.
205. McKnight, A., et al., *A broad range of chemokine receptors are used by primary isolates of human immunodeficiency virus type 2 as coreceptors with CD4.* J Virol, 1998. **72**(5): p. 4065-71.
206. Shimizu, N., et al., *An orphan G protein-coupled receptor, GPR1, acts as a coreceptor to allow replication of human immunodeficiency virus types 1 and 2 in brain-derived cells.* J Virol, 1999. **73**(6): p. 5231-9.
207. Rucker, J., et al., *Utilization of chemokine receptors, orphan receptors, and herpesvirus-encoded receptors by diverse human and simian immunodeficiency viruses.* J Virol, 1997. **71**(12): p. 8999-9007.
208. Deng, H.K., et al., *Expression cloning of new receptors used by simian and human immunodeficiency viruses.* Nature, 1997. **388**(6639): p. 296-300.
209. Sol, N., et al., *Usage of the coreceptors CCR-5, CCR-3, and CXCR-4 by primary and cell line-adapted human immunodeficiency virus type 2.* J Virol, 1997. **71**(11): p. 8237-44.
210. Owen, S.M., et al., *Genetically divergent strains of human immunodeficiency virus type 2 use multiple coreceptors for viral entry.* J Virol, 1998. **72**(7): p. 5425-32.

211. Bron, R., et al., *Promiscuous use of CC and CXC chemokine receptors in cell-to-cell fusion mediated by a human immunodeficiency virus type 2 envelope protein.* J Virol, 1997. **71**(11): p. 8405-15.
212. Shi, Y., et al., *Evolution of human immunodeficiency virus type 2 coreceptor usage, autologous neutralization, envelope sequence and glycosylation.* J Gen Virol, 2005. **86**(Pt 12): p. 3385-96.
213. Weber, J., *The pathogenesis of HIV-1 infection.* Br Med Bull, 2001. **58**: p. 61-72.
214. Mattapallil, J.J., et al., *Massive infection and loss of memory CD4+ T cells in multiple tissues during acute SIV infection.* Nature, 2005. **434**(7037): p. 1093-7.
215. Brenchley, J.M., et al., *T-cell subsets that harbor human immunodeficiency virus (HIV) in vivo: implications for HIV pathogenesis.* J Virol, 2004. **78**(3): p. 1160-8.
216. Brenchley, J.M., et al., *Differential Th17 CD4 T-cell depletion in pathogenic and nonpathogenic lentiviral infections.* Blood, 2008. **112**(7): p. 2826-35.
217. Brenchley, J.M., et al., *Microbial translocation is a cause of systemic immune activation in chronic HIV infection.* Nat Med, 2006. **12**(12): p. 1365-71.
218. Clark, S.J., et al., *High titers of cytopathic virus in plasma of patients with symptomatic primary HIV-1 infection.* N Engl J Med, 1991. **324**(14): p. 954-60.
219. Daar, E.S. and D.D. Ho, *Relative resistance of primary HIV-1 isolates to neutralization by soluble CD4.* Am J Med, 1991. **90**(4A): p. 22S-26S.
220. Veazey, R.S., et al., *Gastrointestinal tract as a major site of CD4+ T cell depletion and viral replication in SIV infection.* Science, 1998. **280**(5362): p. 427-31.
221. Li, Q., et al., *Peak SIV replication in resting memory CD4+ T cells depletes gut lamina propria CD4+ T cells.* Nature, 2005. **434**(7037): p. 1148-52.
222. Rosenberg, E.S., et al., *Immune control of HIV-1 after early treatment of acute infection.* Nature, 2000. **407**(6803): p. 523-6.
223. Cohen, M.S., et al., *Prevention of HIV-1 infection with early antiretroviral therapy.* N Engl J Med, 2011. **365**(6): p. 493-505.
224. Ho, D.D., et al., *Rapid turnover of plasma virions and CD4 lymphocytes in HIV-1 infection.* Nature, 1995. **373**(6510): p. 123-6.
225. Piatak, M., Jr., et al., *Determination of plasma viral load in HIV-1 infection by quantitative competitive polymerase chain reaction.* AIDS, 1993. **7 Suppl 2**: p. S65-71.
226. Schacker, T.W., et al., *Biological and virologic characteristics of primary HIV infection.* Ann Intern Med, 1998. **128**(8): p. 613-20.
227. Doyle, T., C. Goujon, and M.H. Malim, *HIV-1 and interferons: who's interfering with whom?* Nat Rev Microbiol, 2015. **13**(7): p. 403-13.
228. Clerici, M. and G.M. Shearer, *A TH1-->TH2 switch is a critical step in the etiology of HIV infection.* Immunol Today, 1993. **14**(3): p. 107-11.
229. Herbeuval, J.P., et al., *CD4+ T-cell death induced by infectious and noninfectious HIV-1: role of type 1 interferon-dependent, TRAIL/DR5-mediated apoptosis.* Blood, 2005. **106**(10): p. 3524-31.
230. Hardy, G.A., et al., *Interferon-alpha is the primary plasma type-I IFN in HIV-1 infection and correlates with immune activation and disease markers.* PLoS One, 2013. **8**(2): p. e56527.

231. Marshall, H.D., S.L. Urban, and R.M. Welsh, *Virus-induced transient immune suppression and the inhibition of T cell proliferation by type I interferon.* J Virol, 2011. **85**(12): p. 5929-39.
232. Keele, B.F., et al., *Characterization of the follicular dendritic cell reservoir of human immunodeficiency virus type 1.* J Virol, 2008. **82**(11): p. 5548-61.
233. Fauci, A.S., et al., *NIH conference. Immunopathogenic mechanisms in human immunodeficiency virus (HIV) infection.* Ann Intern Med, 1991. **114**(8): p. 678-93.
234. Haynes, B.E., et al., *Medical response to catastrophic events: California's planning and the Loma Prieta earthquake.* Ann Emerg Med, 1992. **21**(4): p. 368-74.
235. Lifson, A.R., et al., *Long-term human immunodeficiency virus infection in asymptomatic homosexual and bisexual men with normal CD4+ lymphocyte counts: immunologic and virologic characteristics.* J Infect Dis, 1991. **163**(5): p. 959-65.
236. Samson, M., et al., *Resistance to HIV-1 infection in caucasian individuals bearing mutant alleles of the CCR-5 chemokine receptor gene.* Nature, 1996. **382**(6593): p. 722-5.
237. Huang, Y., et al., *The role of a mutant CCR5 allele in HIV-1 transmission and disease progression.* Nat Med, 1996. **2**(11): p. 1240-3.
238. Quillent, C., et al., *HIV-1-resistance phenotype conferred by combination of two separate inherited mutations of CCR5 gene.* Lancet, 1998. **351**(9095): p. 14-8.
239. Barassi, C., et al., *Induction of murine mucosal CCR5-reactive antibodies as an anti-human immunodeficiency virus strategy.* J Virol, 2005. **79**(11): p. 6848-58.
240. Clerici, M., et al., *Serum IgA of HIV-exposed uninfected individuals inhibit HIV through recognition of a region within the alpha-helix of gp41.* AIDS, 2002. **16**(13): p. 1731-41.
241. Sheppard, H.W., et al., *The characterization of non-progressors: long-term HIV-1 infection with stable CD4+ T-cell levels.* AIDS, 1993. **7**(9): p. 1159-66.
242. Guergnon, J., et al., *Single-nucleotide polymorphism-defined class I and class III major histocompatibility complex genetic subregions contribute to natural long-term nonprogression in HIV infection.* J Infect Dis, 2012. **205**(5): p. 718-24.
243. Shacklett, B.L., *Understanding the "lucky few": the conundrum of HIV-exposed, seronegative individuals.* Curr HIV/AIDS Rep, 2006. **3**(1): p. 26-31.
244. Avettand-Fenoel, V., et al., *HIV-DNA in rectal cells is well correlated with HIV-DNA in blood in different groups of patients, including long-term non-progressors.* AIDS, 2008. **22**(14): p. 1880-2.
245. Dalmasso, C., et al., *Distinct genetic loci control plasma HIV-RNA and cellular HIV-DNA levels in HIV-1 infection: the ANRS Genome Wide Association 01 study.* PLoS One, 2008. **3**(12): p. e3907.
246. Deeks, S.G. and B.D. Walker, *Human immunodeficiency virus controllers: mechanisms of durable virus control in the absence of antiretroviral therapy.* Immunity, 2007. **27**(3): p. 406-16.
247. Manel, N., et al., *A cryptic sensor for HIV-1 activates antiviral innate immunity in dendritic cells.* Nature, 2010. **467**(7312): p. 214-7.

248. Lahouassa, H., et al., *SAMHD1 restricts the replication of human immunodeficiency virus type 1 by depleting the intracellular pool of deoxynucleoside triphosphates.* Nat Immunol, 2012. **13**(3): p. 223-8.
249. Rice, G.I., et al., *Mutations involved in Aicardi-Goutieres syndrome implicate SAMHD1 as regulator of the innate immune response.* Nat Genet, 2009. **41**(7): p. 829-32.
250. Crow, Y.J. and J. Rehwinkel, *Aicardi-Goutieres syndrome and related phenotypes: linking nucleic acid metabolism with autoimmunity.* Hum Mol Genet, 2009. **18**(R2): p. R130-6.
251. Goujon, C., et al., *SIVSM/HIV-2 Vpx proteins promote retroviral escape from a proteasome-dependent restriction pathway present in human dendritic cells.* Retrovirology, 2007. **4**: p. 2.
252. Luban, J., et al., *Human immunodeficiency virus type 1 Gag protein binds to cyclophilins A and B.* Cell, 1993. **73**(6): p. 1067-78.
253. Franke, E.K., H.E. Yuan, and J. Luban, *Specific incorporation of cyclophilin A into HIV-1 virions.* Nature, 1994. **372**(6504): p. 359-62.
254. Goujon, C., et al., *With a little help from a friend: increasing HIV transduction of monocyte-derived dendritic cells with virion-like particles of SIV(MAC).* Gene Ther, 2006. **13**(12): p. 991-4.
255. Manel, N. and D.R. Littman, *Hiding in plain sight: how HIV evades innate immune responses.* Cell, 2011. **147**(2): p. 271-4.
256. Lee, K., et al., *Flexible use of nuclear import pathways by HIV-1.* Cell Host Microbe, 2010. **7**(3): p. 221-33.
257. Price, A.J., et al., *CPSF6 defines a conserved capsid interface that modulates HIV-1 replication.* PLoS Pathog, 2012. **8**(8): p. e1002896.
258. Chauveau, L., et al., *HIV-2 infects resting CD4+ T cells but not monocyte-derived dendritic cells.* Retrovirology, 2015. **12**: p. 2.
259. Kalams, S.A., et al., *Association between virus-specific cytotoxic T-lymphocyte and helper responses in human immunodeficiency virus type 1 infection.* J Virol, 1999. **73**(8): p. 6715-20.
260. Rosenberg, E.S., et al., *Vigorous HIV-1-specific CD4+ T cell responses associated with control of viremia.* Science, 1997. **278**(5342): p. 1447-50.
261. Ortiz, M., et al., *No longitudinal mitochondrial DNA sequence changes in HIV-infected individuals with and without lipoatrophy.* J Infect Dis, 2011. **203**(5): p. 620-4.
262. Douek, D.C., et al., *HIV preferentially infects HIV-specific CD4+ T cells.* Nature, 2002. **417**(6884): p. 95-8.
263. Porichis, F., et al., *Responsiveness of HIV-specific CD4 T cells to PD-1 blockade.* Blood, 2011. **118**(4): p. 965-74.
264. D'Souza, M., et al., *Programmed death 1 expression on HIV-specific CD4+ T cells is driven by viral replication and associated with T cell dysfunction.* J Immunol, 2007. **179**(3): p. 1979-87.
265. Kaufmann, D.E., et al., *Upregulation of CTLA-4 by HIV-specific CD4+ T cells correlates with disease progression and defines a reversible immune dysfunction.* Nat Immunol, 2007. **8**(11): p. 1246-54.
266. Martins, G.A., et al., *Blimp-1 directly represses Il2 and the Il2 activator Fos, attenuating T cell proliferation and survival.* J Exp Med, 2008. **205**(9): p. 1959-65.
267. Thiele, S., et al., *miR-9 enhances IL-2 production in activated human CD4(+) T cells by repressing Blimp-1.* Eur J Immunol, 2012. **42**(8): p. 2100-8.

268. Allan, J.S., et al., *Major glycoprotein antigens that induce antibodies in AIDS patients are encoded by HTLV-III.* Science, 1985. **228**(4703): p. 1091-4.
269. Pitcher, C.J., et al., *HIV-1-specific CD4+ T cells are detectable in most individuals with active HIV-1 infection, but decline with prolonged viral suppression.* Nat Med, 1999. **5**(5): p. 518-25.
270. Kaufmann, D.E., et al., *Limited durability of viral control following treated acute HIV infection.* PLoS Med, 2004. **1**(2): p. e36.
271. Iannello, A., S. Samarani, and A. Ahmad, *Comment on "HIV-specific IL-21 producing CD4+ T cells are induced in acute and chronic progressive HIV infection and are associated with relative viral control".* J Immunol, 2010. **185**(10): p. 5675; author reply 5675.
272. Ferre, A.L., et al., *HIV controllers with HLA-DRB1*13 and HLA-DQB1*06 alleles have strong, polyfunctional mucosal CD4+ T-cell responses.* J Virol, 2010. **84**(21): p. 11020-9.
273. Soghoian, D.Z., et al., *HIV-specific cytolytic CD4 T cell responses during acute HIV infection predict disease outcome.* Sci Transl Med, 2012. **4**(123): p. 123ra25.
274. Kader, M., et al., *Alpha4(+)beta7(hi)CD4(+) memory T cells harbor most Th-17 cells and are preferentially infected during acute SIV infection.* Mucosal Immunol, 2009. **2**(5): p. 439-49.
275. Alimonti, J.B., T.B. Ball, and K.R. Fowke, *Mechanisms of CD4+ T lymphocyte cell death in human immunodeficiency virus infection and AIDS.* J Gen Virol, 2003. **84**(Pt 7): p. 1649-61.
276. Cooper, A., et al., *HIV-1 causes CD4 cell death through DNA-dependent protein kinase during viral integration.* Nature, 2013. **498**(7454): p. 376-9.
277. Gandhi, R.T., et al., *HIV-1 directly kills CD4+ T cells by a Fas-independent mechanism.* J Exp Med, 1998. **187**(7): p. 1113-22.
278. Laurent-Crawford, A.G., et al., *The cytopathic effect of HIV is associated with apoptosis.* Virology, 1991. **185**(2): p. 829-39.
279. Terai, C., et al., *Apoptosis as a mechanism of cell death in cultured T lymphoblasts acutely infected with HIV-1.* J Clin Invest, 1991. **87**(5): p. 1710-5.
280. Zhang, Y.J., et al., *Induction of apoptosis by primary HIV-1 isolates correlates with productive infection in peripheral blood mononuclear cells.* AIDS, 1997. **11**(10): p. 1219-25.
281. Jekle, A., et al., *In vivo evolution of human immunodeficiency virus type 1 toward increased pathogenicity through CXCR4-mediated killing of uninfected CD4 T cells.* J Virol, 2003. **77**(10): p. 5846-54.
282. Meyaard, L., et al., *Programmed death of T cells in HIV-1 infection.* Science, 1992. **257**(5067): p. 217-9.
283. Muro-Cacho, C.A., G. Pantaleo, and A.S. Fauci, *Analysis of apoptosis in lymph nodes of HIV-infected persons. Intensity of apoptosis correlates with the general state of activation of the lymphoid tissue and not with stage of disease or viral burden.* J Immunol, 1995. **154**(10): p. 5555-66.
284. Finkel, T.H., et al., *Apoptosis occurs predominantly in bystander cells and not in productively infected cells of HIV- and SIV-infected lymph nodes.* Nat Med, 1995. **1**(2): p. 129-34.
285. Rosok, B., et al., *Correlates of latent and productive HIV type-1 infection in tonsillar CD4(+) T cells.* Proc Natl Acad Sci U S A, 1997. **94**(17): p. 9332-6.

286. Glushakova, S., et al., *Infection of human tonsil histocultures: a model for HIV pathogenesis.* Nat Med, 1995. **1**(12): p. 1320-2.
287. Zeng, M., A.T. Haase, and T.W. Schacker, *Lymphoid tissue structure and HIV-1 infection: life or death for T cells.* Trends Immunol, 2012. **33**(6): p. 306-14.
288. Doitsh, G., et al., *Abortive HIV infection mediates CD4 T cell depletion and inflammation in human lymphoid tissue.* Cell, 2010. **143**(5): p. 789-801.
289. Munoz-Arias, I., et al., *Blood-Derived CD4 T Cells Naturally Resist Pyroptosis during Abortive HIV-1 Infection.* Cell Host Microbe, 2015. **18**(4): p. 463-70.
290. Baldauf, H.M., et al., *SAMHD1 restricts HIV-1 infection in resting CD4(+) T cells.* Nat Med, 2012. **18**(11): p. 1682-7.
291. Ablasser, A., et al., *Cell intrinsic immunity spreads to bystander cells via the intercellular transfer of cGAMP.* Nature, 2013. **503**(7477): p. 530-4.
292. Konig, R., et al., *Global analysis of host-pathogen interactions that regulate early-stage HIV-1 replication.* Cell, 2008. **135**(1): p. 49-60.
293. Brass, A.L., et al., *Identification of host proteins required for HIV infection through a functional genomic screen.* Science, 2008. **319**(5865): p. 921-6.
294. Pereira-Lopes, S., et al., *The exonuclease Trex1 restrains macrophage proinflammatory activation.* J Immunol, 2013. **191**(12): p. 6128-35.
295. Allen, I.C., et al., *NLRX1 protein attenuates inflammatory responses to infection by interfering with the RIG-I-MAVS and TRAF6-NF-kappaB signaling pathways.* Immunity, 2011. **34**(6): p. 854-65.
296. Moore, C.B., et al., *NLRX1 is a regulator of mitochondrial antiviral immunity.* Nature, 2008. **451**(7178): p. 573-7.
297. Abdul-Sater, A.A., et al., *Enhancement of reactive oxygen species production and chlamydial infection by the mitochondrial Nod-like family member NLRX1.* J Biol Chem, 2010. **285**(53): p. 41637-45.
298. Tattoli, I., et al., *NLRX1 is a mitochondrial NOD-like receptor that amplifies NF-kappaB and JNK pathways by inducing reactive oxygen species production.* EMBO Rep, 2008. **9**(3): p. 293-300.
299. Lei, Y., et al., *The mitochondrial proteins NLRX1 and TUFM form a complex that regulates type I interferon and autophagy.* Immunity, 2012. **36**(6): p. 933-46.
300. Barouch, D.H., et al., *Rapid Inflammasome Activation following Mucosal SIV Infection of Rhesus Monkeys.* Cell, 2016. **165**(3): p. 656-67.
301. Guo, H., et al., *NLRX1 Sequesters STING to Negatively Regulate the Interferon Response, Thereby Facilitating the Replication of HIV-1 and DNA Viruses.* Cell Host Microbe, 2016. **19**(4): p. 515-28.
302. Brinkmann, V., et al., *Interferon alpha increases the frequency of interferon gamma-producing human CD4+ T cells.* J Exp Med, 1993. **178**(5): p. 1655-63.
303. Swiecki, M. and M. Colonna, *Type I interferons: diversity of sources, production pathways and effects on immune responses.* Curr Opin Virol, 2011. **1**(6): p. 463-75.
304. Wang, Y., et al., *Timing and magnitude of type I interferon responses by distinct sensors impact CD8 T cell exhaustion and chronic viral infection.* Cell Host Microbe, 2012. **11**(6): p. 631-42.
305. Biron, C.A., *Interferons alpha and beta as immune regulators--a new look.* Immunity, 2001. **14**(6): p. 661-4.

306. Davidson, S., et al., *Pathogenic potential of interferon alphabeta in acute influenza infection.* Nat Commun, 2014. **5**: p. 3864.
307. Fraietta, J.A., et al., *Type I interferon upregulates Bak and contributes to T cell loss during human immunodeficiency virus (HIV) infection.* PLoS Pathog, 2013. **9**(10): p. e1003658.
308. Gougeon, M.L. and J.P. Herbeuval, *IFN-alpha and TRAIL: a double edge sword in HIV-1 disease?* Exp Cell Res, 2012. **318**(11): p. 1260-8.
309. Cousens, L.P., et al., *Two roads diverged: interferon alpha/beta- and interleukin 12-mediated pathways in promoting T cell interferon gamma responses during viral infection.* J Exp Med, 1999. **189**(8): p. 1315-28.
310. Nguyen, K.B., et al., *Critical role for STAT4 activation by type 1 interferons in the interferon-gamma response to viral infection.* Science, 2002. **297**(5589): p. 2063-6.
311. Bromberg, J.F., et al., *Transcriptionally active Stat1 is required for the antiproliferative effects of both interferon alpha and interferon gamma.* Proc Natl Acad Sci U S A, 1996. **93**(15): p. 7673-8.
312. Lee, C.K., et al., *STAT1 affects lymphocyte survival and proliferation partially independent of its role downstream of IFN-gamma.* J Immunol, 2000. **164**(3): p. 1286-92.
313. Tanabe, Y., et al., *Cutting edge: role of STAT1, STAT3, and STAT5 in IFN-alpha beta responses in T lymphocytes.* J Immunol, 2005. **174**(2): p. 609-13.
314. Touzot, M., et al., *Combinatorial flexibility of cytokine function during human T helper cell differentiation.* Nat Commun, 2014. **5**: p. 3987.
315. Swiecki, M., N.S. Omattage, and T.J. Brett, *BST-2/tetherin: structural biology, viral antagonism, and immunobiology of a potent host antiviral factor.* Mol Immunol, 2013. **54**(2): p. 132-9.
316. Sauter, D., *Counteraction of the multifunctional restriction factor tetherin.* Front Microbiol, 2014. **5**: p. 163.
317. Perreau, M., et al., *Follicular helper T cells serve as the major CD4 T cell compartment for HIV-1 infection, replication, and production.* J Exp Med, 2013. **210**(1): p. 143-56.
318. Allain, J.P., et al., *Antibody to HIV-1, HTLV-I, and HCV in three populations of rural Haitians.* J Acquir Immune Defic Syndr, 1992. **5**(12): p. 1230-6.
319. von Sydow, M., et al., *Interferon-alpha and tumor necrosis factor-alpha in serum of patients in various stages of HIV-1 infection.* AIDS Res Hum Retroviruses, 1991. **7**(4): p. 375-80.
320. Borrow, P., *Innate immunity in acute HIV-1 infection.* Curr Opin HIV AIDS, 2011. **6**(5): p. 353-63.
321. Stylianou, E., et al., *Interferons and interferon (IFN)-inducible protein 10 during highly active anti-retroviral therapy (HAART)-possible immunosuppressive role of IFN-alpha in HIV infection.* Clin Exp Immunol, 2000. **119**(3): p. 479-85.
322. Stetson, D.B. and R. Medzhitov, *Type I interferons in host defense.* Immunity, 2006. **25**(3): p. 373-81.
323. Silvin, A. and N. Manel, *Innate immune sensing of HIV infection.* Curr Opin Immunol, 2015. **32**: p. 54-60.
324. Fuller, M.J., et al., *Maintenance, loss, and resurgence of T cell responses during acute, protracted, and chronic viral infections.* J Immunol, 2004. **172**(7): p. 4204-14.

325. Wherry, E.J., et al., *Viral persistence alters CD8 T-cell immunodominance and tissue distribution and results in distinct stages of functional impairment.* J Virol, 2003. **77**(8): p. 4911-27.
326. Agnellini, P., et al., *Impaired NFAT nuclear translocation results in split exhaustion of virus-specific CD8+ T cell functions during chronic viral infection.* Proc Natl Acad Sci U S A, 2007. **104**(11): p. 4565-70.
327. Mackerness, K.J., et al., *Pronounced virus-dependent activation drives exhaustion but sustains IFN-gamma transcript levels.* J Immunol, 2010. **185**(6): p. 3643-51.
328. Sandler, N.G., et al., *Type I interferon responses in rhesus macaques prevent SIV infection and slow disease progression.* Nature, 2014. **511**(7511): p. 601-5.
329. Lahaye, X., et al., *Nuclear Envelope Protein SUN2 Promotes Cyclophilin-A-Dependent Steps of HIV Replication.* Cell Rep, 2016.
330. Kauffmann, A., R. Gentleman, and W. Huber, *arrayQualityMetrics--a bioconductor package for quality assessment of microarray data.* Bioinformatics, 2009. **25**(3): p. 415-6.
331. Carvalho, B.S. and R.A. Irizarry, *A framework for oligonucleotide microarray preprocessing.* Bioinformatics, 2010. **26**(19): p. 2363-7.
332. Ritchie, M.E., et al., *limma powers differential expression analyses for RNA-sequencing and microarray studies.* Nucleic Acids Res, 2015. **43**(7): p. e47.
333. Culhane, A.C., et al., *MADE4: an R package for multivariate analysis of gene expression data.* Bioinformatics, 2005. **21**(11): p. 2789-90.
334. Langfelder, P. and S. Horvath, *WGCNA: an R package for weighted correlation network analysis.* BMC Bioinformatics, 2008. **9**: p. 559.
335. Subramanian, A., et al., *Gene set enrichment analysis: a knowledge-based approach for interpreting genome-wide expression profiles.* Proc Natl Acad Sci U S A, 2005. **102**(43): p. 15545-50.
336. Heinz, S., et al., *Simple combinations of lineage-determining transcription factors prime cis-regulatory elements required for macrophage and B cell identities.* Mol Cell, 2010. **38**(4): p. 576-89.
337. Kwon, A.T., et al., *oPOSSUM-3: advanced analysis of regulatory motif over-representation across genes or ChIP-Seq datasets.* G3 (Bethesda), 2012. **2**(9): p. 987-1002.
338. Zambelli, F., G. Pesole, and G. Pavesi, *Pscan: finding over-represented transcription factor binding site motifs in sequences from co-regulated or co-expressed genes.* Nucleic Acids Res, 2009. **37**(Web Server issue): p. W247-52.
339. Iwasaki, A. and R. Medzhitov, *Control of adaptive immunity by the innate immune system.* Nat Immunol, 2015. **16**(4): p. 343-53.
340. Bruchard, M., et al., *The receptor NLRP3 is a transcriptional regulator of TH2 differentiation.* Nat Immunol, 2015. **16**(8): p. 859-70.
341. Wu, J., et al., *Cyclic GMP-AMP Is an Endogenous Second Messenger in Innate Immune Signaling by Cytosolic DNA.* Science, 2012.
342. Li, X.D., et al., *Pivotal roles of cGAS-cGAMP signaling in antiviral defense and immune adjuvant effects.* Science, 2013. **341**(6152): p. 1390-4.
343. Meyts, I. and J.L. Casanova, *A human inborn error connects the alpha's.* Nat Immunol, 2016. **17**(5): p. 472-4.
344. Tang, C.H., et al., *Agonist-Mediated Activation of STING Induces Apoptosis in Malignant B Cells.* Cancer Res, 2016. **76**(8): p. 2137-52.

345. Kranzusch, P.J., et al., *Ancient Origin of cGAS-STING Reveals Mechanism of Universal 2',3' cGAMP Signaling.* Mol Cell, 2015. **59**(6): p. 891-903.
346. Pillai, S., et al., *Tank binding kinase 1 is a centrosome-associated kinase necessary for microtubule dynamics and mitosis.* Nat Commun, 2015. **6**: p. 10072.
347. Pannicke, U., et al., *Deficiency of innate and acquired immunity caused by an IKBKB mutation.* N Engl J Med, 2013. **369**(26): p. 2504-14.
348. Torres, J.M., et al., *Inherited BCL10 deficiency impairs hematopoietic and nonhematopoietic immunity.* J Clin Invest, 2014. **124**(12): p. 5239-48.
349. Courtois, G., et al., *A hypermorphic IkappaBalpha mutation is associated with autosomal dominant anhidrotic ectodermal dysplasia and T cell immunodeficiency.* J Clin Invest, 2003. **112**(7): p. 1108-15.
350. Greil, J., et al., *Whole-exome sequencing links caspase recruitment domain 11 (CARD11) inactivation to severe combined immunodeficiency.* J Allergy Clin Immunol, 2013. **131**(5): p. 1376-83 e3.
351. Stepensky, P., et al., *Deficiency of caspase recruitment domain family, member 11 (CARD11), causes profound combined immunodeficiency in human subjects.* J Allergy Clin Immunol, 2013. **131**(2): p. 477-85 e1.
352. Chien, Y., et al., *Control of the senescence-associated secretory phenotype by NF-kappaB promotes senescence and enhances chemosensitivity.* Genes Dev, 2011. **25**(20): p. 2125-36.
353. Colanzi, A. and C. Sutterlin, *Signaling at the Golgi during mitosis.* Methods Cell Biol, 2013. **118**: p. 383-400.
354. Pourcelot, M., et al., *The Golgi apparatus acts as a platform for TBK1 activation after viral RNA sensing.* BMC Biol, 2016. **14**: p. 69.
355. Onorati, M., et al., *Zika Virus Disrupts Phospho-TBK1 Localization and Mitosis in Human Neuroepithelial Stem Cells and Radial Glia.* Cell Rep, 2016. **16**(10): p. 2576-92.
356. Kim, J.H., et al., *High cleavage efficiency of a 2A peptide derived from porcine teschovirus-1 in human cell lines, zebrafish and mice.* PLoS One, 2011. **6**(4): p. e18556.
357. Asensio, V.C., et al., *Interferon-independent, human immunodeficiency virus type 1 gp120-mediated induction of CXCL10/IP-10 gene expression by astrocytes in vivo and in vitro.* J Virol, 2001. **75**(15): p. 7067-77.
358. Ahonen, C.L., et al., *Dendritic cell maturation and subsequent enhanced T-cell stimulation induced with the novel synthetic immune response modifier R-848.* Cell Immunol, 1999. **197**(1): p. 62-72.
359. Garland, S.M., *Imiquimod.* Curr Opin Infect Dis, 2003. **16**(2): p. 85-9.
360. Lombardi, V., et al., *Human dendritic cells stimulated via TLR7 and/or TLR8 induce the sequential production of Il-10, IFN-gamma, and IL-17A by naive CD4+ T cells.* J Immunol, 2009. **182**(6): p. 3372-9.
361. Trinchieri, G., *Interleukin-12 and the regulation of innate resistance and adaptive immunity.* Nat Rev Immunol, 2003. **3**(2): p. 133-46.
362. Parrish-Novak, J., et al., *Interleukin 21 and its receptor are involved in NK cell expansion and regulation of lymphocyte function.* Nature, 2000. **408**(6808): p. 57-63.
363. Parrish-Novak, J., et al., *Interleukin-21 and the IL-21 receptor: novel effectors of NK and T cell responses.* J Leukoc Biol, 2002. **72**(5): p. 856-63.

364. Ahluwalia, J.K., et al., *Human cellular microRNA hsa-miR-29a interferes with viral nef protein expression and HIV-1 replication.* Retrovirology, 2008. **5**: p. 117.
365. Adoro, S., et al., *IL-21 induces antiviral microRNA-29 in CD4 T cells to limit HIV-1 infection.* Nat Commun, 2015. **6**: p. 7562.
366. Micci, L., et al., *Paucity of IL-21-producing CD4(+) T cells is associated with Th17 cell depletion in SIV infection of rhesus macaques.* Blood, 2012. **120**(19): p. 3925-35.
367. Pallikkuth, S., et al., *Maintenance of intestinal Th17 cells and reduced microbial translocation in SIV-infected rhesus macaques treated with interleukin (IL)-21.* PLoS Pathog, 2013. **9**(7): p. e1003471.
368. Schmitt, N., et al., *Human dendritic cells induce the differentiation of interleukin-21-producing T follicular helper-like cells through interleukin-12.* Immunity, 2009. **31**(1): p. 158-69.
369. Ueno, H., J. Banchereau, and C.G. Vinuesa, *Pathophysiology of T follicular helper cells in humans and mice.* Nat Immunol, 2015. **16**(2): p. 142-52.
370. Munroe, M.E. and G.A. Bishop, *A costimulatory function for T cell CD40.* J Immunol, 2007. **178**(2): p. 671-82.
371. Blair, P.J., et al., *CD40 ligand (CD154) triggers a short-term CD4(+) T cell activation response that results in secretion of immunomodulatory cytokines and apoptosis.* J Exp Med, 2000. **191**(4): p. 651-60.
372. Royle, C.M., et al., *HIV-1 and HIV-2 differentially mature plasmacytoid dendritic cells into IFN-producing cells or APCs.* J Immunol, 2014. **193**(7): p. 3538-48.
373. Sahlender, D.A., et al., *Optineurin links myosin VI to the Golgi complex and is involved in Golgi organization and exocytosis.* J Cell Biol, 2005. **169**(2): p. 285-95.
374. Roncagalli, R., et al., *Quantitative proteomics analysis of signalosome dynamics in primary T cells identifies the surface receptor CD6 as a Lat adaptor-independent TCR signaling hub.* Nat Immunol, 2014. **15**(4): p. 384-92.
375. Dalgleish, A.G., et al., *The CD4 (T4) antigen is an essential component of the receptor for the AIDS retrovirus.* Nature, 1984. **312**(5996): p. 763-7.
376. Klatzmann, D., et al., *T-lymphocyte T4 molecule behaves as the receptor for human retrovirus LAV.* Nature, 1984. **312**(5996): p. 767-8.
377. Lim, E.S., et al., *The ability of primate lentiviruses to degrade the monocyte restriction factor SAMHD1 preceded the birth of the viral accessory protein Vpx.* Cell Host Microbe, 2012. **11**(2): p. 194-204.

7 Appendix